Volume 21, Number 3

September, 1966

SOVIET ATOMIC ENERGY

АТОМНАЯ ЭНЕРГИЯ
(ATOMNAYA ÉNERGIYA)

TRANSLATED FROM RUSSIAN

CONSULTANTS BUREAU

SOVIET ATOMIC ENERGY

Soviet Atomic Energy is a cover-to-cover translation of *Atomnaya Énergiya*, a publication of the Academy of Sciences of the USSR.

An arrangement with Mezhdunarodnaya Kniga, the Soviet book export agency, makes available both advance copies of the Russian journal and original glossy photographs and artwork. This serves to decrease the necessary time lag between publication of the original and publication of the translation and helps to improve the quality of the latter. The translation began with the first issue of the Russian journal.

Subscription
(12 Issues): $95

Single Issue: $30
Single Article: $15

Order from:

CONSULTANTS BUREAU
227 West 17th Street, New York, New York 10011

SOVIET ATOMIC ENERGY

A translation of *Atomnaya Énergiya*

Volume 21, Number 3 September, 1966

CONTENTS

CONTENTS

(continued)

NOTE

The Table of Contents lists all material that appeared in the original Russian journal. Items originally published in English or generally available in the West are not included in the translation and are shown in brackets. Whenever possible, the English-language source containing the omitted items is given.

The Russian press date (podpisano k pechati) of this issue was 8/29/1966. Publication therefore did not occur prior to this date, but must be assumed to have taken place reasonably soon thereafter.

ANALYZING THE OXYGEN CONTENT OF CERTAIN METALS BY RECORDING THE DELAYED NEUTRONS PRODUCED IN THE $O^{18}(\gamma, p)N^{17}$ REACTION

M. M. Dorosh, N. P. Mazyukevich, and V. A. Shkoda-Ul'yanov

UDC 543.53

This article considers the possibility of utilizing the $O^{18}(\gamma, p)N^{17}$ reaction for determining the concentration of oxygen in metal ingots by recording delayed neutrons. Calculations are made to determine the yields from oxygen impurities in thick blocks of Be, Ti, and Zr. The construction of high-current medium-energy accelerators makes it possible to work out a continuous analysis of metals and alloys.

The growing industry of heat-resistant metals and alloys for nuclear power engineering, airplane and rocket design, and scientific research requires the development of new, sufficiently rapid and accurate methods for determining impurities; of special importance are admixtures of the gases H_2, N_2, and O_2, whose presence reduces the plasticity of metal parts and structures.

Because of the serious technological difficulties involved in determining the presence of small quantities of oxygen in certain metals (e.g., in Be, Ti, or Zr [1, 2]), the development of new analytical methods for detecting oxygen and the improvement of the existing methods are becoming particularly urgent problems. The currently used methods of vacuum melting and large-volume dissolution of metals have a sensitivity of 10^{-1}-10^{-2}% [1, 3] and, furthermore, are laborious and time-consuming. To determine the amount of various gases (including oxygen) contained in metals by means of nuclear reactors, we activate a specimen with a flux of neutrons, gamma quanta, or high-density charged particles, and then measure the induced β or γ activity. The average sensitivity obtained for oxygen is 10^{-3}-10^{-4}% [4, 5]. However, it is not always possible to use this method for rapid analysis under industrial conditions because of the complicated equipment needed, the long time required for irradiation, and a number of other factors. In practice it is often necessary to know the average oxygen content in a specific part of the ingot or in the ingot as a whole. This problem can be solved by using the photoneutron method, owing to the following special features of this method. In the first place, in large specimens an electron-photon avalanche is produced when the incident beam is absorbed; secondly, the neutrons emitted by nuclei on γ-ray absorption have a large average path length and will easily pass through a specimen which is thick enough to absorb the primary beam completely.

Analysis utilizing methods of nuclear physics, which requires a high-intensity irradiator, may be introduced into factory practice by using high-current accelerators (microtrons, linear accelerators, high-current betatrons). Today such accelerators have already been designed and built [6-9]; they are characterized by a relatively high electron-beam current (10-100 μA or higher) and small size. The use of such accelerators provides increased opportunities for analyzing metals and alloys at production sites by recording the products of various nuclear reactions immediately — either during or after the irradiation period. It therefore seems desirable to develop an analytical method in which delayed-neutron precursors are produced and the yield of these neutrons is measured.

Reference [10] suggests determining the presence of oxygen by recording the delayed neutrons produced by the disintegration of the radioactive N^{17} nucleus formed in the $O^{17}(n, p)N^{17}$ and $O^{18}(n, d)N^{17}$ reactions when the specimen is irradiated with a neutron flux from a reactor in the $O^{17}(n, p)N^{17}$ and $O^{18}(n, d)N^{17}$ reactions and in the $O^{18}(t, \alpha)N^{17}$ reaction caused by tritium from the $Li^6(n, \alpha)H^3$ reaction. Such a large number of reactions forming N^{17} may often create some inconvenience in analyzing the specimen for oxygen, but this difficulty can be avoided if an electron or photon beam is used instead of the primary neutron flux. In this case the specimen under

Translated from Atomnaya Énergiya, Vol. 21, No. 3, pp. 163-166, September, 1966. Original article submitted April 24, 1964; revised May 16, 1966.

Maximum Delayed-Neutron Yield Q(E) for 10^{-4}% Oxygen in Various Metals (neutrons/100 μA · sec)

E, MeV	$Q_{Be}(E)$	$Q_{Ti}(E)$	$Q_{Zn}(E)$
18	10	20	30
19	40	60	80
20	70	140	170
21	130	240	270
22	200	370	400
23	300	540	590
24	480	780	830

investigation (e.g., a metal ingot) must at the same time be part of a Faraday cup used to measure the incident radiation flux precisely [11] (which is much easier than precisely measuring the neutron flux by using the neutrons as primary radiation sources), and a source of delayed neutrons produced by the $O^{18}(\gamma, p)N^{17}$ reaction. As was shown in [12], the contribution of the $O^{17}(n, p)N^{17}$ reaction is negligible in comparison with that of the $O^{18}(\gamma, p)N^{17}$ reaction. It should be noted that the specimen dimensions for which the electron or photon radiation effective for the $O^{18}(\gamma, p)N^{17}$ reaction is almost completely absorbed are small in comparison with the path length of the neutrons formed in the photo-nuclear reactions. This makes it possible to minimize the contribution of all the reactions produced by neutrons and yielding the isotope N^{17}.

Thus, suppose that a specimen containing oxygen is irradiated with a beam of electrons or gamma quanta and that an electron-photon avalanche is produced in the specimen for a specified beam energy and sufficiently large specimen dimensions. In O^{18} nuclei, gamma quanta with an energy above the threshold energy (E = 16.4 MeV) give rise to a (γ, p) reactions, forming the beta-active isotope N^{17} with a half-life of $T_{1/2}$ = 4.15 sec. Each N^{17} nucleus undergoes beta disintegration and is converted into the stable isotope O^{16} and a neutron. Schematically the reaction may be represented as follows:

Each disintegration is accompanied by the emission of one neutron, and therefore the resulting neutron "activity" may also be characterized by a half-life of 4.15 sec. Irradiation for about 20 sec saturates the specimen with the active isotope N^{17}. When saturation is achieved in the activation process, the number of nuclei formed per second is equal to the number of delayed neutrons emitted by the specimen per second. The recording can be carried out either during the intervals between accelerator pulses or after the irradiation has stopped and saturation has been achieved. In either case, however, the counting apparatus should be turned on some time after (about 1000 μsec after) the accelerator pulse. During this time the prompt neutrons formed in the photonuclear reactions are slowed down to thermal energies and are absorbed, so that there is virtually no error introduced into the delayed-neutron counting by the contribution of the prompt neutrons.

Thus, we have a new method for measuring the concentration of oxygen in metals and alloys. This conclusion is supported by numerical calculations.

The total number of (γ, p) reactions involving O^{18} (or the maximum number of delayed neutrons) can be found by calculation according to the Belen'kii-Tamm theory [13]. We used the value for the cross section for the $O^{18}(\gamma, p)$ reaction given in [12], and the critical energies given in [14]; the concentration of O^{18} in natural oxygen was assumed to be 0.2%, and the concentration of oxygen in the metal was taken to be 10^{-4}%.

The maximum yields Q(E) were calculated for an electron current of 100 μA from the accelerator (see table and Fig.). By using these data, we can estimate the time needed for recording the neutrons with a given statistical accuracy, and we can also determine the N^{17} saturation level of the specimen.

Let us assume that the counting rate is constant; this is entirely possible if the recording is carried out during the short time intervals between the accelerator pulses. Let the efficiency of the counting apparatus be k = 1%, the given statistical accuracy of the recording be $\delta = \pm 5\%$, and the duration of the transmission-system pulse be τ = 10,000 μsec, for a frequency of f = 50 cps. As can be seen from the table, for an accelerator current of 100 μA and an electron energy of about 25 MeV the number of active N^{17} nuclei (or delayed neutrons) produced per second in a titanium specimen is $Q(25) \approx 1000$ nuclei/μA · sec. Then the counting rate is $kf\tau Q = 5$ neutrons/sec. From the formula for the statistical accuracy,

$$\delta = \frac{1}{\sqrt{kf\tau Qt}}$$

we find the measurement time

$$t = \frac{1}{kf\tau Q\delta^2} \approx 1.5 \text{ min.}$$

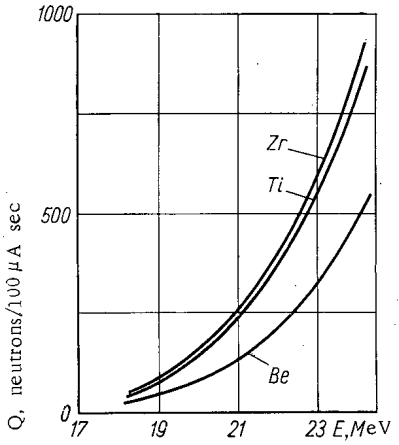

Number of delayed neutrons versus energy of electron beam (for oxygen concentration of 10^{-4} % in metals).

i.e., a value convenient for use in analysis . From the graph showing the yields (see Fig), we see that this value also holds in the case of zirconium, but in the case of beryllium the measurement time required when other conditions remain the same is approximately twice as long. It should be noted that we can reduce the value of t somewhat for the constant value of δ by increasing the neutron-counting efficiency k and increasing τ.

An apparatus for recording after saturation can be set up without any technical difficulty. This procedure is preferable in the cases when the irradiation is carried out with an accelerator which has a high beam current (of the order of 1 mA or more) or when the specimen contains more than 10^{-4}% oxygen.

Using the formula

$$Q_n(E) = \frac{Q(E)\,T_{1/2}}{\ln 2}\left(1 - e^{-\frac{t \ln 2}{T_{1/2}}}\right),$$

we find that the delayed-neutron yield $Q_n(E)$ obtained after irradiation for $t = 5 \cdot T_{1/2}$ (energy 25 MeV, accelerator current 100 μA, oxygen content of the titanium 10^{-4}%) is about 6000 neutrons. Industrial titaniums usually contain more than 0.01% oxygen [15], and for these the total number of delayed neutrons at saturation should be no less than $6 \cdot 10^5$ for the experimental condition under consideration. This yield can be recorded with sufficient accuracy in a short time (the measurement time will be no more than 1 min), and this is a considerable advantage of the proposed analytical method.

In our calculations we used an electron-current value of 100 μA, which can be achieved even today in some types of accelerator, and we considered data obtained for just this magnitude of current. From these data we can also decide how suitable this type of analysis would be for other conditions (different current values, oxygen concentrations, etc). In particular, if we consider that the oxygen contamination in industrially produced ingots is about 100 times as high as the values used in our calculations, we see that the results will not change when the accelerator current is 1/100 of our value, i.e., 1 μA. This current can be achieved today without any practical difficulty. In view of what we have said concerning the purity of industrially produced metal and present-day possibilities of accelerator technology, we may conclude that the idea described here is worth testing experimentally. *

In conclusion, it should be noted that in the proposed method for determining the oxygen content of metals (or other substances), the isotope composition of oxygen in the specimen (i.e., the percentage of the isotope O^{18} in the oxygen impurities) is assumed to be known precisely. Where there is reason to suppose that the isotope distribution of oxygen in the specimen will be different from the natural distribution, the actual distribution should be determined once for the particular industrial scheme used in producing the metal (or other substance) involved.

LITERATURE CITED

1. J. Darwin and J. Baddery, Beryllium [Russian translation]. Moscow, Izd-vo inostr. lit. (1962).
2. N. F. Litvinova and Z. M. Turovtseva, Methods of Determining Impurities in Pure Metals [in Russian]. In: "Proceedings of the Commission on Analytical Chemistry," Vol. XII. Moscow, Izd-vo AN SSSR (1960).

* Preliminary experimental results were obtained while this article was being prepared for publication. The delayed-neutron yield of Cu + CuO specimens with different amounts of CuO (specimen weight, 1.5 kg) was measured with BF_3 when these specimens were irradiated to the point of saturation with the bremsstrahlung spectrum of a betatron with an upper limit of 25 MeV (intensity of 25-30 R/min at a distance of 1 m from the target). The sensitivity of the method was about 1% of oxygen in copper (error of the results ±10%, analysis time ≈ 10 min). By using high-intensity irradiating apparatus [9-16] (e.g., the betatron [8] and the microtron [16] developed at the Tomsk Polytechnic Institute and the Institute of Physical Problems of the Academy of Sciences of the USSR are capable of producing more than 1000 R/min, and 3000 R/min, respectively, at a distance of 1 m from the target) and a more efficient counting apparatus, we can increase the sensitivity of this method by several orders of magnitude.

3. I. A. Berezin and V. I. Malyshev, Zh. analit. khim., 17, 1101 (1962).
4. I. A. Maslov, Zavodsk. laboratoriya, 1, 51 (1964).
5. L. Bate, Nucleonics, 21, 72 (1963).
6. Atomnaya Énergiya, 5, 589 (1958).
7. S. P. Kapitsa, V. N. Bykov, and V. P. Melekhin, ZhÉTF, 41, 368 (1961).
8. V. A. Moskalev et al., Summaries of Report Delivered at the Fourth Inter-Universities Scientific Conference on Electron Accelerators, Feb. 13-17 (1962) [in Russian]. Tomsk, Tomsk University Press, p. 41 (1962).
9. O. A. Val'dner, A. A. Glazkov, and A. N. Finogenov, Pribory i tekhnika éksperimenta, 3, 29 (1963).
10. S. Amiel and M. Peisakh, Atomnaya Énergiya, 14, 535 (1963).
11. V. A. Shkoda-Ul'yanov et al., Author's Certificate No. 163782.
12. W. Stephens, J. Halpern, and R. Sher. Phys. Rev., 82, 511 (1951).
13. S. Z. Belen'kii, Avalanche Processes in Cosmic Rays [in Russian]. Moscow-Leningrad, Gostekhteorizdat (1948).
14. O. I. Dovzhenko and A. A. Pomanskii, ZhÉTF, 45, 268 (1963).
15. Nonferrous Metals and Alloys. Testing Methods [in Russian]. Part 2. Moscow, Izd-vo standartov (1964).
16. S. P. Kapitsa, Atomnaya Énergiya, 18, 203 (1965).

All abbreviations of periodicals in the above bibliography are letter-by-letter transliterations of the abbreviations as given in the original Russian journal. *Some or all of this periodical literature may well be available in English translation.* A complete list of the cover-to-cover English translations appears at the back of the first issue of this year.

ACCELERATION OF ELECTRONS IN THE ANNULAR PHASOTRON OF THE P. N. LEBEDEV PHYSICAL INSTITUTE OF THE ACADEMY OF SCIENCES OF THE USSR

L. N. Kazanskii, V. N. Kanunnikov,
A. A. Kolmenskii, E. P. Ovchinnikov,
V. A. Papadichev, S. S. Semenov,
A. P. Fateev, and B. N. Yablokov

UDC 621.384.612.3:621.384.612.4

The physical bases for the selection of parameters in the phasotron of the Lebedev Physical Institute ("FIAN") and details of its construction are considered. The start-up procedure for the accelerator is described. Results obtained on working with a beam are discussed.

A new accelerator was started in the Lebedev Physical Institute in October 1965; this was an electron radial-sector annular phasotron (the KF) [1]. The annular magnet of the accelerator consists of 40 similar units. Strong focusing is ensured by the fact that the field in neighboring units varies on the same radial law but in opposite directions [2, 3]. The constancy of the field in time enables a high-intensity particle beam to be achieved and permits storage of the particles. The construction of the magnet makes it possible to realize the so-called symmetry (or two-beam) condition [4, 5], enabling acceleration, storage, and collision of beams simultaneously rotating in opposite directions to be carried out. The KF provides for the use of inductive and resonance (phasotron) acceleration of the electrons and also the study of special acceleration conditions (stochastic, "phase-shift," etc.).

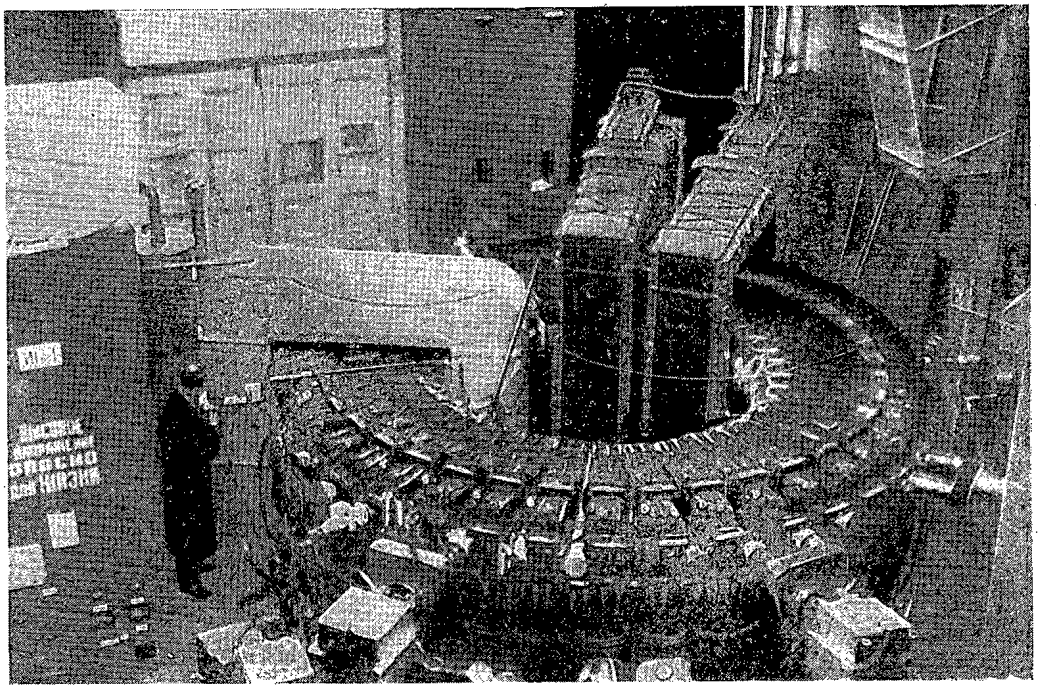

Fig. 1. General view of the apparatus.

Translated from Atomnaya Énergiya, Vol. 21, No. 3, pp. 166-176, September, 1966. Original article submitted March 5, 1966.

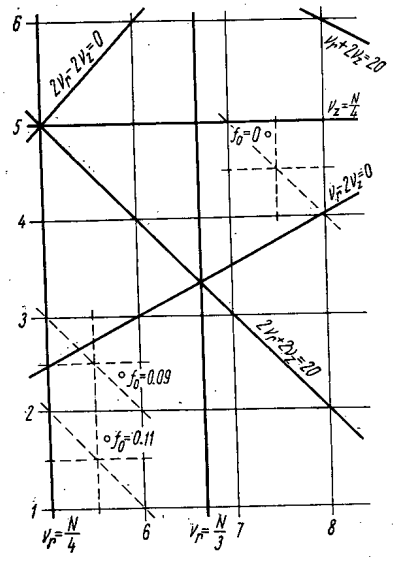

Fig. 2. Stability diagram of the KF (figures near the circles show the corresponding values of the constant component f_0).

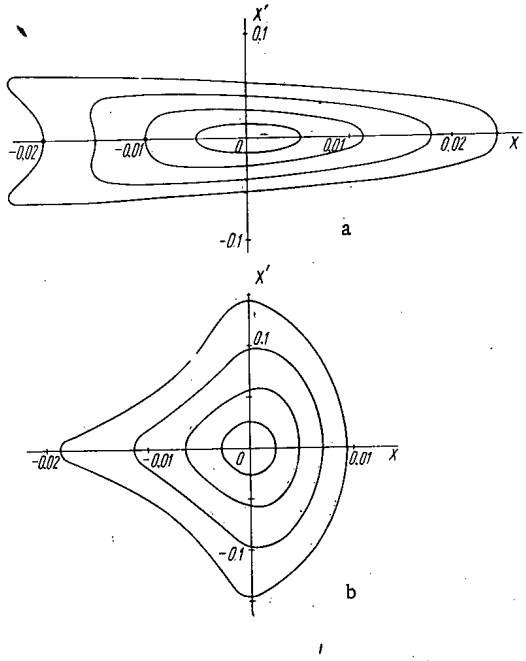

Fig. 3. Phase diagram describing the radial motion of particles in the ideal field of the KF; a) In the middle of the positive units; b) in the middle of the negative units.

TABLE 1. Tolerances for the Deviation of the Magnetic Field in the KF from the Calculated Value (n=16, f_0=0.09)

Ideal field	
Δn (over the radius, identical for all azimuths)	0.06
Δf0	10^{-3}
Perturbed field	
Distortion of median plane, mm:	
"resonance" harmonic	0.1
nearest neigboring harmonics	0.2
higher harmonics	0.3
Azimuthal asymmetry, %:	
"resonance" harmonic	0.1
neighboring and higher harmonics	0.2 to 0.3
Δn with respect to azimuth, identical in the region	
δr ≈ 6 cm	0.02

Note. It is supposed that the permissible frequency variation is $\Delta\nu \lesssim 0.1$.

The KF was set up in order to make an experimental study of the possibilities of accelerators of the annular-phasotron type in various special conditions of acceleration and particle storage.

The general form of the apparatus is shown in Fig. 1, in which we see the electromagnet units, the injection pulse generator, the betatron cores, and the resonator. The principal parameters of the accelerator are as follows:

Number of elements of periodicity N	20
Field index n	16
Number of betatron oscillations per turn (f_0 = 0.09):	
radial	5.79
vertical	2.38

Extent of working region of the field	117 to 160 cm
Working field strength	27 to 4200 Oe
Origin of profiled pole	150 cm
Vertical gap at radius 120 cm	7 cm
Azimuthal dimension of unit	5°
Total weight of magnet	15 ton
Magnet power supply	75 kW
Frequency of rotation of particles:	
initial	19.7 Mc/sec
at critical energy	33.9 Mc/sec
final	29.5 Mc/sec
Power of hf system	17 kW
Injection energy	80 keV
Critical energy	2.11 Mev
Final energy	30 MeV

Working Point and Tolerances for the Deviation of the Magnetic Field from the Calculated Value

The ideal magnetic field of the radial-sector annular phasotron, ensuring geometric similarity of the orbits, may be written in general form [6, 8] as

$$H_z|_{z=0} = H_0\left(\frac{r}{r_0}\right)^n (f_0 + \cos N\theta + f_3 \cos 3N\theta + f_5 \cos 5N\theta + \ldots);$$

$$H_r|_{z=0} = H_\theta|_{z=0} = 0,$$

where N is the number of elements of periodicity, and n the magnetic-field index.

In the KF the higher harmonics f_3, f_5, etc. make up no more than 6 to 7% of the fundamental harmonic.

The position of the working point on the stability diagram (Fig. 2) depends mainly on n, N, and the constant component f_0; in selecting it and determining the magnet parameters, nonlinear effects have to be taken into account.

In contrast to ordinary focusing accelerators, tolerances in the annular phasotron, with its considerable n value, are established principally on the basis of the limiting amplitudes of the betatron oscillations. This is because of the severe non-linearity of the magnetic field, leading to the appearance of nonlinear resonances. Especially dangerous are the "ideal" nonlinear resonances, in particular the $\nu_r = N/3$, $\nu_r = N/4$, $\nu_r + 2\nu_r = N$, $2\nu_r - 2\nu_z = 0$ and $2\nu_r + 2\nu_z = N$, present in the ideal field. (In Fig. 2 these resonances are shown by thick lines.) If the working point of the accelerator is placed close to one of the resonances indicated, pulsations of betatron oscillations take place, the value of these depending on the initial amplitude of the oscillations. For a certain "limiting" amplitude, the pulsations lead to the loss of particles in the injector or on the chamber walls.

Table 1 shows the tolerances for the parameters of the KF magnetic field, obtained by numerical calculation in an electronic computer. The results were analyzed by means of phase diagrams (Fig. 3), which enabled the limiting amplitudes and frequencies of the oscillations to be determined quite accurately from data relating to the initial turns.

Field-Stability Requirements. For the betatron oscillations, practically any perturbation of the magnetic field is slow and can only lead to a change in the working point and breadth of the resonance bands.

On the basis of the tolerances indicated in Table 1 we see that the azimuthal distortion of the field at any moment in time must not exceed 0.1%. Since the field in the KF depends considerably on the radius, the azimuthal distortions are very sensitive to distortions of n in the units. Hence the tolerance for the resonance azimuthal harmonic of instability of n is very rigorous.

Table 2 shows the tolerances for the instability of the magnetic field and the value of n, calculated on the assumption that the total displacement of the working point is no greater than 0.1.

TABLE 2. Tolerances for the Instability of Magnetic Field with $f_0 = 0.09$

Form of perturbation	Frequency of perturbation	Tolerance	What it affects
Change in n, simultaneous for all azimuths	any	0.06	Position of working point
Drift of constant field component f_0	any	10^{-3}	ditto
Azimuthal asymmetry of field (resonance harmonic)	any	0.1	Width of resonance band
Change in n with respect to azimuth (resonance harmonic)	any	0.02*	ditto
Resonance perturbations of field, %	10 to 150 kc/sec	$2 \cdot 10^{-3}$	Amplitude of synchrotron oscillations
Slow changes in field, %	<10 kc/sec	8/fcps	ditto
Rapid changes (jumps) in field, %	>150 kc/sec	$5 \cdot 10^{-2}$	ditto
Noise perturbation of field (mean square)	10 to 150 kc/sec	0.02%	ditto

* Assuming n const. over the radius (near $\delta r \approx 6$ cm).

TABLE 3. Current in the Windings for f_0=0.09

Windings	Current, A	
	Positive units	Negative units
I	206.7	167.1
II	8.516	6.884
III	0.8516	0.6884
On the yoke	8.1	5.8

Accelerator Magnet

The most reasonable way of forming the magnetic field of the annular phasotron [8-11] is the use of ampere-turns distributed over the surface of the magnetic poles. The shape of the pole surface may in general be arbitrary, but it must be remembered that in order to ensure similarity of the magnetic field it is simplest if all the dimensions of the magnet determining the shape of the field are made to increase in proportion to the radius. In order to make better use of the useful volume of the gap, the turns of the distributed winding are laid in grooves in the poles. The requirement for accuracy in the positioning of the conductors extends to accuracy in the finishing of the grooves. The characteristic tolerance for the accuracy of finish is ± 0.1 mm.

In the region of high magnetic fields (r = 150 to 160 cm), profiled poles are used instead of distributed windings, the gap between the poles being reduced by a factor of several times. This is quite permissable since the amplitude of the betatron oscillations is here considerably reduced.

The KF electromagnet units (see Fig. 1) are set on the circumference of an annular stand welded from nonmagnetic steel and consisting of two insulated halves. The divisions in the stand coincide with the insulating divisions of the vacuum chamber. The units are fixed to the stand by means of supports adjustable in position for all degrees of freedom. Each unit consists of two identical "beams" (upper and lower), shaped pole tips, and a stand for the rear yoke. The azimuthal width of a unit (with respect to the iron) is 5°. The vertical gap, equal to 7 cm at a radius of 120 cm, rises in proportion to the radius up to r = 150 cm.

The width of all the grooves is the same in the radial sense and equals 8 mm; the depth is determined by the number and cross section of the conductors. The step between the grooves in the radial sense equals 15 mm, which prevents any magnetic-field distortions due to the discrete nature of the winding [9]. The currents in the distributed windings for $f_0 = 0.09$ are given in Table 3. (The primary windings are made of tubing 6 mm in diameter and are water-cooled).

In order to obtain the required field distribution, a winding on the yoke is necessary in addition to the distributed windings [8, 11]; this compensates the stray field of the distributed windings in the initial radii due to the finite magnetic conductivity of the yoke. The yoke winding consists of individual sections, which enables the necessary number of turns to be selected when correcting the azimuthal distortions of the field in the initial radii. No precise adjustment was made to the form of the shaped pole. The shape of the pole was only maintained with respect to the median line of the unit, so that the pole could subsequently be finished after connecting up the multiwire conductors in the region of the distributed turns.

After assembly, the constancy of the field index along the radius, for optimum current in the yoke

winding, was verified for all the units. The measurements were made on a testing device equipped with a system for supplying stabilized current (± 0.05%) to three units [12].

Magnet Supply System. This system has to ensure a high stability of the magnetic field in time (see Table 2) and reproducibility of its characteristics from one switching-on to another. When the magnet is switched on or off in an irregular manner, additional distortions of field and field gradient appear. Hence the following requirements are imposed upon the switching-on and off processes: 1) a matched (accuracy $5 \cdot 10^{-4}$) standard rise of the currents in all the windings at a given velocity; 2) the absence of any surge at the end of the current rise (accuracy $5 \cdot 10^{-4}$); 3) a standard switch-off procedure (as rapid as possible) for the currents in the windings. Stabilization of the currents must be no worse than $3 \cdot 10^{-4}$. It should be noted that, in the absence of a field-stabilization system at small radii, there requirements would be an order more rigorous [13].

For feeding the windings with a 200-A current, two dc generators of 65 kW each are employed. Other windings of the magnet and the excitation windings of the two generators are fed from a supplementary generator of 13 kW dc. Voltage pulses are suppressed and the steady components of current stabilized by tube units connected in parallel to the excitation windings of the generators and each magnet-winding circuit.

The magnet is switched on by the simultaneous closing of contacts in the circuit of each generator. The linear current rise is ensured by feeding a negative-feedback voltage signal through a dc amplifier and Rc circuit to the tube network of the control units. When the magnet is switched off, the contacts open, and the commutation currents are shunted by the diodes. In this way all switchings-off of the magnet (including accidental ones) are made identical.

Arrangement of the Magnet Units. The magnet units have several well-finished surfaces on which all the attachments for measuring the position of the units are mounted. For measuring the radial and vertical position of the units, a rotating gage furnished with micrometers is used. The azimuthal position of the unit is measured with a theodolite. For measuring the slope of the unit relative to the upper beam, an attachment incorporating two levels is provided.

The deviations of the measured position parameters of the units from the ideal case are converted into magnetic-field distortion harmonics. The azimuthal asymmetry due to inaccuracy in the positioning of the units is 0.01 to 0.02%, and the distortion of the median plane 0.01 mm.

Magnetic Measurements. According to the table of tolerances, the dangerous harmonics of the azimuthal field distortions $\Delta H_{z,k}/H_{z,20} \leqslant 10^{-3}$, where k is the number of the harmonic. For this we must satisfy the following condition for the distortion of the field in each unit (on the assumption of the statistical independence of the deviations in each unit): $\Delta H_z \approx \sqrt{\frac{N}{2}}\,\Delta H_{z,k} \leqslant 3 \cdot 10^{-3}$. An analogous requirement is laid on the radial component of the magnetic field $H_{r,k}/H_{z,20} \leqslant 10^{-3}$. The influence of the azimuthal component H_θ on the z motion is six or seven times weaker than the corresponding influence of H_r. Dangerous harmonics of H_θ are the supplementary harmonics $H_{\theta,\,20\pm k}$, which, combining with the 20-th harmonic of the orbit ripple, give low harmonics in the distortion of the median plane.

Measurement of all three components of magnetic field H_r, H_θ, H_z in the injection region (r = 120 cm) is effected by a compensation method, using a magnetometer [13]. For moving the pickup, the same rod that was used for gaging the positions of the magnet units is employed. Before installing the chamber in the magnet, the rod is rotated by a small motor and the measured data are fed to an automatic record. In the presence of the chamber, the tube carrying the pickup is passed through openings in the chamber opposite each of the units. This system enables the pickup to be set at the same radius in different units to an accuracy of ± 0.01 mm and displacements along the radius to be made to an accuracy of ± 0.03 mm. The constancy of coordinate z on displacing the pickup along the radius is ensured to an accuracy of not worse than 0.1 mm. The azimuthal displacements can be fixed to an accuracy of 10" with the theodolite.

The results of measuring H_z, H_r, and H_θ, after correction, are shown in Fig. 4, from which we see that the values of the harmonics lie within the tolerances laid down.

The ratio of the constant component of magnetic field to the fundamental harmonic was measured to an accuracy of 1.5%, which for $f_0 = 0.9$ corresponded to $\Delta\nu_z \leqslant 0.04$ and $\Delta\nu_r \leqslant 0.015$.

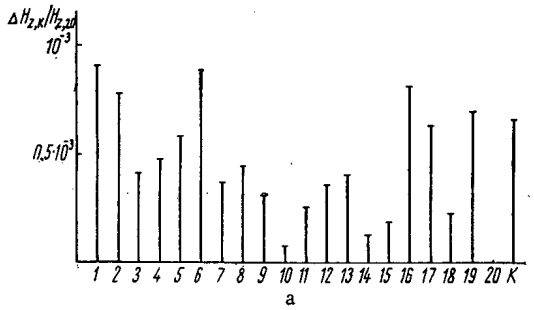

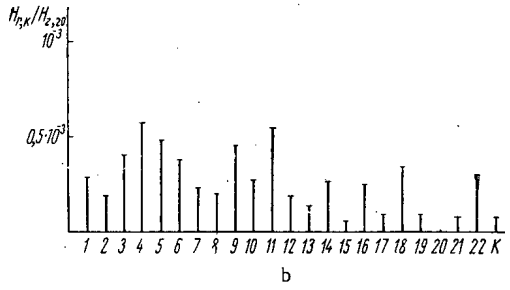

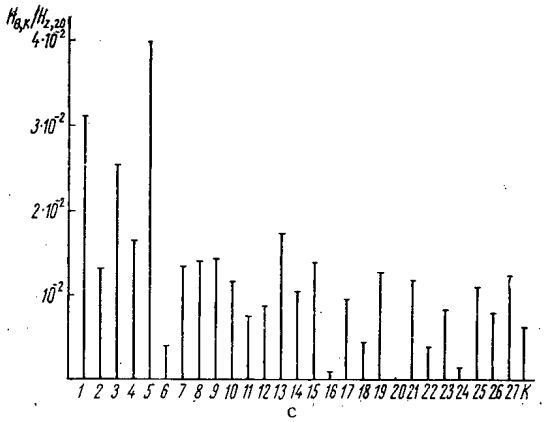

Fig. 4. Results of measuring a) H_z, b) H_r, and H_θ after correction (r = 120 cm).

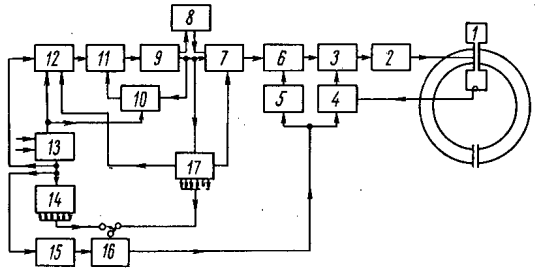

Fig. 5. Block diagram of the hf system; 1) Resonator; 2) power amplifier, 29 to 35 Mc/sec; 3) amplitude modulator; 4) comparison system; 5) unit for measuring the amplitude program; 6) amplitude modulator; 7) phase reverser; 8) phase shifter; 9) generator; 10) automatic adjustment for initial frequency; 11) frequency modulator; 12) frequency programmer; 13) synchronizer; 14) key delay unit; 15) amplitude programmer; 16) key; 17) frequency monitor.

Control system. For controlling the field stability, a system for measuring the field at small radii is employed; this is based on measuring the magnetic potential difference between the upper and lower beams. Magnetically-conducting frameworks are fixed to the upper and lower beams, on their end surfaces. In the gap between these conductors is a magnetic-field pickup on the same type as that used for the magnetic measurements. The signals from the pickup pass through a step selector to an automatic recorder. The system "runs around" the ring in 15 min and records any changes of field associated with irregular connection, short-circuiting of the turns in the windings, displacement of the units, and so forth.

Accelerating System of the KF

Acceleration of particles in the KF is effected at the beginning of the cycle by the eddy field of two betatron cores and later by means of the hf voltage.

The betatron condition is used for the rapid extraction of particles from the injector and their acceleration to about 350 keV, on reaching which the particles are drawn into the phasotron condition of acceleration. Use of preliminary betatron acceleration considerably narrows the range of frequency modulation, increasing the initial frequency from 19 to some 29 Mc/sec. Acceleration is effected during the growth of the magnetic flux; the fall in flux is retarded by the inclusion of a damper [14]. The two betatron cores can accelerate the particles up to 4.5 MeV.

The hf acceleration system incorporates a frequency-modulated generator with a range of 15 to 35 Mc/sec, units for forming the frequency and amplitude programs, delay systems, and a system for tying to the selected frequency values (Fig. 5). For the critical energy $E_{cr} = \sqrt{1+n}\ E_0 = 2.1$ MeV the automatic phasing in the KF vanishes, and special measures have to be employed for further hf acceleration. In order to carry the electrons through the critical energy, a phase shifter and electronic switch are employed; by this means a phase jump in the hf voltage is introduced at the moment at which the critical energy is reached. The phase jump may be regulated between 10 and 180° by including sections of coaxial

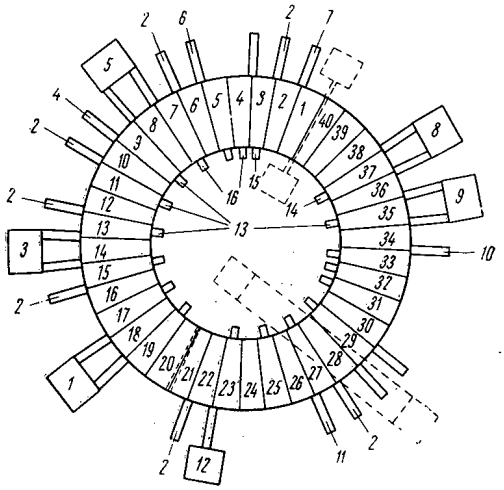

Fig. 6. Arrangement of vacuum chamber; 1) Pump No. 1; 2) mirror; 3) pump No. 2; 4) measuring unit; 5) pump No. 3; 6) Faraday cylinder No. 2; 7) Faraday cylinder No. 1; 8) pump No. 4; 9) pump No. 5; 10) photomultiplier; 11) Faraday cylinder No. 3; 12) diffusion pump; 13) grid; 14) induction electrode; 15) screen; 16) injectors.

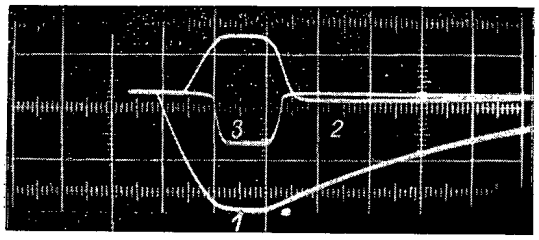

Fig. 7. Pulse to the injector cathode (1); pulse to the inflector (2); current from the inflector (3). Multiturn injection; time base 2.5 μsec/cm.

cable of various lengths. The particles may also be carried through the critical energy without any phase throw by rapidly switching the accelerating voltage off and on.

The voltage from the output of the frequency-modulated generator falls on to a power amplifier, the load of which is a resonator shunted with a resistance of 50 Ω. The equivalent capacity of the resonator is 800 pF, and the power of the amplifier is 15 kW.

The frequency programs are formed in constant R, L, and C elements by means of electronic switches. The amplitude program is formed in diodes. The principal parameters of the hf system are the following:

Multiplicity	1
Initial frequency	29 Mc/sec
Frequency at critical energy	33.5 to 34.5 Mc/sec
Maximum amplitude of accelerating voltage	600 V
Rate of frequency modulation:	
at beginning of cycle	10^4 Mc/sec^2
at end of cycle	3 Mc/sec^2
Permissible rate of frequency change:	
on approaching critical energy	10^4 Mc/sec^2
at the instant of phase shift	10^3 Mc/sec^2
Reproducibility of maximum frequency from cycle to cycle	10^{-4}
Total acceleration time	5.5 msec

Vacuum Chamber

The vacuum chamber of the KF has the form of a torus, the cross section of which largely reproduces the form of the gap in the electromagnet. The chamber is made of nonmagnetic steel sheet 4 mm thick; in the gaps between the magnet units, 40 fins 10 mm thick are welded for the sake of rigidity. The camera is divided into two parts insulated by polystyrene and rubber seals; in order to prevent the direct incidence of the beam these are covered with metal screens. The chamber has 26 tubes leading off from the outer side of the ring and 19 from the inner (Fig. 6). To some of the outer tubes are connected titanium pumps each rated at 100 liter/sec; the working vacuum is 2.10^{-6} mm Hg. The other outer tubes and those of the inner set which are not occupied by injectors are used for siting recording apparatus.

In the inner wall of the chamber are 21 additional openings through which instruments may be inserted for measuring the magnetic field within each unit, just as in the case of the inner tubes.

Injection System

The injector is a Pierce electron gun designed for a working voltage of up to 100 kV and furnished

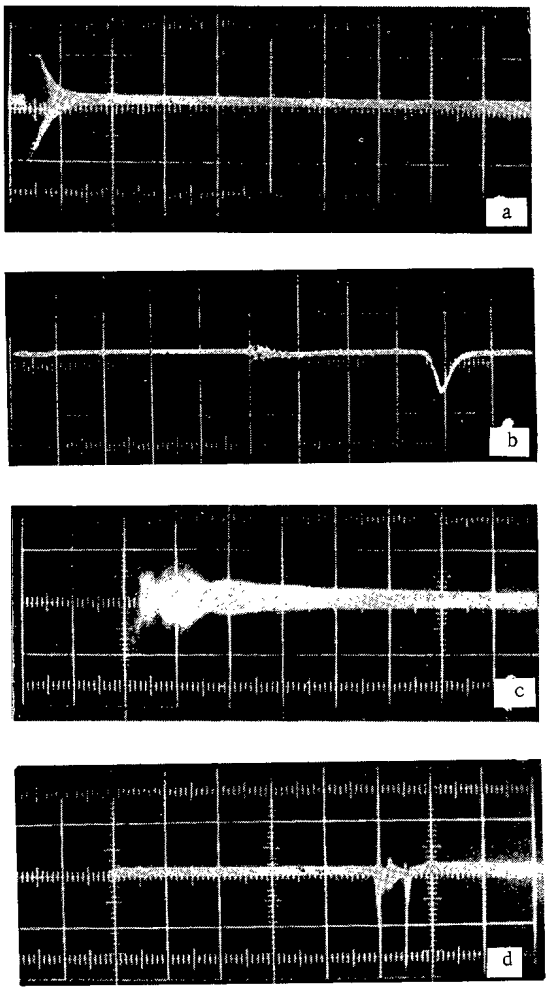

Fig. 8. Spontaneous breakaway of the beam from the injector in the constant magnetic field of an annular phasotron; a) Pulse from signal electrode, beam rapidly debunches; b) pulse from accelerated particles (betatron) to the photomultiplier (betatron pulse switched on 12 μsec after injection, set in the center of the frame; scan velocity 2.5 μsec/cm); c) multiturn injection, signal from electrostatic signal electrode (beam bunched and debunched several times); d) multiturn injection, pulse from accelerated particles to photomultiplier (lifetime of broken-off beam 150 μsec, scan velocity 20 μsec/cm, pulse of betatron core shifted 100 μ from injection).

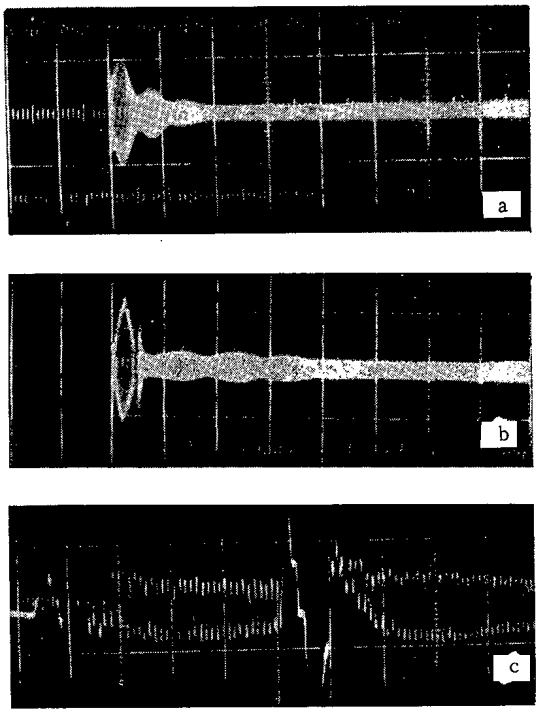

Fig. 9. Spontaneous bunching and debunching of the beam; a) Bunching and debunching for multiturn injection without acceleration, with a period of about 25 μsec, scan velocity 60 μsec/cm; b) bunching and debunching for multiturn injection after betatron acceleration, betatron pulse switched on 25 μsec after injection, bunching-debunching period about 50 μsec; c) initial section of oscillograms, scan velocity 0.5 μsec/cm.

with an electrostatic inflector for rotating the beam through 90°. The voltage to the inflector plate is supplied through a separate insulated lead. The current at the output from the injector reaches 0.4 A; the dimensions of the beam are no greater than 2 mm in the horizontal direction and 10 mm in the vertical (divergence of ± 1.5 and ± 0.5° respectively). The injection angle is controlled within ± 3.5° by the inflector voltage.

The injector is fed from a negative-pulse generator supplying an extracting voltage to the cathode of the electron gun (3 μsec, 20 to 100 kV), a positive-pulse generator for the inflector (2.5 μsec, 0 to 25 kV), and a generator for supplying additional short positive voltage pulses (25 nsec, 3.5 kV) to the inflector for single-turn injection (Fig. 7).

Starting the Annular Phasotron

The KF incorporates units with magnetic fields of different sign; hence injection may take place either in a positive (focusing in the radial direction) or negative unit. Each has advantages and disadvantages. According to linear theory, the envelope of the radial betatron oscillations has a maximum in a

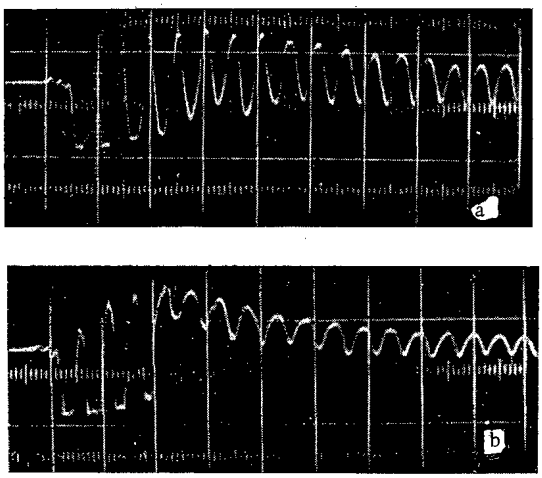

Fig. 10. Oscillograms of the first turns of the beam (without acceleration); signal from electrostatic signal electrode scan velocity 0.1 μsec/cm.

positive unit and a minimum in the negative. Since the vertical aperture is much smaller than the radial in annular phasotrons, injection would be more advantageously carried out in a negative unit, the vertical motion in which is favorably conditioned. In starting the accelerator it turned out, however, that injection in either positive or negative unit was about equally favorable.

Since the tolerances relating to the perturbation harmonics were satisfied, no field correction was made during the start-up process. An exception was the fine adjustment of f_0 at small radii, effected by shifting the reference level of the field-stabilization monitors. This correction was made after obtaining a circulating beam and betatron acceleration. The correction facilitated adjustment of the various particle-capture conditions and also improved the stability of the beam.

For observing the first turns, grids covered with a luminophore of about 0.5 "transparency" were used; these enabled the position of the beam to be recorded to about 1.5 mm. For measuring the beam current in the first turn and calibrating the recording equipment, Faraday cylinders were employed.

The circulating beam is indicated by means of inductive electrodes 4 cm wide covering a range of 116 to 147 cm over the radius. The use of inductive electrodes for recording the beam proved to be feasible, not only for single-turn injection and in the hf-acceleration condition, but also for multiturn injection and in the inductive-acceleration condition, thanks to the "self-bunching" of the beam. The use of inductive electrodes enabled such interesting effects as the spontaneous "breakaway" of the beam from the injector to be observed.

For recording the accelerated beam, a scintillator movable over the whole working region is used.

The starting of the accelerator takes place in several stages: first, the initial turn is obtained (injection energy varied between 70 and 90 keV), then several turns are obtained (capture), then comes betatron acceleration, and finally the phasotron condition.

After finishing the magnetic measurements, the first turn (for injection in a focusing unit) was studied; this confirmed the good quality of the magnetic field. After adjusting the position of the injector by means of the grids and Faraday cylinders, the "broken-off" circulating beam could be recorded on the signal electrode, both for single-turn and multiturn injection. Then the condition of inductive acceleration was obtained, first for injection in a focusing unit, and later for injection in a defocusing unit. At this stage the constant component of the magnetic field at small radii was adjusted with respect to the maximum of the accelerating current. As a result of this, the intensity of the accelerated beam was increased by approximately an order.

For optimum field adjustment and a current of about 50 mA in the first turn, the actual beam "broke off" from the injector and circulated in the chamber for some tens of microseconds. The life-time of the "broken-off" beam was measured by throwing it on to the target by means of a betatron pulse delayed relative to the injection pulse. The life-time of the beam was greater than the bunching-debunching period, as may be seen by comparing the oscillograms of signals from the inductive electrodes and the photomultiplier (Fig. 8).

The effect of the beam breakaway from the injector was observed for both single-turn and multiturn injection (in the latter case the effect occurs over a wider range of injection angles). For multiturn injection, the beam spontaneously bunches itself, as may be seen with the inductive electrodes. This phenomenon of bunching and debunching of the beam may take place both before acceleration and during betatron acceleration (Fig. 9). By adjusting the constant field component at the injection radius (by displacing the working point on the stability diagram) and the inflector voltage (initial conditions), we can set up different particle-capture conditions for the first turns (Fig. 10). The upper oscillogram of Fig. 10 shows

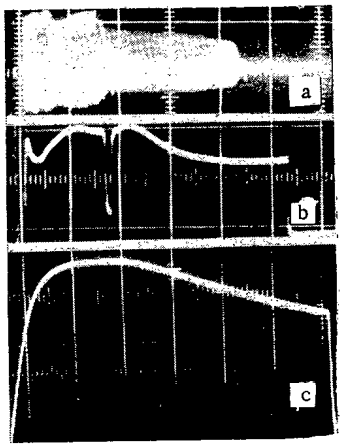

Fig. 11. Transition through the critical energy by switching off the amplitude of the accelerating voltage in the neighborhood of the critical energy; a) Signal from inductive electrodes; b) envelope of accelerating-voltage amplitude; c) change in the frequency of the accelerating voltage with time.

the case in which the intensity of the initial turns falls off smoothly and the intensity of the broken-off circulating beam is small. In the oscillogram of Fig. 10b (after an adjustment of some 3% with respect to the constant component and 1° in angle), we see a sharp fall in current after the fourth turn; the intensity of the broken-off beam, however, is an order greater.

Thanks to the bunching of the particles in the course of betatron acceleration, it was possible to make exact measurements of the particle-rotation frequency at the critical energy, using the beat signal of the signal-electrode voltage mixed with the voltage from a standard-signal generator.

Inclusion of the accelerating hf voltage enabled phasotron acceleration up to the critical energy (2.1 MeV) to be obtained almost immediately after selecting the optimum frequency and the right instant for switching on the accelerating field. The particles were drawn into the phasotron accelerating condition, both for a slow rise in the amplitude of the hf voltage (in 100 μsec, equal to approximately 10 to 15 periods of the synchrotron oscillations) and also for an "instantaneous" rise in amplitude.

The transition through the critical energy was effected either by adjusting the amplitude or shifting the phase. The efficiency of the transition was about the same in both cases. Fig. 11 shows oscillograms of the voltage from the signal electrodes and photomultiplier, together with the envelope of the hf voltage and the frequency-modulation program.

Measurement of the betatron-oscillation frequency by a hf method showed that the actual working point differed very little from the calculated value $\nu_r = 5{\cdot}82$; $\nu_z = 2{\cdot}40$).

In the phasotron condition, the electrons are accelerated to 10 MeV, which corresponds to the end of the region of the distributed windings. The intensity is about 2.10^9 electrons/pulse (10^{11} electrons/sec).

The following took part in the work associated with the starting of the accelerator: V. S. Voronin, D. D. Krasil'nikov, A. N. Lebedev, O. A. Smirnov, V. G. Gapanovich, N. V. Platonov, G. T. Ponomarev, V. A. Ryabov, N. A. Skalkina, E. F. Troyanov, G. I. Kharlamova, L. N. Chekanova, and also a number of technicians and mechanics, to whom the authors express their sincere thanks.

Members of various other organizations took part in developing the FIAN annular phasotron; among these special mention must be made of NIIÉFA colleagues N. A. Monoszon, B. V. Rozhdestvenskii, K. M. Kozlov, A. M. Stolov, V. A. Titov, V. B. Zalmanzon, and E. A. Dmitriev.

LITERATURE CITED

1. A. A. Kolomenskii et al., "Atomnaya Énergiya", 20, 513 (1966).
2. A. A. Kolomenskii, V. A. Petukhov, and M. S. Rabinovich, in "Some Questions in the Theory of Cyclic Accelerators" [in Russian], Moscow, Izd. AN SSSR, p.7 (1955); "Pribory i tekhnika éksperimenta", No.2, 26 (1956).
3. K. Symon, Phys. Rev., 98, 1152 (1955).
4. A. A. Kolomenskii, ZhÉTF, 33, 298 (1957).
5. T. Ohlawa, Rev. Scient. Instrum., 29, 108 (1958).
6. A. A. Kolomenskii, "Atomnaya Énergiya", 3, 492 (1957).
7. A. P. Fateev, ZhTF, 31, 238 (1961).
8. V. N. Kanunnikov and A. P. Fateev, ZhTF, 29, 1228 (1959).
9. V. N. Kanunnikov, Pribory i tekhnika éksperimenta, No.2, 136 (1960).
10. V. N. Kanunnikov et al., Proc. of the Intern. Conf. on High Energy Accelerators and Instrumentations, CERN, p.89 (1959).
11. V. N. Kanunnikov, ZhTF, 33, 592 (1963).
12. V. S. Voronin and V. N. Kanunnikov, Pribory i tekhnika éksperimenta, No.1, 143 (1966).
13. V. S. Voronin and V. N. Kanunnikov, Ibid., No.2, 160 (1965).
14. L. N. Kazanskii and V. N. Kanunnikov, Ibid., No.4, 217 (1965).

TRANSVERSE COHERENT INSTABILITY OF A CHARGED PARTICLE BUNCH

N. S. Dikanskii and A. N. Skrinskii

UDC 621.384.60

The instability condition of a bunch of charged particles (instability due to finite conductivity of the accelerator chamber walls) is derived.

The finite conductivity of vacuum chamber walls is responsible for a coherent transverse instability in a beam of particles rotating in the accelerator magnetic track. This phenomenon has been discussed [1, 2] with reference to a continuous beam. This article discusses the effect in a short bunch oscillating as a single entity. The treatment is also applied to a continuous beam.

The curvature of the beam trajectory, and wave effects, are neglected when we find electromagnetic fields in the interior of the vacuum chamber. We shall treat the chamber as a uniform toroid with highly conducting walls and with no additional elements in its interior, In such a case the electric field inside the chamber can be given by

$$E_\Sigma = E_b + E_{ic}, \tag{1}$$

where E_b is the beam free-space electric field, and E_{ic} is the electric field associated with charges induced on the conducting walls of the chamber.

For the magnetic field, similarly,

$$H_\Sigma = H_b + H_{ic}, \tag{2}$$

where H_b is the beam free-space magnetic field and H_{ic} is the magnetic field associated with current induced in the conducting walls of the chamber.

We assume for simplicity that the linear density (ρ) of beam particles varies slightly in azimuth at distances commensurate with the transverse dimensions of the chamber shortened γ times. Using the notation of Fig. 1, we can state this condition as $\rho \Big/ \frac{d\rho}{dy} \gg \frac{H}{\gamma}$ (it can be shown that this restriction is not essential to find the growth rate). Moreover, $\beta = \frac{v}{c} = 1$ (where this is possible).

The total fields are determined, in our approximation, at each azimuthal value of the local instantaneous particle beam density, when the walls are ideally conducting, and the fields vanish as the beam is removed. If the wall conductivity σ is not infinite, then E_b and H_b continue to "track" the instantaneous beam density. But the transverse components of E_{ic} vanish rapidly as the beam departs (in a time on the order of the charge relaxation time), while the magnetic field associated with the induced currents flowing in a layer of finite thickness still persist for quite a while in the chamber interior. The coherent transverse instability is in fact related to the slow pace at which this residual field disappears.

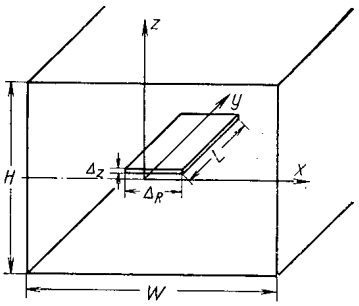

Fig. 1. Geometry of beam and accelerator chamber.

We now find the magnetic field remaining inside a tube after a single pass (parallel to the tube axis) of a short bunch (with geometry and notation as in Fig. 1). First consider a subsidiary problem (with the provisional assumption Δ_R, $\Delta_z \ll H \ll W$). The field due to "wall" currents of a beam uniform along the length of a tube with linear charge density $e\rho$ with ideally conducting chamber walls, can be found by summing over the reflection fields. The x-component of the field is approximately

Translated from Atomnaya Énergiya, Vol. 21, No. 3, pp. 176-179, September, 1966. Original article submitted October 22, 1965; revised May 23, 1966.

$$H_{ic}^{\sigma=\infty} \approx \frac{4e\rho}{H^2}(z+2z_b), \tag{3}$$

where z is the coordinate of the observation point; z_b is the coordinate of the beam center; $z, z_b \ll H$. The same holds for H_{ic} in the first few moments after a beam of the same density appears, again with finite wall conductivity. But in this case H_{ic} will decrease with time because the magnetic field gradually diffuses to the walls. In a time t the field penetrates to a depth $\delta \approx \left(\frac{c^2}{4\pi\sigma} t\right)^{1/2}$ into each of the walls so that the distance between the walls is increased by the order of magnetic $2\frac{\delta}{2} = \delta$. At that point, consequently,

$$H_{ic}(t) \approx H_{ic}^{\sigma=\infty} + \frac{dH_{ic}^{\sigma=\infty}}{dH}\delta \approx H_{ic}^{\sigma=\infty} - \frac{4ec\rho}{H^3\sqrt{\pi\sigma}}(z+2z_b)\sqrt{t}. \tag{4}$$

This makes it immediately clear that, following the passage of a particle bunch of finite duration τ, which can be presented as two density steps of opposed polarity shifted τ in time, there remains a field

$$\Delta H_\sigma(t) \approx -\frac{4ec\rho}{\sqrt{\pi}H^3\sqrt{\sigma}}(z+2z_b)\left(\sqrt{t}-\sqrt{t-\tau}\right) \tag{5}$$

(this time is counted from the instant the bunch begins to form).

When $t \gg \tau$, this formula becomes

$$\Delta H_\sigma(t) \approx -\frac{2c}{\sqrt{\pi}H^3\sqrt{\sigma}}(e\rho\tau)(z+2z_b)\,t^{-1/2}. \tag{6}$$

It is important that the residual field of the bunch be determined by the total charge $e\rho\tau c$ and that it is independent of the bunch duration. Here the slow rate of decay of the residual field, as well as its sign (opposite to the sign of the reflection field) becomes conspicuous.

Accurate calculations involving a Fourier expansion of a widely spaced periodic sequence of the bunches using Leontovich boundary conditions yields a similar expression for ΔH_σ:

$$\Delta H_\sigma(t) = -\frac{\pi ec}{3H^3\sqrt{\sigma}}\cdot\frac{\rho\tau\,(z+2z_b)}{\sqrt{t}}\,\Phi, \tag{7}$$

where

$$\Phi = \Phi\left(\frac{\Delta_z}{H}, \frac{\Delta_R}{W}, \frac{H}{W}\right) = 1$$

when

$$\left(\frac{\Delta_z}{H}, \frac{\Delta_R}{W}, \frac{H}{W}\right) \ll 1.$$

The field remaining after the passage of a beam with arbitrary $\rho(t)$ and $z_b(t)$ can be stated in the same approximation, as usual, in the form of superposed fields left over from short bunches into which any beam can be broken down, i.e., in the form of the integral

$$\Delta H_\sigma(t) = \frac{\pi ec}{3H^3\sqrt{\sigma}}\int_{t_0}^{t}\frac{\rho(\tau)\,[z+2z_b(\tau)]}{\sqrt{t-\tau}}\,d\tau, \tag{8}$$

where t_0 is the effective time of onset of the process.

Note that the integrals diverge, in the general case, in the limit $t_0 \to -\infty$, because the Leontovich conditions are not satisfied at very low frequencies; in other words, the skin layer thickness is commensurate with the wall thickness and with other characteristic dimensions.

The equation of particle betatron oscillations, taking account of the magnetic field left at each azimuth by particles which have passed by up to time t can be stated as

$$\ddot{z}(t) + \omega^2 z(t) = \frac{A}{2}z(t)\int_{t_0}^{t}\frac{\rho(\tau)}{\sqrt{t-\tau}}\,d\tau + A\int_{t_0}^{t}\frac{z_b(\tau)\,\rho(\tau)}{\sqrt{t-\tau}}\,d\tau, \tag{9}$$

where

$$A = \frac{2\pi e^2 c}{3\gamma m H^3\sqrt{\tau}}\,\Phi.$$

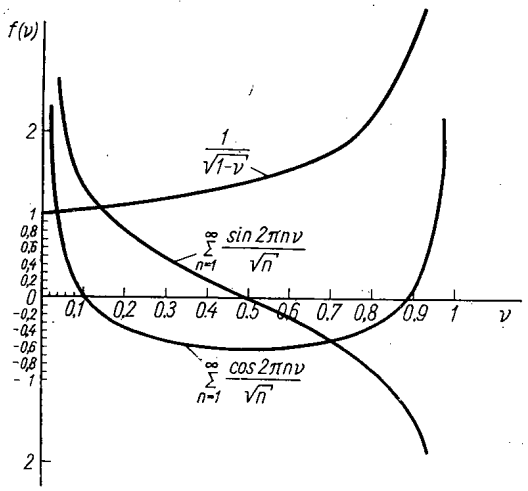

Fig. 2.

The first term in the right-hand member is not due to oscillations of the beam center, and is equivalent to some stationary steady-state distortion of the principal magnetic field; this term is therefore discarded.

We now analyze the stability of betatron oscillations by treating the right-hand member as a small perturbation, and assuming the oscillations to be symmetric about the chamber axis. This allows the approximation that $z_b(\tau)$ constitutes steady-state beam oscillations, so that the integral converges in the limit t_0 and the equation of the oscillation acquires the form

$$\ddot{z}(t)+\omega^2 z(t)=A\int_{-\infty}^{t}\frac{z_b(\tau)\rho(\tau)\,d\tau}{\sqrt{t-\tau}}=A\int_{0}^{\infty}\frac{z_b(t-\tau)\rho(t-\tau)}{\sqrt{\tau}}\,d\tau. \qquad (10)$$

Now consider the case of a single short bunch oscillating as a single entity. The equation of the bunch particle oscillations is, in the approximation we are using,

$$\ddot{z}(t)+\omega^2 z(t)=\frac{AN}{c}\sum_{n=1}^{\infty}\frac{z(t-nT)}{\sqrt{n\bar{T}}}\,, \qquad (11)$$

where T is the period of revolution. The right-hand side of the equation is the force exerted by the magnetic field left over from preceding passes of the bunch on the particle at each azimuth.

In the first approximation by the method of averaging, we find the instability growth rate for a short bunch

$$\delta=\left\{\frac{da}{dt}\Big/\alpha\right\}=-\frac{\pi r_e RcN\Phi}{3H^3\sqrt{T\sigma\gamma\nu}}\sum_{n=1}^{\infty}\frac{\sin 2\pi n\nu}{\sqrt{n}}\,, \qquad (12)$$

where R is the average radius of the orbit, N is the number of particles belonging to the bunch, r_e is the classical radius of the electron, ν is the dimensionless frequency of the oscillations. $\sum_{n=1}^{\infty}\frac{\sin 2\pi n\nu}{\sqrt{n}}$ is plotted as a function of ν in Fig. 2. The growth rate is positive (instability case) when $k-1/2<\nu<k$, and negative when $k<\nu<k+1/2$, where $k=0, 1, 2, \ldots$, because of the periodicity and asymmetry of each term in the series.

The instability will occur in a "one-frequency" system at $\delta > 1/\tau_0$, where τ_0 is the decay time of the oscillations (e.g., the radiation decay time).

By using Eq. (10), we can find the growth rate for a beam continuous in azimuth:

$$\delta=\pm\frac{\pi r_e RcN\Phi}{3H^3\sqrt{T\sigma\gamma\nu}}\cdot\frac{1}{\sqrt{m\mp\nu}} \qquad (13)$$

(m is the mode number, as in the formula derived in [1]).

We shall now consider the possible stabilization of an instability by Landau damping in reference to a single short bunch. This damping will not occur under the condition

$$\left|\frac{\Delta\omega}{\omega_k-\bar{\omega}}\right|\ll 1,$$

where $\bar{\omega}$ is the average frequency of bunch particle oscillations in the absence of coherent oscillations; ω_k is the frequency of coherent bunch oscillations; $\Delta\omega$ is the rms spread of particle oscillation frequencies.

Stabilization is possible when the opposite condition prevails (as is usually the case).

The spread of particle betatron oscillation frequencies is due to nonlinearity of the effective focusing

field for a finite beam phase volume, with the main contributions to the spread being made by:

1) nonlinearity of the external guide field;

2) the presence of ions in the electron beam (this contribution is proportional to $\alpha N/\gamma$, where α is the compensation factor);

3) the transverse electromagnetic self-field of the bunch (this contribution is proportional to BN/γ^3, where B is the bunching coefficient).

The contribution of individual particles to the shift of coherent bunch oscillations about the average frequency of oscillations is made by:

1) the electromagnetic self-field of the bunch (this affects only $\bar{\omega}$, with the contribution proportional to BN/γ^3);

2) the electromagnetic image field (this affects ω_k mostly, and the contribution is proportional to BN/γ^3);

3) the residual magnetic field due to the finite conductivity of the chamber walls (affects ω_k mainly, and the contribution is proportional to N/γ ($\sigma^{1/2}$ and is independent of B).

The electric field of the ions affects $\bar{\omega}$ and ω_k identically in the case of an electron beam, and makes no contribution to the frequency shift.

The total shift, for a bunch with a round transverse section of radius of r_0 and of uniform density, can be stated as:

$$\omega_k - \bar{\omega} \approx \frac{r_e RcN}{\nu\gamma^3 r_0^2 L} - \frac{r_e RcN}{\nu\gamma^3 \left(\frac{H}{2}\right)^2 L} - \frac{\pi}{3} \times \frac{r_e RcN\Phi}{\nu\gamma H^3 \sqrt{T\sigma}} \sum_{n=1}^{\infty} \frac{\cos 2\pi n\nu}{\sqrt{n}},$$

where L is the bunch length. $\sum_{n=1}^{\infty} \frac{\cos 2\pi n\nu}{\sqrt{n}}$ is plotted as a function of ν in Fig. 2.

Note in summary that a long bunch is apparently unstable only to excitation of coherent bunch oscillations as a whole (with all bunch particles on the same trajectory) when its particles execute synchrotron phase motion at frequency $\Omega \gg \delta$. In that case the short-bunch calculations above will apply.

The authors are indebted to B. V. Chirikov, M. M. Karliner, and B. Gittel'man for their highly valued comments, and to V. L. Auslender for his interest in the progress of the work.

LITERATURE CITED

1. L. Laslett, V. Neil, and A. Sessler, Rev. Scient. Instrum., 36, 436 (1965).
2. V. I. Balvekov and A. A. Kolomenskii, Atomnaya Énergiya, 19, 126 (1965).

A CRITERION FOR THE EFFICIENCY OF UTILIZATION OF NUCLEAR FUEL

V. V. Batov and Yu. I. Koryakin

UDC 338.409.4:621.039

Practical experience in the design and operation of power reactors raises a number of problems concerned with maximizing the efficiency of utilization of the nuclear fuel in the reactor. The present article develops and defines a criterion for this efficiency.

The complicated interrelationship among nuclear physics, thermal, economic, and other factors affecting the efficiency of utilization of fuel, necessitates the establishment of a criterion for measuring it. This criterion should be fairly general: it must take account of all the efficiency factors involved in various reactors and fuel cycles and must at the same time give an unambiguous definition of efficiency.

The present article is an attempt to determine this criterion in a form suitable for practical use and to investigate the conditions under which it is applicable.

Let us consider a single-zone thermal reactor with a uniform initial fuel charge, operating without partial recharging (the entire active zone is recharged at one time when the fuel reaches its average burn-up fraction). The fuel cycle of such a reactor may be either open (with the fuel discarded after burn-up) or closed (with regeneration of the fuel). Let us apply the general criterion for the efficiency of the utilization of productive capital [1] to nuclear power engineering and consider separately the part relating to nuclear fuel:

$$E_t = C_t + pK_t, \tag{1}$$

where C_t and K_t are, respectively, the annual expenditures and the productive capital of the nuclear power station which go for nuclear fuel; p is a normalization coefficient designed to take account of the efficiency of the productive capital.

There are two ways of defining the normal expenditures. In the first case in accordance with [2], when we define the components of the expenditures on the basis of selling price, we do not include associated capital investments* in calculating the total capital investment, and consequently

$$K_t = K_c, \tag{2}$$

where K_c is the amount of circulating assets accounted for by the necessary supplies of nuclear fuel, semifinished products, and other items used for operation, calculated on the basis of selling prices. In the second case, the components of the expenditures are determined on the basis of the prime cost of the consumed output, and the productive capital must also include the associated capital investment K_a, i.e.,

$$K_t = K_c + K_a. \tag{3}$$

Let us consider the first case. We introduce the following notation: $\tilde{C}(t) = \tilde{C}_i(t)$ is the sale price of the nuclear fuel as it moves through the fuel cycle; i is the number of the step in the fuel cycle; $T_i = t_i - t_{i-1}$ is the time for processing a batch of nuclear fuel (with an output corresponding to 1 kg of uranium with initial enrichment) in the i-th step, in years. By processing we mean any operation performed on the nuclear fuel which causes a change in its value (e.g., preparation of fuel elements, irradiation of fuel in the reactor, storage of depleted nuclear fuel, regeneration, etc.); Q is the thermal power of the reactor; N is the electrical power of the reactor; η is the reactor efficiency; G is the charge inventory of the reactor; t_s is the start of the run; T_r is the duration of the reactor run; B is the average burn-up reaction of the nuclear fuel; φ is the coefficient of utilization of the rated power of the nuclear power station.

* Capital investments for fuel extraction and processing (including transportation) by the fuel-cycle enterprise serving the nuclear power station.

Translated from Atomnaya Énergiya, Vol. 21, No. 3, pp. 179-184, September, 1966. Original article submitted April 26, 1966.

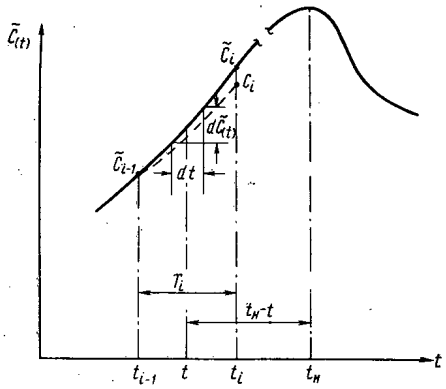

Fig. 1. Value of nuclear fuel as a function of time as it moves through the fuel cycle: $\tilde{C}_i-\tilde{C}_{i-1}$ is the cost of processing the nuclear fuel in the i-th step of the fuel cycle, in rubles/kg of uranium of initial enrichment; $d\tilde{C}(t)$ is the change in price of the output of the fuel cycle over a time interval dt, in rubles/kg of uranium of initial enrichment; t_s-t is the time during which the value is "frozen" at $\frac{1}{2}d\tilde{C}(t)$.

The amount of circulating assets for the fuel cycle is determined, according to the procedures described in [1, 2], on the basis of their turnover, the change in the value of the fuel during the processing in each step of the cycle, and is calculated for the time at which the use of the fuel in the reactor begins.

Figure 1 shows the change in the nuclear-fuel value as it moves through the fuel cycle. If the cycle begins with the extraction of the uranium ore, then the $\tilde{C}(t)$ curve starts at the origin. The value of the nuclear fuel is increased by the past or present work done on it during the processing, and is decreased by the generation of electrical energy.

The circulating assets for the fuel cycle consist of two parts: fuel costs and processing costs.

Let us designate the first part of the circulating assets (those included in the cost of the nuclear fuel at the beginning of the i-th step and remaining unchanged throughout the processing time T_i) by K_{1i} and the second part of the circulating assets (included in the cost of processing the nuclear fuel) by K_{2i}. Then

$$K_c = \sum_i (K_{1i} + K_{2i}) = K_{1c} + K_{2c}. \quad (4)$$

The amount of circulating assets included in the value of the nuclear fuel at the beginning of each step of the cycle and calculated for the time when this fuel begins to be used in the reactor may be written in the form

$$K_{1c} = \frac{G\varphi}{T_r} \sum_i \tilde{C}_{i-1} T_i (1+p)^{t_s - t_i} \quad (5)$$

$$(i = 1, 2, \ldots; \tilde{C}_0 = 0).$$

Let us consider the second part of the circulating assets (processing).

It follows from Fig. 1 that an increase in the value of the nuclear fuel by an amount of $d\tilde{C}(t)$ during a time interval dt causes an increase in the converted value of the nuclear fuel at time t_i:

$$dK_{2i}(t) = k_{n_i} \frac{G\varphi}{T_r} T_i d\tilde{C}(t) (1+p)^{t_i - t}, \quad (6)$$

where $k_{n_i} = \frac{1}{n_i+1}$ $(n_i \geqslant 0)$; n_i is the exponent in the case when the function $\tilde{C}_i = \tilde{C}_i(t)$ is represented as a power of t. In the case when $n_i = 1$ (a linear function), $k_1 = 1/2$, and

$$dK_{2i}(t) = \frac{1}{2} \cdot \frac{G\varphi}{T_r} T_i d\tilde{C}(t) (1+p)^{t_i - t}. \quad (7)$$

We assume that within each step the function $\tilde{C}_i = \tilde{C}_i(t)$ is linear (this is an acceptable approximation, since the intervals T_i are small in comparison with a calendar year and the industrial processes take place at uniform rates); then

$$\tilde{C}_i(t) = \tilde{C}_{i-1} + \frac{\tilde{C}_i - \tilde{C}_{i-1}}{T_i} (t - t_i), \quad (8)$$

and hence

$$\frac{d\tilde{C}_i(t)}{dt} = \frac{\tilde{C}_i - \tilde{C}_{i-1}}{T_i}. \quad (9)$$

Since

$$K_{2i} = \int_{t_{i-1}}^{t_i} dK_{2i}(t), \quad (10)$$

we can use (9) and substitute (7) into Eq. (10) and integrate to obtain

$$K_{2i} = \frac{1}{2} \cdot \frac{G\varphi}{T_r} (\tilde{C}_i - \tilde{C}_{i-1}) \frac{[(1+p)^{T_i} - 1]}{\ln (1+p)}. \quad (11)$$

It should be noted that if income is received in discrete payments (at the end of each year), formula (11) is changed slightly:

$$K_{2i} = \frac{1}{2} \cdot \frac{G\varphi}{T_r} (C_i - C_{i-1}) \frac{[(1+p)^{T_i} - 1]}{p}. \quad (11')$$

The value of the circulating assets for the fuel cycle that are included in the cost of processing the nuclear fuel in each step, recomputed for the time when this fuel begins to be used in the reactor, is one of the form

$$K_{2c} = \sum_i K_{2i} (1+p)^{t_s - t_i} \quad (12)$$

or using Eq. (11),

$$K_{2c} = \frac{1}{2} \cdot \frac{G\varphi}{T_r} \sum_i (C_i - C_{i-1}) \times \frac{[(1+p)^{T_i} - 1]}{\ln (1+p)} (1+p)^{t_s - t_i} \quad (13)$$

If we substitute (5) and (13) into Eq. (4), we obtain the total amount of circulating assets for the fuel cycle, recomputed for the time when the nuclear fuel begins to be used in the reactor:

$$K_c = \frac{G\varphi}{T_r} \sum_i \left\{ \tilde{C}_{i-1} T_i + \frac{1}{2} (\tilde{C}_i - \tilde{C}_{i-1}) \frac{[(1+p)^{T_i} - 1]}{\ln (1+p)} \right\} (1+p)^{t_s - t_i}. \quad (14)$$

Noting that the cost of nuclear fuel consumed per year is

$$C_t = \frac{G\varphi}{T_r} \sum_i (\tilde{C}_i - \tilde{C}_{i-1}) \quad (15)$$

and substituting (14) and (15) into Eq. (1), we obtain an equation giving a criterion for the efficiency of utilization of nuclear fuel for a single-zone thermal reactor with a uniform initial fuel charge:

$$\tilde{E}_t = \frac{G\varphi}{T_r} \sum_i \left\{ (\tilde{C}_i - \tilde{C}_{i-1}) + p \left[\tilde{C}_{i-1} T_i + \frac{1}{2} (C_i - C_{i-1}) \frac{[(1+p)^{T_i} - 1]}{\ln (1+p)} \right] (1+p)^{t_s - t_i} \right\} \text{ rubles/year}. \quad (16)$$

Noting that

$$\bar{B} = 365 \frac{QT}{G},$$

we find

$$e_t = \frac{100}{24} \cdot \frac{1}{\bar{B}\eta} \sum_i \left\{ (C_i - C_{i-1}) + p \left[\tilde{C}_{i-1} T_i + \frac{1}{2} \times (C_i - C_{i-1}) \frac{[(1+p)^{T_i} - 1]}{\ln (1+p)} \right] \times (1+p)^{t_s - t_i} \right\} \text{ kopeks/kW·h} \quad (17)$$

The first term on the right side of Eq. (17) is the fuel component of the value of the reactor-generated electrical energy when the expenditure components are determined on the basis of selling prices:

$$\tilde{c}_t = \frac{100}{24} \cdot \frac{\sum_i (C_i - C_{i-1})}{\bar{B}\eta} = \sum_i c_{fi}, \quad (18)$$

where C_{fi} is that part of the value of the electrical energy which is due to the expenses of the i-th step of the fuel cycle or to the processing of the nuclear fuel in this step.

Equations (16) and (17) are obtained on the assumption that the income connected with the movement of the nuclear fuel through the fuel cycle is received continuously. It is easily shown that if the increment is received in discrete installments (at the end of each year), Eqs. (16) and (17) change only slightly: the quantity $\ln (1+p)$ is the second term on the right side of Eqs. (16) and (17) is replaced by p.

If we consider that

$$(1+p)^{t_s - t_i} \approx 1 + p(t_s - t_i);$$
$$(1+p)^{T_i} \approx 1 + pT_i;$$
$$\ln (1+p) \approx p,$$

we obtain an approximate expression for the criterion measuring the efficiency of utilization of the nuclear fuel:

$$\tilde{e}_t = \frac{100}{24}\frac{1}{\bar{B}\eta}\sum_i \left\{(\tilde{C}_i - \tilde{C}_{i-1}) + \frac{1}{2}pT_i \times (C_i + C_{i-1})[1 + p(t - t_i)]\right\} \quad (19)$$

Formulas (16) and (17) are the equations for the criterion of the efficiency of utilization of nuclear fuel for a single-zone thermal reactor with a uniform initial charge in the case when the expenditure components on the basis of selling price are calculated in a linear approximation given by the function $\tilde{C}_i = \tilde{C}_i(t)$ and on the assumption that the income connected with the value of the nuclear fuel is received continuously.

The approximate formula for the criterion of the efficiency of utilization of nuclear fuel (19), was obtained from formula (17) by substituting simple interest for compound interest and discrete income for continuous income. The approximate formula (19) is suitable for practical use: it is simpler than formula (17) and at the same time gives a satisfactory accuracy for the calculations.

Let us consider the second case, when the annual income is calculated on the basis of cost, i.e., taking associated capital investment into account.

The annual expenses for the nuclear fuel are defined by the expression (see Fig. 1)

$$C_t = \frac{G\varphi}{T_r}\sum_i (C_i - \tilde{C}_{i-1}), \quad (20)$$

and the fuel component of the value of the electrical energy produced by the nuclear reactor is

$$c_t = \frac{100}{24}\cdot\frac{1}{\bar{B}\eta}\sum_i (C_i - \tilde{C}_{i-1}) = \sum_i c_{t\,i}. \quad (21)$$

As in the preceding case, the amount of the circulating assets is determined from the formula

$$K_c = \frac{G\varphi}{T_r}\sum_i \left\{C_{i-1}T_i + \frac{1}{2}(C_i - C_{i-1})\frac{[(1+p)^{T_i} - 1]}{\ln(1+p)}\right\}(1+p)^{t_s - t_i}. \quad (22)$$

Let us assume that all the enterprises in the fuel cycle have already been built and are operating normally; then the associated capital investment may be defined by the expression

$$K_a = \frac{G\varphi}{T}\sum_i k_{sp.a.i}, \quad (23)$$

where $k_{sp.a.i.}$ represents the specific associated capital investment in the i-th enterprise in the fuel cycle, in rubles·year/kg of uranium.

Substituting (20), (22), and (23) into Eq. (21), we find

$$E_t = \frac{G\varphi}{T_r}\sum_i \left\{(C_i - \tilde{C}_{i-1}) + p(1+p)^{t_s - t_i} \times \left[C_{i-1}T_i + \frac{1}{2}\cdot\frac{[(1+p)^{T_i} - 1]}{\ln(1+p)}(C_i - \tilde{C}_{i-1})\right] + pk_{sp.a.i}T_i\right\} \text{ rubles/year}, \quad (24)$$

and hence

$$e_t = \frac{100}{24}\cdot\frac{1}{\bar{B}\eta}\sum_i \left\{(C_i - \tilde{C}_{i-1}) + p(1+p)^{t - t_i} \times \left[C_{i-1}T_i + \frac{1}{2}\cdot\frac{[(1+p)^{T_i} - 1]}{\ln(1+p)}(C_i - \tilde{C}_{i-1})\right] + pk_{s.a.i}T_i\right\} \text{ kopeks/kW·h}. \quad (25)$$

By comparing formulas (17) and (25), obtained by two different methods for the criterion of the efficiency of utilization of nuclear fuel, we can see that they will be identical provided that

$$\sum_i \left\{(\tilde{C}_i - C_i) + p(1+p)^{t_s - t_i}\left[(\tilde{C}_{i-1} - C_{i-1}) \times T_i + \frac{1}{2}(\tilde{C}_i - C_i)\frac{[(1+p)^{T_i} - 1]}{\ln(1+p)}\right]\right\} = p\sum_i k_{sp.a.i}T_i, \quad (26)$$

which states that the additional products calculated on the basis of the difference between selling price and cost of the fuel-cycle output in the first case are equal to the additional products calculated on the basis of associated capital investment in the second case. In practice it must be taken into consideration that selling prices do not always reflect the cost of labor which is essential to society (the cost to the national economy), and therefore the more easily obtainable definition of the fuel component of the calculated expenses according to formula (17) should be checked by finding the fuel components of the calculated expenses according to formula (25).

If the cost of labor essential to the society is correctly reflected by the selling prices, Eq. (26) will hold and formulas (17) and (25), which define the two criteria for the efficiency of utilization of nuclear fuel, will become identical.

Let us consider a multi-zone reactor. This may be a thermal reactor with one or more fission zones, a fast reactor with an active zone and blankets, or a thermal reactor with a non-uniform initial fuel charge. Strictly speaking, even if the initial loading of a reactor is uniform, it will become non-uniform soon after the start of operation, because the fuel burn-up in the active zone is not uniform.

Let ρ_j denote the fraction of reactor power represented by the j-th zone:

$$\rho_j = \frac{Q_j}{Q} \quad \left(\sum_j \rho_j = 1\right)$$

and let $\bar{B}_j$ represent the burn-up fraction of the j-th zone (this also means an average burn-up fraction, but averaged over the smaller amount of fuel; in the limiting case, this is averaged over each channel or even part of a channel):

$$\bar{B}_j = \frac{365 \cdot Q_j T_{kj}}{G_j}.$$

Let us consider each j-th zone as a single-zone reactor for which all the foregoing equations hold; we then obtain the equation for the fuel component of the value and the fuel component of the calculated expenses for a multi-zone reactor for the case in which the expenses are calculated on the basis of a selling price:

$$\tilde{c}_t = \frac{100}{24} \cdot \frac{1}{\eta} \sum_i \sum_j \frac{\rho_j}{\bar{B}_j} (\tilde{C}_{i,j} - \tilde{C}_{i-1,j}); \tag{27}$$

$$\tilde{e}_t = \frac{100}{24} \cdot \frac{1}{\eta} \sum_i \sum_j \frac{\rho_j}{\bar{B}_j} \left\{ (\tilde{C}_{ij} - \tilde{C}_{i-1,j}) + p(1+p)^{t_{j-t_{ij}}} \left[\tilde{C}_{i-1,j} T_{ij} + \frac{1}{2} (\tilde{C}_{ij} - \tilde{C}_{i-1,j}) \frac{[(1+p)^{T_{ij}} - 1]}{\ln(1+p)} \right] \right\}. \tag{28}$$

If in formula (28) we replace the compound interest by simple interest and the continuous income by discrete income, we obtain an approximate formula for the criterion of the efficiency of utilization of nuclear fuel for a multizone reactor:

$$\tilde{e}_t = \frac{100}{24} \cdot \frac{1}{\eta} \sum_i \sum_j \frac{\rho_j}{\bar{B}_j} \left\{ (\tilde{C}_{ij} - \tilde{C}_{i-1,j}) + \frac{1}{2} pT_{ij} (\tilde{C}_{i,j} + \tilde{C}_{i-1,j}) [1 + p(t_{s\,j} - t_{ij})] \right\}. \tag{29}$$

Similarly, we can obtain the equations for C_t and E_t for the case in which the expenses are determined on the basis of cost; we shall not show this in the present article. When we derived formulas (27) and (28), we assumed that the power of the j-th zone was constant only for time intervals of length ΔT_k between two successive variants of a j-zone reactor. For example, in the case of a reactor which is recharged in steady-state operation, ΔT_k represents the time between two successive partial rechargings (Fig.2). In other words, formulas (27) and (28) determine the amounts of the fuel component of the value and the fuel component of the calculated expenses for electrical energy only within each of these time intervals ΔT_k. The average values $\tilde{\bar{C}}_t$ and $\tilde{\bar{e}}$ for individual periods can be obtained by ordinary averaging. Thus, in the case when the reactor is recharged in steady-state operation we have

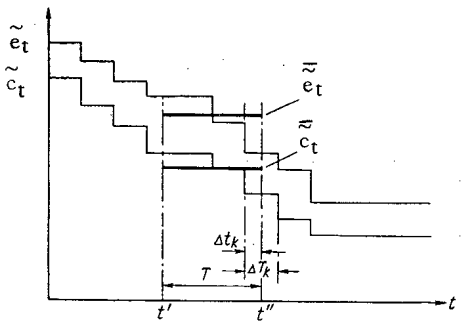

Fig. 2. Fuel component of value and fuel component of calculated expenses for electrical energy for a reactor recharged in operation.

$$\tilde{\bar{c}} = \frac{\sum_k \tilde{c}_{t\,k} \Delta t_k}{T};$$

$$\tilde{\bar{e}} = \frac{\sum_k \tilde{e}_{t\,k} \Delta t_k}{T},$$

where ΔT_k is the time between the k-th and (k+1)-st partial rechargings; T is the period of time under consideration ($T = t'' - t'$); Δt_k is the part of the interval ΔT_k which lies in the time interval T.

As can be seen from Fig. 2, when we recharge the reactor in steady-state operation, we reduce the fuel

component of the value and the fuel component of the calculated expenses from some initial value to an equilibrium value which corresponds to steady-state partial recharging of the reactor.

In conclusion, the authors express their gratitude to V. B. Lytkin for his valuable comments on the article.

LITERATURE CITED

1. Typical Procedure for Determining the Economic Efficiency of Capital Investment and New Technological Processes in the National Economy of the USSR [in Russian]. Moscow, Gosplanizdat (1960).
2. Fundamental Procedure for Technical and Economic Calculations in Power Engineering [in Russian]. Moscow, Gostekhizdat (1959).

ACTIVATION OF CORROSION PRODUCTS IN NUCLEAR REACTORS

A. P. Veselkin and A. V. Nikitin

UDC 621.039.56

Questions of the mass transfer and activation of corrosion products in nuclear reactors incorporating water under pressure and in boiling reactors are considered. The state of the problem is outlined and the difficulty of solution indicated. A mathematical formulation of the problem and a solution of the mass-transfer equations for the stationary case are presented, together with an approximate solution of the nonstationary problem for the accumulation of Co^{60}. Existing experimental data are analyzed on the basis of the solutions and mass-transfer coefficients averaged over several reactor systems are obtained for the deposition ($\omega = 3.5 \cdot 10^{-5}$ sec^{-1}) and erosion ($\gamma = 5.10^{-8}$ sec^{-1}) of particles.

Information on the extent of radioactive contamination in active reactors [1-7] and recommendations on methods of calculating this [6-10] exist in the literature. For boiling reactors, however, no such recommendations have been made.

It was shown in [10] that the mathematical complication of the problem does not lead to any great increase in the accuracy of the solution, owing to inadequate knowledge of the mass-transfer coefficients. In addition to this, some limitations imposed in earlier papers are not very well-founded. Thus in some papers not all the sources of radioactivity in the system were taken into account, while in others the deposition of radioactive nuclei in the active zone was neglected.

In this paper we shall endeavor to find a solution valid for boiling reactors and satisfying the demands of accuracy, simplicity, and physical clarity. We considered the following mechanism for the mass-transfer of impurities in the reactor. Nonradioactive target nuclei appear in the circulation system as a result of the corrosion of the structural material in the circuit. An oxide film forms on the surface of the metal and emission of metal ions into the water takes place [11, 12]. The outer layer of the oxide film is formed under the influence of the deposition of particles from the flow of water and as a result of the erosion of the surface. The increase in the inner oxide film (subsequently called the base film) is a diffusion-controlled process, and the rate of film growth falls with time. The thickness of the outer film (subsequently called the superficial film) is stabilized under the influence of the competing processes and remains constant. For a stainless-steel surface the typical thickness of the superficial film is 1 to 10 μ [6, 8, 10].

Despite the presence of an ion exchanger, the concentration of metal molecules and ions in the water increases with time and may reach saturation as regards solubility, whereupon a solid phase, particles of various sizes, will begin to separate out of solution. On circulating through the system, these particles, together with erosion products, will settle on the surface. In zones with maximum variation in the velocity and density of the heat carrier (the so-called particle traps), selective deposition of particles may take place.

In boiling reactors two extra sources of impurities appear: corrosion of the structural materials in the vapor and condensation parts of the system and in leakage in the condenser. The mechanism underlying the carrying away of the reactor-water impurities with the vapor is the same as in boiler systems using organic fuel, and is due to two processes: dissolution of the impurities in the vapor and removal of the impurities with the moisture [13, 14]. The first process is only important in systems with pressures above 40 to 100 absolute atm (depending on the element) [15]. In a turbine, owing to the sharp fall in vapor pressure and solubility, impurities may be deposited on the walls. A proportion of the impurities (over and above those soluble in the exhaust vapor) may fall immediately into the condenser, since the depostion process takes place at a finite velocity, and the time for the vapor to pass through the turbine is short. The formation of the superficial film in the turbine is also affected by processes of erosion and washing with moist vapor.

Translated from Atomnaya Énergiya, Vol. 21, No. 3, pp. 184-189, September, 1966. Original article submitted December 27, 1965 and in final form April 20, 1966.

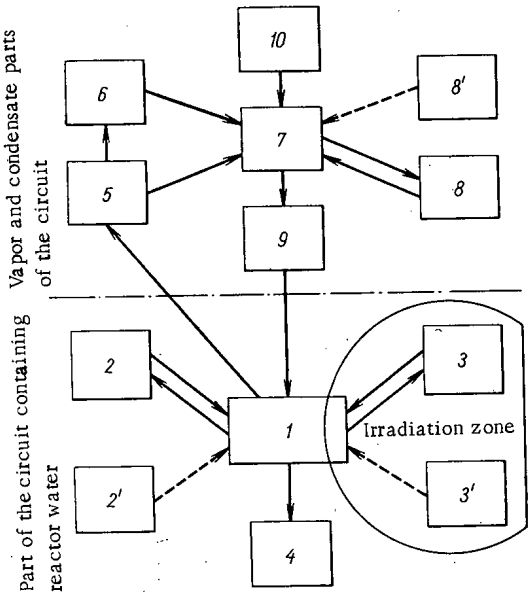

Diagram for the mass transfer of corrosion products in a boiling nuclear reactor; 1) Impurities in the reactor water; 2) film on nonirradiated reactor surfaces; 2') construction materials outside the irradiation zone; 3) film in the active zone of the reactor; 3') construction material in the active zone of the reactor; 4) filter for purifying the reactor water; 5) impurities in the vapor; 6) film in the turbine; 7) impurities in the condensate; 8) film on surface wetted by the condensate; 8') construction material in the vapor and condensate parts of the circuit; 9) filter for purifying the supply water; 10) inleakage of impurities in the condenser; - - - - - diffusion of ions; ——— mass transfer of particles.

The activation of the corrosion products takes place in three ways: a) activation of the structural material in the active zone of the reactor with subsequent emission into the water; b) activation of the impurities in the reactor water on passing through the active zone of the reactor; c) activation of the film of corrosion products in the active zone of the reactor.

Apart from the mass-transfer processes just described, radioactive decay must be considered for radioactive nuclei. The burn-up of nuclei in the neutron flux and mass transfer associated with the kinetic energy of recoil nuclei are not very important [10].

For some reactor systems [1, 10] mass transfer by means of molecular and ionic diffusion plays a secondary part, except for the emission of "fresh" corrosion products into the water. This is indicated, first by the similarity between the chemical composition of the superficial film and the impurities in the water [1], and secondly by the fact that the chemical composition of the water impurities and the superficial film differs from that of the constructional material [1].

Thus the role of the basis oxide film in the radioactive contamination of the system is subordinate, and may eliminate it from consideration. For the same reason we may refrain from separating out the dissolved component of impurities in the heat carrier.

These points seriously limit the generality of the solution and partly explain the pessimism of some workers and their attachment to empirical methods. The next problem in the study of mass transfer and activation of corrosion products is the generalization and systematization of experience in the use of power reactors and the carrying out of special experiments in order to select the correct model (or models) and determine the mass-transfer coefficients.

Mass-Transfer Equations

In accordance with the mass-transfer diagram (see Fig), the equations for the total amount of the i-th element accumulating in each of the media have the following form (indices 1, 2, etc. in the equations correspond to the enumeration of the media in the Fig): for the target nuclei

$$\left.\begin{aligned} &\frac{dN_1}{dt} = -(\lambda_0+\omega)N_1+\gamma(N_2+N_3)+Q_1;\\ &\frac{dN_2}{dt} = \omega\frac{S_2}{S_1}N_1-\gamma N_2;\quad \frac{dN_3}{dt} = \omega\frac{S_3}{S_1}N_1-\gamma N_3, \end{aligned}\right\} \tag{1}$$

where

$$\left.\begin{aligned} &Q_1 = Q_2+Q_3+(1-\varepsilon_9)(Q_8+Q_{10});\\ &Q_2 = \sum_m C_2^m S_2^m f_s^m;\\ &Q_3 = \sum_m C_3^m S_3^m f_s^m;\\ &Q_8 = \sum_m C_8^m S_8^m f_s^m; \end{aligned}\right\} \quad \left.\begin{aligned} &\lambda_0 = \frac{\varepsilon_4 G_4 + kG_5}{V_1};\\ &S_l = \sum_m S_l^m; \end{aligned}\right\} \tag{2}$$

for total activities

$$\left.\begin{aligned}
&\frac{dA_1}{dt} = -(\lambda_0+\omega+\lambda)A_1+\gamma A_2+\gamma A_3+\lambda\sigma\Phi_\varepsilon\frac{N_0 f_n}{A}N_1+q_3+q_7;\\
&\frac{dA_2}{dt} = \omega\frac{S_2}{S_1}A_1-(\gamma+\lambda)A_2;\quad \frac{dA_3}{dt} = \omega\frac{S_3}{S_1}A_1-(\gamma+\lambda)A_3+\lambda\sigma\Phi_0\frac{N_0 f_n}{A}N_3;\\
&\frac{dA_4}{dt} = \varepsilon_4\frac{G_4}{V_1}A_1-\lambda A_4;\quad A_5(t) = \frac{V_5}{V_1}kA_1(t);\quad \frac{dA_6}{dt} = \alpha k\frac{G_5}{V_1}A_1-(\lambda+\gamma_6)A_6;\\
&A_7(t) = (1-\alpha)k\frac{V_7}{V_1}A_1(t)+\gamma_6\frac{V_7}{G_5}A_6(t);\quad \frac{dA_8}{dt} = \omega A_7-(\lambda+\gamma)A_8;\quad \frac{dA_9}{dt} = \varepsilon_9\frac{G_5}{V_7}A_7-\lambda A_9,
\end{aligned}\right\} \tag{3}$$

where

$$q_3 = \sigma\Phi_0(1-e^{-\lambda t})\frac{N_0 f_n}{A}Q_3;\quad q_7 = (1-\varepsilon_9)\frac{G_7}{V_7}A_7. \tag{4}$$

The summation in Eqs. (2) is carried out over all the construction materials. The accumulation of target nuclei in the vapor and condensate parts of the circuit is not of interest for the present problem.

At present there is no satisfactory means of allowing for the particle traps. The irreversible deposition of particles in traps and supplementary scavenging of the reactor water may be taken into account by varying the value of λ_0. In setting up the equations it was assumed that the time of motion of the condensate was not large $\left(\omega\frac{V_7}{G_7}\ll 1\right)$ and that the fall in activity resulting from the deposition of particles on the walls could be neglected.

Solution of Eqs. (1) to (4) for arbitrary initial conditions is in practice only possible by computer methods; the authors are setting up a program for this at the present time in company with O. Ya. Shakh and N. A. Ger'eva. In many cases, however, it is important to know simply the maximum values of radioactive impurities. This information is given by the asymptotic solution of the problem for $t\to\infty$. For zero initial conditions and constant rate of emission of the reactor materials, this solution has the form

$$N_1^\infty = \frac{Q_1}{\lambda_0};\quad N_2^\infty = \frac{\omega}{\lambda_0\gamma}\cdot\frac{S_2}{S_1}Q_1;\quad N_3^\infty = \frac{\omega}{\lambda_0\gamma}\cdot\frac{S_3}{S_1}Q_1; \tag{5}$$

$$A_1^\infty = \frac{\left[\sigma\Phi_0(\gamma+\lambda)Q_3+\sigma\Phi_\varepsilon(\gamma+\lambda)\frac{\lambda}{\lambda_0}Q_1+\sigma\Phi_0\omega\frac{\lambda}{\lambda_0}\cdot\frac{S_3}{S_1}Q_1\right]}{\omega\lambda+(\lambda_0+\lambda)(\gamma+\lambda)}\cdot\frac{N_0 f_n}{A}; \tag{6}$$

$$A_2^\infty = \frac{\left[\sigma\Phi_0 Q_3+\sigma\Phi_\varepsilon\frac{\lambda}{\lambda_0}Q_1+\sigma\Phi_0\frac{\omega\lambda}{\lambda_0(\gamma+\lambda)}\cdot\frac{S_3}{S_1}Q_1\right]\omega\frac{S_2}{S_1}}{\omega\lambda+(\lambda_0+\lambda)(\gamma+\lambda)}\cdot\frac{N_0 f_n}{A}; \tag{7}$$

$$A_3^\infty = \frac{\left\{\sigma\Phi_0 Q_3+\sigma\Phi_\varepsilon\frac{\lambda}{\lambda_0}Q_1+\sigma\Phi_0\frac{\lambda}{\lambda_0}Q_1\frac{\left[(\lambda_0+\lambda)(\gamma+\lambda)+\omega\gamma\frac{S_3}{S_1}+\omega\lambda\right]}{\gamma(\gamma+\lambda)}\right\}\omega\frac{S_3}{S_1}}{\omega\lambda+(\lambda_0+\lambda)(\gamma+\lambda)}\cdot\frac{N_0 f_n}{A}; \tag{8}$$

$$A_4^\infty = \frac{\varepsilon_4 G_4}{\lambda V_1}A_1^\infty; \tag{9}$$

$$A_6^\infty = \frac{\alpha k}{\lambda+\gamma_6}\cdot\frac{G_5}{V_1}A_1^\infty; \tag{10}$$

$$A_7^\infty = k\left(1-\frac{\alpha\lambda}{\lambda+\gamma_6}\right)\frac{V_7}{V_1}A_1^\infty; \tag{11}$$

$$A_8^\infty = \frac{\omega k}{\lambda+\gamma}\cdot\frac{V_7}{V_1}\left(1-\frac{\alpha\lambda}{\lambda+\gamma_6}\right)A_1^\infty; \tag{12}$$

$$A_9^\infty = k\varepsilon_9\left(1-\frac{\alpha\lambda}{\lambda+\gamma_6}\right)\frac{G_5}{V_1}A_1^\infty. \tag{13}$$

Let us consider the main characteristics of the asymptotic solution.

1. The total quantity of corrosion products in the reactor water does not depend on the rates of deposition and erosion of the particles.

2. It is known that the total quantity of corrosion products on the reactor surfaces considerably exceeds their content in the water [1, 6]. Hence from the relation

$$\frac{N_2^\infty+N_3^\infty}{N_1^\infty} = \frac{\omega}{\gamma} \tag{14}$$

we find that $\omega \gg \gamma$.

3. In the numerator of expressions (6) to (8) we have a sum of three terms, each of which corresponds to three possible sources for the appearance of radioactive nuclei in the system: A), B), and C). What is the relative role of these sources?

Activation during the passage of the heat carrier through the active zone (source B) is only important for short-lived nuclei. An approximate criterion is given by the relations $\lambda > \lambda_0$ and $\lambda > \omega$. The role of sources A) and C) may be quite arbitrary; for equilibrium activity of Co^{60} the contribution of source A) increases. In general none of the three sources of activation can be neglected.

4. The part played by the purification of the reactor water in reducing the contamination of the surfaces is mainly determined by competition between impurity removal by the purification system and deposition of particles on the walls, as may be seen from the relation

$$A_1^\infty : A_2^\infty : A_4^\infty \approx \frac{\lambda}{\lambda_0} : \frac{\omega}{\lambda_0\left(1+\frac{\gamma}{\lambda}\right)} \cdot \frac{S_2}{S_1} : 1, \tag{15}$$

For long-lived activity the role of the purification system becomes more important.

5. Solution of the problem for long-lived activity ($\lambda \ll \lambda_0$) is considerably simplified on satisfying the two conditions $\left(\frac{Q_3}{S_3} \approx \frac{Q_1}{S_1}$ and $\lambda \ll \lambda_0 \frac{\Phi_0}{\Phi_e} \cdot \frac{Q_3}{Q_1}\right)$:

$$A_1^\infty = \sigma\Phi_0 \frac{Q_3}{\lambda_0} \cdot \frac{N_0 f_n}{A}; \tag{16}$$

$$A_2^\infty = \sigma\Phi_0 Q_3 \frac{\omega}{\lambda_0(\gamma+\lambda)} \cdot \frac{S_2}{S_1} \cdot \frac{N_0 f_n}{A}; \tag{17}$$

$$A_3^\infty = \sigma\Phi_0 Q_3 \frac{\omega}{\lambda_0(\gamma+\lambda)} \cdot \frac{S_3}{S_1}\left(1+\frac{\lambda}{\gamma} \cdot \frac{Q_1}{Q_3}\right) \frac{N_0 f_n}{A}. \tag{18}$$

6. For experimental study it is convenient to use the specific activity referred to unit mass of impurities. For relations (16) to (18) we obtain:

$$a_1^\infty = \frac{A_1^\infty}{\sum_i N_{1i}^\infty} = \sigma\Phi_0 \frac{Q_3}{\sum_i Q_{1i}} \cdot \frac{N_0 f_n}{A}; \tag{19}$$

$$a_2^\infty = \frac{A_2^\infty}{\sum_i N_{2i}^\infty} = \sigma\Phi_0 \frac{\gamma}{\gamma+\lambda} \cdot \frac{Q_3}{\sum_i Q_{1i}} \cdot \frac{N_0 f_n}{A}; \tag{20}$$

$$a_3^\infty = \frac{A_3^\infty}{\sum_i N_{3i}^\infty} = \sigma\Phi_0 \frac{Q_3}{\sum_i Q_{1i}} \times \frac{\gamma}{\gamma+\lambda}\left(1+\frac{\lambda}{\gamma} \cdot \frac{Q_1}{Q_3}\right) \frac{N_0 f_n}{A}. \tag{21}$$

The slight dependence of the specific activities on the mass-transfer coefficient should be noted.

7. By comparing expressions (19) to (21) we see that $a_3 > a_1 > a_2$, for short-lived isotopes this inequality intensified.

8. The accumulation of activity in the primary circuit of the reactor containing water under pressure is a particular case of the problem in question for $G_5 = 0$.

Solution of the Nonstationary Problem

Since the characteristic equation of system (1) to (3) is at least cubic, it is difficult to solve without making substantial simplifying assumptions. The solution given below is principally valid for the accumulation of isotope Co^{60} on nonirradiated surfaces. This solution is obtained on the following assumptions: 1) Equilibrium is attained with respect to the mass transfer of the target nuclei, i.e., $\lambda_0 t \gg 1$, $\omega t \gg 1$, $\gamma t \gg 1$;

TABLE 1. Mass-Transfer Constants of the Corrosion Products of Various Nuclear Reactors

Isotope	ω, sec^{-1}	γ, sec^{-1}	λ_0, sec^{-1}	ω/γ	Literature
Fe^{59}	$3.5\cdot10^{-5}$	$5\cdot10^{-8}$	10^{-5}	700	[6]
Fe^{59}	—	—	—	720	[1]
Fe^{59}	$6\cdot10^{-2}$	$2.6\cdot10^{-7}$		$2.3\cdot10^{5}$	
Co^{60}	$7\cdot10^{-2}$	$2.3\cdot10^{-7}$		$3\cdot10^{5}$	
Cu^{64}	$9.4\cdot10^{-6}$	$2.8\cdot10^{-6}$	$1.9\cdot10^{-5}$	3.4	
Cr^{51}	$1.3\cdot10^{-4}$	$4\cdot10^{-9}$		$3.2\cdot10^{4}$	[7]
Sb^{122}	$4.5\cdot10^{-3}$	$1.5\cdot10^{-5}$		300	
Sb^{124}	$4.5\cdot10^{-3}$	small		large	
—	$5.8\cdot10^{-6}$	$4.4\cdot10^{-6}$	$5.7\cdot10^{-5}$	1.3	[8]
—	10^{-6}	$5\cdot10^{-6}$		0.2	

TABLE 2. Relative Mass-Transfer Velocity for Various Oxides in the Dresden APS

Oxides	$\left(\frac{\omega}{\gamma}\right)_i / \left(\frac{\omega}{\gamma}\right)_{Fe_2O_3}$
Fe_2O_3	1.0
Cr_2O_3	0.76
NiO	0.88
CuO	0.34

2) activation source B) is not taken into account (see above analysis); 3) the radioactivity of the impurities in the reactor water is independent of time.

On these assumptions

$$A_2(t) = A_2^{\infty}(1 - e^{-pt}), \tag{22}$$

where A_2^{∞} is found from expression (7) without the term corresponding to activation source B) and

$$p = (\gamma + \lambda)\frac{\lambda_0(\gamma+\lambda) + \omega\lambda}{\lambda_0(\gamma+\lambda) + \omega\left(\gamma\frac{S_2}{S_1} + \lambda\right)}. \tag{23}$$

For preferential accumulation of activity on the reactor surfaces $p \approx \lambda S_1/S_2$, and for accumulation of activity in the filter $p \approx \gamma + \lambda$. The accumulation of activity on the surfaces washed by the condensate is analogous to expression (22).

Analysis of Experimental Data

Since the nuclear-physics constants and circuit parameters required for the calculation are usually known, computing errors are mainly determined by the accuracy of the mass-transfer coefficients (especially the deposition and erosion rates); information regarding these constants is very meager, however, and quite contradictory (Table 1) [7, 8]. We may suppose that $\omega \gg \gamma$, and it follows, from the time for establishing equilibrium activity of the reactor water [1], that in order of magnitude $\gamma \sim 10^{-7}$ sec^{-1}.

Information regarding the growth of oxide films was obtained by means of a radioactive indicator, Fe^{59}, in the SM-1 reactor [6]. Analysis of existing data with respect to the relations derived above showed that for samples with various holding periods the quantities ω and γ lay within the limits of $\omega = (0.9\text{–}5)\cdot10^{-5}$ sec^{-1} and $\gamma = (3\text{–}7)\cdot10^{-8}$ sec^{-1}. For samples with holding periods of more than 1000 h the best agreement was obtained for $\omega = 3.5\cdot10^{-5}$ sec^{-1} and $\gamma = 5\cdot10^{-8}$ sec^{-1}.

It is known that the water of the Dresden Atomic-Power Station contains 70 g of corrosion products and the surface of the circuit 50 kg [1]. Hence in view of relation (14) $\omega/\gamma = 720$, which agrees closely with the data of [6]. From chemical analysis of the corrosion film and impurities in the water [1] we may draw certain conclusions regarding the relative velocity of mass transfer for various oxides (Table 2). It follows from the tabulated data that the values of ω/γ are of the same order for the oxides of Fe, Cr, and Ni, i.e., they are carried around the circuit mainly in the form of particles. On analyzing other data with respect to water-cooled, water-moderated reactors, a value of $\omega/\gamma = 440$ to 1000 with respect to iron was obtained.

The values of mass-transfer constants obtained in the DIDO circuit differ considerably from data relating to other reactor systems (see Table 1); the thickness of the superficial oxide film is about 200 μ the relative efficiency of the purification system in comparison with the deposition on the reactor surfaces equals 0.2% for Fe^{59}, 5% for Co^{60}, and so on. In view of the unusual conditions in the system (material carbon steel, water pH 10.5, corrosion products in the dissolved state), the use of constants taken from [7] when analyzing other reactor systems demands caution.

The mass-transfer coefficients recommended in [8] do not agree with experimental data obtained with other reactors.

The data available in the literature are insufficient to enable final conclusions to be drawn regarding the deposition and erosion coefficients. We can only recommend a ratio of around 700 for these coefficients. The values of coefficients given in this paper should be considered approximate. It is felt that the true values will be rather higher than those recommended, although the authors have no concrete evidence to support this as yet.

The authors have been greatly aided by discussions with M. A. Styrikovich and his colleagues and also with V. V. Gerasimov et al. The authors are grateful to B. A. Alekseev and O. Ya. Shakh for a useful exchange of views.

NOTATION USED

t	operating time of the reactor;
N_l	total amount of the i-th element in the l-th medium (index i usually omitted);
A_l	total activity of i-th isotope in l-th medium;
a_l	specific activity of i-th isotope per unit weight of impurity in l-th medium;
Q_l	rate of access of the i-th element into the reactor water from the l-th medium;
q_l	rate of access of the activity of the i-th isotope from the l-th medium into the reactor water;
V_l	weight of heat carrier in the l-th medium;
S_l^m	surface of the m-th construction material in the l-th medium;
C_l^m	effective corrosion rate (emission rate) of the m-th construction material in the l-th medium;
G_l	flow of heat carrier in the l-th medium;
$\varepsilon_4, \varepsilon_9$	efficiency of purifying filters for the reactor and supply water;
α	proportion of activity deposited from the vapor into the turbine;
λ_0	time constant for purification of the reactor water;
p	effective time constant for the accumulation of activity on the wall;
k	apparent distribution coefficient of the impurities between the saturated vapor and boiling water.

The rest of the notation is taken from [8].

LITERATURE CITED

1. F. Brutschy et al., Corrosion of Reactor Materials, Vol. 1, Vienna, IAEA, p. 133 (1962).
2. E. U. Kramer, Boiling-Water Nuclear Reactors [Russian translation]. Moscow, IL (1960).
3. V. Hall et al., Nucleonics, 19, No. 3, 80 (1961).
4. Power Reactor Technology, 4, No. 3, 56 (1961).
5. C. Breden et al., AEG-Euratom Conference on Aqueous Corrosion of Reactor Materials, Brussels, TID-7587, p. 48 (1959).
6. C. Bergen, Nucleonics, 20, No. 6, 70 (1962).
7. G. Walton and E. Hesford, Corrosion of Reactor Materials, Vol. 2. Vienna, IAEA, p. 547 (1962).
8. Protection of Nuclear Reactors, Edited by T. Rockwell [Russian translation]. Moscow, IL (1958).
9. D. L. Broder, K. K. Popkov, and S. M. Rubanov, Biological Protection of Naval Reactors [in Russian]. Leningrad, "Sudostronenie, " (1964).
10. S. Yerazunis et al., KAPL-M-SMB-98. May 27 (1959).
11. Corrosion and Wear in Water-Cooled Reactors. Edited by De Pol [Russian translation]. Leningrad (1958).
12. P. A. Akol'zin and V. V. Gerasimov, Corrosion of Construction Materials in Nuclear and Thermal Power Stations [in Russian]. Moscow, "Vysshaya shkola" (1963).
13. M. A. Styrikovich, Processes in Boilers [in Russian]. Moscow-Leningrad, Gosénergoizdat (1954).
14. O. I. Martynova, Doctor's Dissentation [in Russian]. Moscow (1963).
15. M. A. Styrikovich, "Atomnaya Énergiya," 15, 214 (1963).

THERMODYNAMIC PROPERTIES OF THE γ-PHASE IN THE URANIUM-ZIRCONIUM SYSTEM

G. B. Fedorov and E. A. Smirnov

UDC 621.039.542.32:536.77

Alloying with zirconium has a beneficial effect on uranium fuel; the corrosion resistance, dimensional stability, and some physicomechanical properties are all improved [1-5].

It is therefore of interest to study the thermodynamic and diffusion properties of uranium-zirconium alloys at temperatures above 750°C, for which unlimited solubility exists between these metals.

EXPERIMENTAL

The thermodynamic properties of the uranium-zirconium system were studied by measuring the emf of the electrochemical cell

$$U\ (\text{solid}) \mid U^{+3} + (KCl - NaCl) \mid U - Zr\ (\text{alloy}).$$

In setting up the cell we used data relating to the equilibrium potentials of uranium and zirconium in molten NaCl and KCl, the oxidation-reduction potentials of these metals relative to the chlorine comparison electrode, the polarization of uranium and zirconium anodes during electrolysis, and the measured heats of formation of uranium and zirconium chlorides [6-8]. Comparison of existing information shows that in the uranium-zirconium pair the more electropositive element is uranium and that the stable valence of uranium in the temperature range studied equals +3. The experimental electrochemical cell is shown in Fig. 1. After assembly it is placed in a furnace evacuated to a residual pressure of 10^{-2} mm Hg and held for 2 h at 500°C in order to remove traces of moisture from the electrolytes. After several flushings, the cell is filled with purified argon and heated to 800°C.

Tervalent uranium ions were introduced into the electrolyte by anodic dissolution, for which a double-walled alundum cylinder was used. Inside the cylinder was a uranium anode and between the

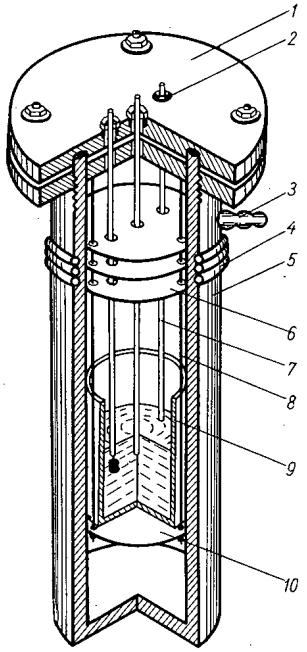

Fig. 1. Arrangement of electromechanical cell: 1) Steel roof with rubber gasket; 2) leads; 3) port for evacuating and admitting argon; 4) copper tube for water cooling; 5) stainless-steel cylinder; 6) molybdenum screens; 7) alundum tubes for introducing Chromel-Alumel thermocouples and tungsten leads for the electrodes; 8) three metal holders; 9) alundum cylinder containing electrolyte; 10) base plate.

Translated from Atomnaya Énergiya, Vol. 21, No. 3, pp. 189-192, September, 1966. Original article submitted February 1, 1966. V. G. Bukatov and V. Ya. Vodyanoi took part in this work.

TABLE 1. EMF Values for Uranium-Zirconium Alloys

Uranium content, at.%	Temperature, °K	Emf, mV	Coefficients of equation E=AT+B	
			A, mV/deg	B, mV
14.1	1030	125.47	0.0111	114.1
	1068	125.78		
	1124	126.53		
	1160	126.80		
27.6	1043	94.64	0.0141	80.12
	1097	95.50		
	1138	95.94		
	1182	96.70		
41.5	1045	20.11	0.0158	12.43
	1039	29.80		
	1132	30.50		
	1184	31.35		
60.5	1048	18.02	0.0179	—0.81
	1082	18.65		
	1121	19.40		
	1178	20.40		
75	1030	14.00	0.0168	—3.504
	1063	14.48		
	1120	15.52		
	1175	16.45		
89	1036	8.62	0.0147	—6.590
	1075	9.21		
	1119	9.80		
	1172	10.70		
94	1039	4.43	0.0116	—7.568
	1123	5.61		
	1165	5.98		

walls a tungsten-wire cathode. The inner wall served as a semipermeable membrane, letting sodium and potassium ions through to the cathode and holding up the uranium ions. Thus uranium trichloride was formed in the inner space and sodium and potassium ions were deposited on the cathode. The current density at the anode during electrolysis was 30 mA/cm^2. The equimolar mixture of sodium and potassium chlorides used contained 0.5 wt.% uranium trichloride.

The alloys were prepared from iodide-type zirconium and electrolytic uranium in an arc furnace with a cooled copper hearth, in an atmosphere of pure argon. The samples for thermodynamic study, 2.2 to 2.4 mm long and about 0.7 cm^2 in cross section, were preliminarily homogenized at 900°C for 100 h, after which they were water-quenched. The samples for diffusion measurements, 6 to 8 mm long and 1 cm^2 in cross section, were subjected to five-fold phase recrystallization (heating to 1000°C and cooling in air) with a subsequent homogenizing anneal for 2 h at 1000°C. The annealing and quenching were carried out in sealed quartz ampoules under continuous evacuation.

The emf were measured over 100 to 200 h by a compensation method for a temperature range of 750 to 910°C. The cell temperature was maintained to an accuracy of ±2°C. At each temperature the emf was measured to an accuracy of ±0.05 mV; the values during heating and cooling agreed to within 0.5 mV. For

TABLE 2. Principal Partial Thermodynamic Functions of the Uranium-Zirconium System at 800°C

N_U	a_U	a_{Zr}	$\Delta\bar{Z}_U$, cal/g-at.	$\Delta\bar{H}_U$, cal/g-at.	$\Delta\bar{S}_U$, cal/g-at.deg	$\Delta\bar{Z}_{Zr}$, cal/g-at.	$\Delta\bar{H}_{Zr}$, cal/g-at.	$\Delta\bar{S}_{Zr}$, cal/g-at.deg
0.141	0.017	0.83	—8730	—7900	0.769	—400	—456	—0.052
0.276	0.045	0.60	—6600	—5555	0.975	—1060	—1167	—0.1
0.415	0.385	0.20	—1980	—810	1.094	—3420	—3580	—0.15
0.605	0.55	0.15	—1280	50	1.239	—4120	—4390	—0.25
0.75	0.62	0.12	—1030	220	1.163	—4770	—4767	0.028
0.89	0.74	0.032	—640	450	1.018	—7360	—4730	2.45
0.94	0.85	0.0036	—340	530	0.806	—12000	—5870	5.7

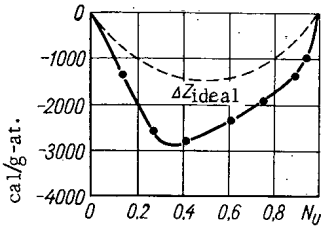

Fig. 2. Integral molar free energy of the uranium-zirconium system at 800°C.

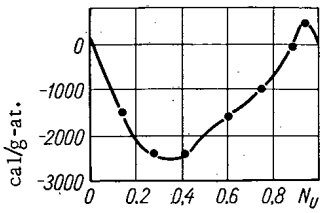

Fig. 3. Integral molar enthalpy of the uranium-zirconium system at 800°C.

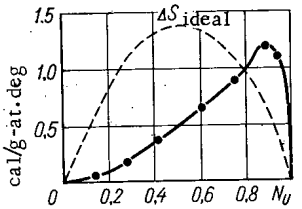

Fig. 4. Integral molar entropy of the uranium-zirconium system at 800°C.

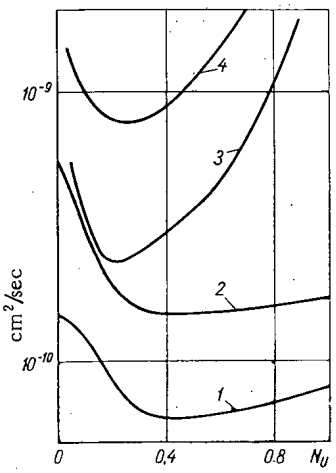

Fig. 5. Coefficients of hetero-diffusion in the uranium-zirconium system as functions of concentration: 1) 800°C; 2) 900°C; 3) 950°C [11]; 4) 1000°C [11].

TABLE 3. Diffusion Coefficients of Uranium and Zirconium in Uranium-Zirconium Alloys ($D \times 10^{10}$ cm²/sec)

Zirconium content, wt%	Diffusing element	Temperature, °C					
		800	900	940	1000	1050	1065
0	Zirconium	0.79	1.5	—	2.7	3.3	—
35	Uranium	—	2.1	—	8.1	—	18
	Zirconium	—	1.2	2.0	4.0	—	7.2
50	Uranium	—	2.6	4.3	8.9	—	20
	Zirconium	—	0.93	—	4.2	—	10.5
70	Uranium	—	3.5	—	12	—	21
	Zirconium	—	0.79	1.4	5.0	—	11
100	Uranium	—	5.6	8	17	—	26

uranium-rich alloys the constancy of the emf was attained more rapidly and the data reproduced to a greater accuracy.

The diffusion of the components in the uranium-zirconium system was studied by means of radioactive isotopes U^{235} and Zr^{95}, which were vacuum-deposited on to the prepared sample surfaces. Diffusion annealing 2 to 10 h in duration was carried out over the temperature range 800 to 1065°C in quartz ampules under continuous evacuation. The temperature was kept constant to ±5°C. The diffusion coefficients were determined by the layer-removal method, the total radioactivity of the remaining part of the sample being determined [9].

The radioactivity was recorded by means of scintillation counters; for recording the α-radiation of U^{235} we used zinc sulfide and for the γ-radiation of Zr^{95} sodium iodide activated by thallium. The emission from the radioactive zirconium was separated from the background of γ-radiation from the uranium samples by means of a differential discriminator.

DISCUSSION

The averaged results of the emf measurements are shown in Table 1. The coefficients of the analytical equation E=AT+B for the temperature dependence of the emf were found by the method of least squares.

The thermodynamic activity of uranium in the alloys was calculated from the formula

$$\log a_U = -\frac{Z_U EF}{2.3RT} = -15\,120\frac{E}{T},$$

and the activity of zirconium by graphical integration of the Gibbs-Duhame equation

$$\log a_{Zr} = -\int_0^{N_U} \frac{\lg a_U}{N_{Zr}^2} dN_U - \frac{N_U}{N_{Zr}} \log a_U.$$

The resultant values are shown in Table 2. The values of emf were also used for calculating the partial and integral molar thermodynamic functions of uranium and zirconium (see Table 2 and Fig. 2 to 4). The partial molar entropy of zirconium was calculated by graphical integration of the Gibbs-Duhame equation and the remaining thermodynamic functions by means of the ordinary thermodynamic relationships. The measured diffusion coefficients in the uranium-zirconium system are shown in Table 3.

The resultant thermodynamic and diffusion characteristics of the uranium-zirconium alloys enabled us to calculate the heterodiffusion coefficient [10] from the Darken formula for 800 and 900°C.

$$\tilde{D} = (N_U D^*_{Zr} + N_{Zr} D^*_U)\left(1 + \frac{\partial \ln f_U}{\partial \ln N_U}\right),$$

where D^*_{Zr} and D^*_U are the diffusion coefficients of the components, f_U is the coefficient of activity of uranium, N_U and N_{Zr} are the atomic proportions of the components.

The calculated concentration/heterodiffusion-coefficient relationships are shown in Fig. 5 together with the data of [11] obtained for higher temperatures by the Matano method.

In the temperature and concentration ranges studied there was a negative deviation of the activities of the two components from Raoult's law. This indicates an intensification of the binding forces between the uranium and zirconium atoms in solid solution as compared with the corresponding forces between atoms of similar types.

We see from Figs. 2-4 that the maximum deviation of the integral thermodynamic functions from the ideal state occurs in the concentration range 30 to 35 at.% uranium, which at lower temperatures corresponds to the range of existence of the δ-phase.

It is well known that the coefficients of heterodiffusion calculated from the Darken formula (using data relating to the diffusion of radioactive isotopes and the concentration dependence of the thermodynamic factor) are more reliable than measurements by the Matano method [12, 13]. However, despite the difference in the methods, the resulting concentration dependence of the coefficients of heterodiffusion agrees with the results of [11, 14]. At high temperatures the concentration dependence of the coefficients of heterodiffusion has a sharp minimum in the range of concentrations corresponding to extremal values of the excess integral thermodynamic function (see Fig. 5); on lowering the temperature temperature this minimum becomes smoother.

LITERATURE CITED

1. V.S. Emel'yanov, and A.I. Evstyukhin, Metallurgy of Nuclear Fuel [in Russian]. Moscow, Atomizdat (1964).
2. A.S. Zaimovskii, V.V. Kalashnikov, and I.S. Golovin, Heat-Evolving Elements of Atomic Reactors [in Russian]. Moscow, Gosatomizdat (1962).
3. G.Ya. Sergeev, V.V. Titova, and K.A. Borisov, Metallurgy of Uranium and Other Reactor Materials [in Russian]. Moscow, Gosatomizdat (1960).
4. Physical Metallurgy of Reactor Materials, Vol. 1. Nuclear-Fuel Materials. Edited by D.M. Skorov [Russian translation]. Moscow, Gosatomizdat (1961).
5. V.V. Gerasimov, Corrosion of Uranium and Its Alloys [in Russian]. Moscow, Atomizdat (1965).
6. M.V. Smirnov, and O.V. Skiba, "Dokl. AN SSSR", 141, 4 (1961).
7. V.E. Komarov, M.V. Smirov, and A.N. Baraboshkin, In the collection "Electrochemistry of Molten-Salt and Solid Electrolytes" [in Russian]. Sverdlovsk, Izd. Instituta élektrokhimiya Ural'skogo filiala AN SSSR, p. 3 (1960); O.V. Skiba, and M.V. Smirnov. Ibid., p. 3 (1961); V.E. Komarov, M.V. Smirnov, and A.N. Baraboshkin. Ibid., p. 25 (1962); O.V. Skiba, M.V. Smirnov, and O.A. Ryzhik. Ibid., p. 41 (1962).
8. Physical Chemistry of Molten Salts and Slags [in Russian]. Moscow, Metallurgizdat (1962).
9. P.L. Gruzin, "Izv. AN SSSR. Otd. tekhn. n.", No. 3, 383 (1963).
10. L. Darken, Trans. AIME, 175, 184 (1948).
11. Y. Adda, and J. Philibert, Compt. rend., 242, 3081 (1965); 243, 1316 (1965).
12. S.D. Gertsriken, and I.Ya. Dekhtyar. Diffusion in Metals and Alloys in the Solid Phase [in Russian]. Moscow, Fizmatgiz (1960).
13. R.L. Fogel'son. "Fiz. metallov i metallovedenie", 19, 212 (1965).
14. N. Müller, Z. Metallkunde, 50, 562 (1959).

X-RAY DIFFRACTION STUDY OF THE DISTRIBUTION OF TEXTURE OVER THE CROSS SECTION OF URANIUM BARS WORKED IN THE α- AND γ-PHASES AND SUBJECTED TO QUENCHING

V. F. Zelenskii, V. V. Kunchenko,
N. M. Roenko, L. D. Kolomiets,
and A. I. Stukalov

UDC 548.735:621.039.543.4

This article contains the results of an x-ray diffraction study of texture distribution over the cross section of a uranium rod worked in the α- and γ-phases and subjected to β- and γ-heat treatment. The pole-density distribution P(hkl) and growth index G_x depend on the conditions of mechanical and heat treatment; this enables the possible nature of dimensional changes taking place over the cross section of the rod in the course of radiation growth to be determined.

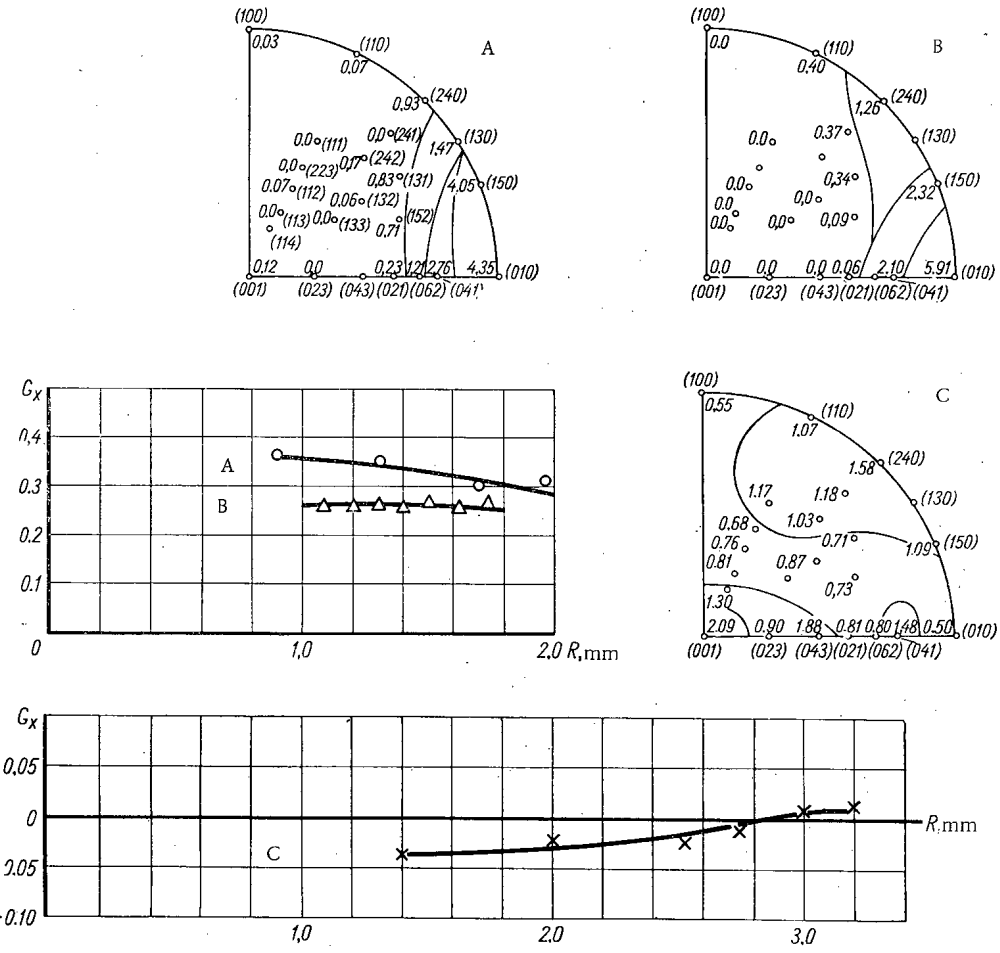

Fig. 1. Reciprocal pole figures for α-worked (A, B) and γ-extruded (C) rods and distribution of growth index G_x over the rod radius.

Translated from Atomnaya Énergiya, Vol. 21, No. 3, pp. 192-197, September, 1966. Original article submitted July 15, 1965; revised February 7, 1966.

When a polycrystalline metal is intensively strained in any one direction, a very considerable texture develops within it; the character and intensity of this is determined by the conditions of plastic deformation. Mechanical methods of finishing metals designed to produce conventional profiles (rods or sheet) produce inhomogeneous distributions of strains and stresses [1, 2]. The strain texture thus has different values at various points in the cross section of such samples.

For textured polycrystalline metals having noncubic crystal lattice symmetry, an inhomogeneous distribution of texture may lead to undesirable consequences in use (for example, leading to the development of thermal stresses [3] and hence buckling or spontaneous cracking of components).

For uranium blocks and rods used as fuel elements in reactors, an inhomogeneous texture distribution may cause inhomogeneous radiation growth over the cross section of the rod [4], leading to breaks in the coating and finally to breakdown of the reactor.

As a rule, the cores of fuel elements are blocks or rods which have been subjected to special heat treatment (quenching from the β- or γ-phase [5-8]). In some cases nonuniform texture distribution over the cross section has been observed [4].

In this paper we present some results of an x-ray diffraction study of texture distribution over the cross section of uranium rods worked in the α- and γ-regions and quenched from the β- and γ-phases.

Distribution of Texture in α-Worked Uranium Rods

The texture was studied by plotting reciprocal pole densities [9], and the growth index G_x for the end sections of the rod [10, 11].

The absolute error in determining P(hkl) and hence G_x is determined primarily by how well the standard (isotropic) sample is chosen or the intensity values J_i(hkl) for the isotropic state calculated [12].

In our case we used J_i(hkl) values calculated for the isotropic state and corrected from a standard sample not having texture (the degree of isotropy was checked by measuring the coefficient of linear thermal expansion in three mutually-perpendicular directions). Instrumental errors were thus excluded, since all the x-ray pictures were taken in a single apparatus under constant conditions. This made it possible to estimate the error in determining P(hkl), which could reach 20% of the measured value (in the case of a relatively coarse-grained metal structure), being determined by the number of crystallites taking part in the diffraction of the x-rays [13].

The x-ray diffraction experiments were made in the URS-50I diffractometer, using filtered CuKα radiation. Subsequent layer removal was effected by electrolytic etching. Uranium of 99.76 to 99.80% purity was used for the experiments.

The samples were prepared in the form of rods or thick wires 4.2 to 6.3 mm in diameter, using the following technology [14]:

A) Extrusion in the α-phase with subsequent rotatory forging and gage drawing at room temperature;

B) Extrusion in the α-phase at high temperatures and gage drawing at 150 to 200°C;

C) Vacuum extrusion at the temperature of the γ-phase.

Figure 1 shows the reciprocal pole figures for metal samples obtained in these ways. The same figure shows the variation of the G_x growth index over the rod cross section, this characterizing the ratio of the contributions of poles of the {010} and {100} types in the direction of the rod axis.

It follows from these data that extrusion in the low-temperature region of the α-phase (scheme A) causes the formation of axial texture of the [010] type along the extrusion direction. In such rods the texture is distributed nonuniformly over the cross section; the contribution of [010] poles is slightly increased at the axis of the rod, but the character of the texture is unchanged.

When the conditions of working are changed (scheme B), the texture and the character of its distribution over the cross section remain practically unaltered. A typical pole figure (see B in Fig. 1) indicates a certain contribution of (240) poles close to (110) in the direction of the rod axis, this being a consequence of high-temperature working with a high degree of reduction (about 95%) [15]. However, we still have a dominating [010] texture in the direction of the rod axis, the character of the texture not changing over the cross section.

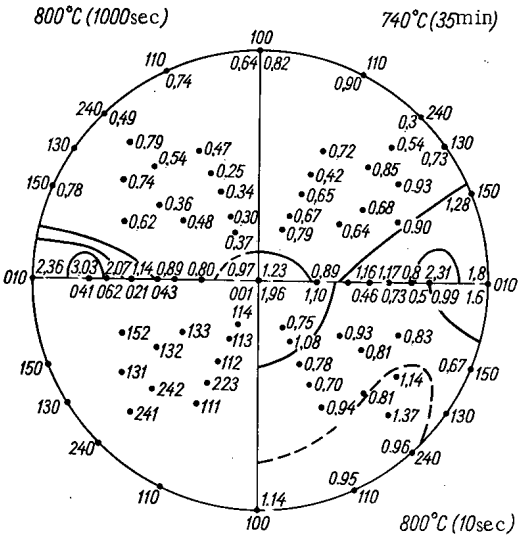

Fig. 2. Distribution of pole density P(hkl) over the cross section of α-worked uranium rods.

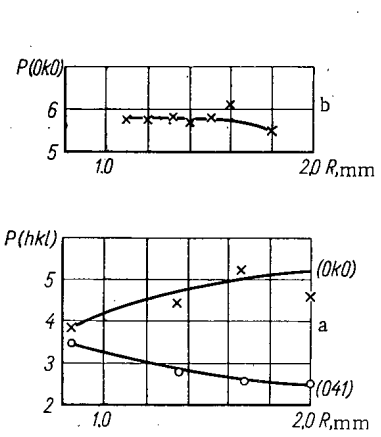

Fig. 3.

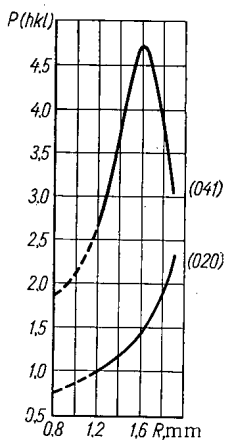

Fig. 4.

Fig. 3. Reciprocal pole figures for uranium rods quenched from the β- and γ-phases.

Fig. 4. Pole-density distribution over the cross section of a γ-quenched rod (1000 sec holding period at 800°C).

Figure 2 shows the variation in the density of the poles determining the type of texture over the radius of the rod for cases A and B.

Extrusion from the γ-phase leads to a qualitatively different texture. In the section of the rod perpendicular to the extrusion direction there is a composite texture, in which the poles of the (001) planes and those close to the (240) and (041) coincide with the axis of the sample.

As the radius diminishes, there is a weak tendency for a relative increase in the contribution of the poles close to the (240). This explains the negative values of the growth index G_x (see C in Fig. 1).

Thus the character of the texture and its distribution over the section of the rods depends on the conditions of thermomechanical treatment. Conditions may be chosen in such a way as to lead to a quasi-homogeneous distribution of texture over the cross section.

It is interesting to consider the texture of rods quenched from the β- and γ-phases of the rods, since this form of heat treatment is usually used in order to break up the texture of the uranium as much as possible. The technological methods developed for the treatment of the uranium cores of fuel elements [6, 11, 14] ensure the production of a quasi-isotropic structure of α-uranium, and hence a satisfactory radiation resistance of the fuel element. However, quenching from the β- or γ-phases does not always lead to desirable results. Certain conditions of heat treatment do not ensure complete elimination of the preferential orientation of crystallites [4, 5]. There is also a nonuniform distribution of the average coefficient of thermal expansion over the cross section of a quenched uranium core [4, 14].

Distribution of Texture Over the Cross Section of β- and γ-Quenched Rods

We studied the distribution of texture in samples quenched from the β-phase (rods obtained by the B method, heated slowly to 740°C in the furnace, held for 35 min, then water-quenched [5, 14] and γ-phase (heated in molten magnesium to 800°C, held 1000 sec, and water-quenched [14]). This kind of heat treatment led to practically the same type of texture (Fig. 3). It was also interesting to trace the distribution of the texture over the cross section of such samples. Figure 4 presents the distribution of pole density P(hkl) for samples quenched from the γ-phase (holding time 1000 sec). The pole-density distribution curves P(hkl) were obtained by successive x-ray diffraction of the rod cross section after electrolytic removal of layers from the cylindrical surface. In the surface zone there was a maximum density of (062) and (041) poles and those close to the [010].

The character of the texture does not vary over the cross section, although the extent to which it is expressed is not uniform (Fig. 5).

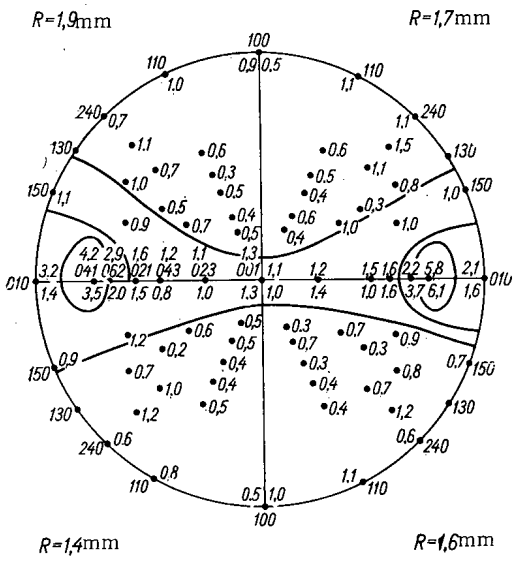

Fig. 5. Reciprocal pole figures for a sample quenched from the γ-phase (800°C, 1000 sec), corresponding to various cross sections.

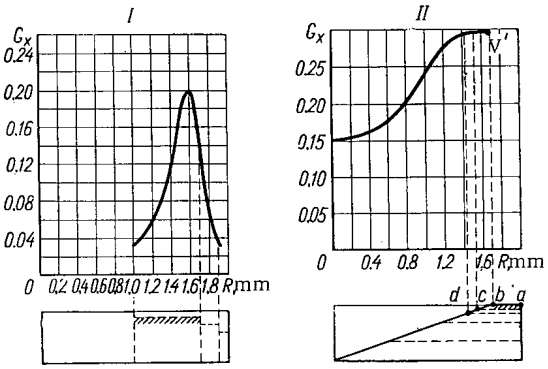

Fig. 6. Distribution of growth index G_x over the cross section of β-quenched rod.

Since the texture is uniaxial and the distribution of the coefficients of thermal expansion of these samples indicate a monotonic increase in their values as radius diminishes [14], we may extrapolate the pole-density distribution curves P(hkl) toward the center of the sample (see broken curve in Fig. 4). The variation in the pole density over the cross sections of samples quenched from the β-phase has an analogous character.

A more complete picture of the possible variation in the coefficient of radial growth over the sample cross section is given by the radial variation of the growth index G_x rather than the distribution curves for the density of individual poles. Figure 6 shows the distribution of growth index G_x over the cross section of a rod quenched from the β-phase. The layer-removal scheme is indicated in the same figure. In Fig. 6I the layers were taken from the cylindrical surface and the x-ray diffraction carried out from the remaining (shaded) circular area. The graph of Fig. 6II is plotted for rings successively increasing in area (ab, then ad, and so on); this was achieved by grinding the end surface of a sample in which conical holes had been drilled. Point b' corresponds to averaging over the surface of ring ab, and the point corresponding to the center of the sample (radius R = O) is obtained by x-ray examination of the whole end section. This made it possible to trace the qualitative picture of the texture distribution over the whole cross section, which cannot be done by taking layers from the outer surface of the sample.

The holding period spent in the β- and γ-phases before quenching affects the coefficient of linear thermal expansion [14]. This is because of the change in the type of texture. Figure 3 shows not only the reciprocal pole figures plotted for samples quenched from the β- and γ-phases (1000 sec at 800°C), but also that of a sample held at 800°C for 10 sec. The texture of this sample differs from that of a sample quenched from the γ-phase with a holding time of 1000 sec, in that the density of poles close to the [100] and [001] is increased. This kind of texture is typical of several cases of quenching from the β-phase, involving rapid heating of the samples into the temperature range corresponding to the existence of the β-phase and a short holding time at this temperature [14].

By comparing data relating to the distribution of texture over the cross section of the rod before and after quenching, we may conclude that the original texture does not have a decisive influence on the formation of texture in the quenched metal, since samples with the same initial texture have very different textures after different forms of heat treatment.

Apparently the texture of the quenched uranium in the present case is determined by the distribution and magnitude of stresses arising in the sample as a result of volume changes during phase transformations and also thermoelastic stresses.

Annealing the uranium at the temperatures of the β- and γ-phases leads to additional "alloying" as a result of the dissolution of inclusions, which reduces the temperature of the phase transformation and thus modifies the effect of stresses on the formation of the texture observed after quenching. This explains

the influence of the holding time (in the temperature range corresponding to the existence of the high-temperature phases) on the intensity and distribution of texture over the cross section.

LITERATURE CITED

1. Ya. S. Umanskii, X-Ray Diffraction of Metals [in Russian], Moscow, Fizmatgiz, p. 291 (1960)
2. S. I. Gubkin, Plastic Deformation (Working) of Metals [in Russian], Vil. 1, Moscow, Metallurgizdat, p. 346 (1960).
3. V. A. Likhachev, "Fiz. metallov i metallovedenie", 2, 792 (1961).
4. J. Gittus et al., Radiation Damage in Reactor Materials, Venice, 7-11 May, 1962, p. 109. Part of the Proceeding of the Symposium on Radiation Damage in Solids and Reactor Materials.
5. F. Foote, In: Metallurgy of Nuclear Power and the Effect of Radiation on Materials [Russian translation]. Contributions of non-Soviet scientists to the International Conference on the Peaceful Use of Atomic Energy (Geneva, 1955). Moscow, Energoizdat, p. 146 (1956).
6. Metallurgy of Reactor Materials (Reviews of the Battelle Institute), Book I. "Nuclear-Fuel Material", [Russian translation], Moscow, Gosatomizdat (1961).
7. A. S. Zaimovskii et al., In: Transactions of the Second International Conference on the Peaceful Use of Atomic Energy (Geneva, 1958). Contributions of Soviet scientists [in Russian], Moscow, Atomizdat, p. 573 (1959).
8. B. Kopelman, Materials for Nuclear Reactors [Russian translation], Moscow, Gosatomizdat, p. 328 (1962).
9. G. Slattery and D. Connelly, TRG Report, 360 (S) (1963).
10. E. Sturcken and W. McDonell, J. Nucl. Mat., 7, 85 (1962).
11. V. E. Ivanov et al., "Atomnaya Énergiya", 18, 357 (1965).
12. G. Harris, Philos. Mag., 43, 113 (1952).
13. P. Morris, J. Appl. Phys., 35, 2553 (1964).
14. V. E. Ivanov et al., "Atomnaya Énergiya", 16, 325 (1964).
15. A. N. Holden, Physical Metallurgy of Uranium [Russian translation], Moscow, Metallurgizdat, p. 103 (1962).

Sr^{90} AND Cs^{137} CONTENT IN AGRICULTURAL PRODUCTS OF WESTERN SLOVAKIA, 1963-1964

S. Cupka, M. Petrasova, and J. Carach

UDC 551.577.7:614.776

The Sr^{90} and Cs^{137} levels in agricultural crops grown in Western Slovakia in 1963-1964 were investigated. Highest content of both isotopes in grains and a relatively low content in legumes were reported, with the lowest content in row crops. The different Cs^{137}/Sr^{90} ratios in the crops studied is accounted for by the sorbing power of the plants and primarily by the amount of radioactive fallout occurring during the period in question.

The purpose of this article is to describe determinations of levels of the most important radioisotopes found in agricultural crops in areas contiguous to nuclear power station sites.

At present, with Sr^{90} and Cs^{137} fallout levels gradually declining, there is interest in investigating migration, extraction of isotopes from the soil by plants, and circulation in the food cycle. Some farm produce containing radioactive materials enters the human organism directly. Other agricultural products are utilized as raw material in the food industry or as fodder for livestock. In the latter case, only a certain fraction of the radioactive materials originally present enter the human organism because of discriminating effects in the metabolism of the livestock. The radioactivity of agricultural products of this type, which make a significant contribution to national crop production, was studied to obtain a quantitative estimate of this effect. Grains, corn, tobacco, and the like were scrutinized (Table 1). Samples were taken at three sites in Western Slovakia: Bratislava-Raca, Bohunice, and Pest'any. One kg assorted grains, 2 kg legumes, 4 kg row crops, and 100 g tobacco and 100 g tobacco leaf, unprocessed, were sampled for analysis. Only the edible portion of potato plants was analyzed. Sugar beet and fodder beet samples were carefully freed of clinging farm soil before being analyzed.

The authors isolated both radioisotopes radiochemically, employing techniques described in the literature [2, 3], and then determined the beta-activity of the isotopes.

Average Sr^{90} and Cs^{137} specific activities in crops grown in Western Slovakia in 1963-1964 are listed in Tables 2 and 3.

The maximum calcium content in grain crops is reported in oats—the minimum in millet. Of all the products studied by the authors, potatoes and corn contain the least calcium, poppy and tobacco the most.

TABLE 1. Contribution of Slovakia and the Western Slovak. District to the Total Agricultural Production of the CSSR, 1964

Crop	Slovakia, %	West. Slovak. District, %	Crop	Slovakia, %	West. Slovak. District, %
Wheat	27.6	18.1	Sugar beet	25.7	20.2
Rye	12.6	4.4	Potatoes	21.0	4.3
Barley	35.7	23.6	Corn (silage)	30.1	16.9
Oats	14.0	4.2	Tobacco	91.2	—
Corn (whole grain)	91.0	76.8	Poppy seeds	16.7	—
Legumes	30.4	—			

District Public Health and Epidemiological Station, Bratislava, CSSR. Translated from Atomnaya Énergiya, Vol. 21, No. 3, pp. 197-201, September, 1966. Original article submitted November 6, 1965; revised April 12, 1966.

TABLE 2. Specific Sr^{90} Activity in 1963-1964 Crops

Crop	No. of sample sites	Calcium content, g/kg		Sr^{90} content, pCi/kg		Sr^{90}/Ca content pCi/g		1963/1964 Sr^{90}/Ca ratio
		1963	1964	1963	1964	1963	1964	
Grains								
Wheat	6	0.45	0.40	108.7	123,8	241.5	309.5	1.3
Rye	4	0.49	0.51	77.3	114.9	157.8	225.7	1.4
Barley	8	0.36	0.43	66.2	162.9	183.9	381.4	2.1
Oats	7	1.06	0.83	62.9	108,1	59.3	130.6	2.2
Millet	2	0.19	0.32	29.7	18.8	156.3	59.4	0.4
Legumes								
Peas	4	1.32	0.88	15.8	10.4	12.0	11.7	1.0
Beans	1	—	1.89	—	25.0	—	13.2	—
Lentils	1	—	0.65	—	14.5	—	22.3	—
Row crops								
Cleaned potatoes	12	0.05	0.05	5.2	2.7	104.0	54.0	0.5
Corn	8	0.05	0.06	3.7	2.1	75.5	35.0	0.5
Sugar beet	4	—	0.22	—	22.4	—	101.8	—
Fodder beet	12	0.51	0.20	17.0	7.4	33.3	37.0	1.1
Miscellaneous crops								
Poppy	2	—	12.56	—	22.0	—	1.9	—
Tobacco	2	—	34.80	—	350.3	—	10.1	—
Fodder beet foliage	5	6.10	—	494.2	—	81.0	—	—

TABLE 3. Specific Cs^{137} Activity in 1963-1964 Crops

Crop	Number of sampling sites	Cs^{137} content, pCi/kg		Cs^{137}/Sr^{90} ratio		1964/1963 Cs^{137} data ratio
		1963	1964	1963	1964	
Row crops						
Wheat	6	180.0	299.2	1.7	2.4	1.7
Rye	4	505.9	344.6	6.5	2.9	0.7
Barley	8	197.2	175.5	3.0	1.1	0.9
Oats	7	290.1	268.4	4.6	2.5	0.9
Millet	2	224.5	248.0	7.6	13.2	1.1
Grains						
Peas	4	310.9	108.5	19.7	10.5	0.3
Beans	1	–	132.7	–	5.3	–
Lentils	1	–	271.8	–	19.4	–
Legumes						
Cleaned potatoes	12	44.0	32.7	8.5	12.1	0.7
Corn	8	150.6	58.6	40.7	27.9	0.4
Sugar beet	4	24.4	15.2	–	0.7	0.6
Fodder beet	12	53.2	11.3	3.1	1.5	0.2
Miscellaneous crops						
Poppy	2	–	117.2	–	5.3	–
Tobacco	2	–	647.1	–	1.8	–
Fodder beet leaves	5	1266.6	–	2.6	–	–

TABLE 4. Average Specific Activities of Sr^{90} and Cs^{137} in 1963-1964 Crops

Isotope	Grains		Legumes		Miscellaneous crops	
	1963	1964	1963	1964	1963	1964
Ca, g	0.51	0.50	1.32	1.14	0.20	0.14
Sr^{90}, pCi/kg	69.0	105.7	15.8	16.6	8.6	8.6
Sr^{90} : Ca, pCi/kg	135.3	211.4	12.0	14.6	43.0	61.4
Cs^{137}, pCi/kg	279.5	265.1	310.9	171.0	68.1	29.4
Cs^{137} : Sr^{90}	4.0	2.5	19.7	10.3	7.9	3.4

The Sr^{90}/Ca ratio is lowest in poppy samples (1.9) and tobacco samples (10.1), owing to the relatively high content of calcium in the product. The Sr^{90} concentration (in strontium units) is much higher in the remaining products, on account of the low calcium content.

Maximum Sr^{90} concentrations were detected in grains (211.4 strontium units) and minimum in legumes (14.6 Sr units). Concentration in row crops was intermediate (61.4 Sr units). The lowest Sr^{90} level in the 1964 crops studies was in the edible part of the potato plant (2.7 pCi/kg) and in corn (2.1 pCi/kg).

A rise in Sr^{90} level in almost all crops above the 1963 level was observed in 1964. The highest increase was observed in barley and oats (the level doubled in these cases). Sr^{90} activity dropped in corn and potatoes (by about 50%).

The maximum specific activity of Sr^{90} and Cs^{137} was observed in tobacco leaf and beets (Cs^{137} content totalled 647.1 pCi/kg, in some cases 1266.6 pCi/kg), followed by grains with an average of 265.1 pCi/kg for 1964, legumes with 171.0 pCi/kg, and finally row crops with a low of 29.4 pCi/kg (Table 3 and 4).

The content of Cs^{137} in agricultural crops was higher than that of Sr^{90} owing to radioactive fallout, in which the Cs^{137} activity is higher than Sr^{90} activity. The Cs^{137}/Sr^{90} ratio in atmospheric fallout usually ranges 1.5 to 2, although it can sometimes surpass that range [4]. The greatest difference in Cs^{137} and Sr^{90} contents is found in corn, where the Cs^{137}/Sr^{90} ratio is 27.9, and in potatoes (12.1). The average Cs^{137}/Sr^{90} ratio for legumes was 10.3 in 1964, and that of the grains millet showed the greatest difference in Cs^{137} and Sr^{90} content.

The 1964 specific activity of Cs^{137} ran below the 1963 figure in all crops studied. A significant decrease as much as 80% was recorded in row crops with the smallest decrease in grains, viz. 5% (see Table 4).

TABLE 5. Cs^{137} and Sr^{90} Content in Atmospheric Fallout Over the Territory of Western Slovakia, 1963-1964

Year	Atmospheric fallout, mm	Fallout density,		Cs^{137}/Sr^{90} ratio
		Cs^{137}	Sr^{90}	
1963	558	29.0	22.5	1.3
1964	555	15.5	16.9	0.9
1964 : 1963	—	0.53	0.75	—

Sr^{90} and Cs^{137} specific activity in plants depends primarily on the amount of those isotopes present in atmospheric fallout. A comparison by the authors of Cs^{137} and Sr^{90} activities in monthly atmospheric fallout reports covering 1963–1964 (Table 5) and in crops (see Table 3) show that the slowdown in the rate of Cs^{137} fallout from the atmosphere also affected Cs^{137} content in plants.

TABLE 6. Relative Amounts of Sr^{90} and Cs^{137} Present in 1964 Crops

Crops compared	Ca	K	Sr^{90}	Sr^{90}:Ca	Cs^{137}
wheat/peas	0.5	0.5	11.9	13.5	2.9
wheat/potatoes	4.8	1.0	20.3	2.4	7.0
peas/potatoes	9.3	1.7	1.7	0.2	2.4
fodder beet foliage/beet .	12.0	0.9	29.1	2.4	23.8

TABLE 7. Distribution of Sr^{90} and Cs^{137} Activities in Potato Tubers

Variable	1963			1964		
	whole tubers	edible part	edible part, %	whole tubers	edible part	edible part, %
weight of wet tuber, g . .	1000	662	66.2	1000	798	79.8
Ca, mg	82	49	59.8	94	53	56.4
Sr^{90}, pCi/kg	11.1	5.2	46.8	6.1	2.7	44.3
Cs^{137}, pCi/kg	61.0	44.0	72.1	44.2	32.7	74.0
Cr^{90}: Ca, pCi/kg	135.4	106.1	—	64.9	50.9	—
Cs^{137}: Sr^{90}	5.5	8.5	—	7.2	12.1	—

Radioactive materials precipitated to the earth's surface are retained mostly in the topsoil layer. Cs^{137} becomes trapped in the top organic layer [5-8], Cs^{137} is taken up by plants from the soil in amounts only one-twentieth the amount of Sr^{90} taken up. The Cs^{137}/Sr^{90} ratio in plant uptake from the soil is roughly 0.03 to 0.20 [9]. The rise in Cs^{137} content in legumes and row crops over the Sr^{90} content can be accounted for only by uptake of cesium which had settled out on the surface of the plant foliage, i.e., traceable directly to atmospheric fallout.

Sr^{90} and Cs^{137} contents also depend on what part of the plant yields the isotope. As far as Sr^{90} is concerned, there are indications that the root system accounts for only 10% of the total amount of this emitter in the plant, whereas the aerial part of the plant concentrates about 90% of the isotope [5, 10].

The isotope distribution in the aerial part of the part is not the same either. Table 6 lists data on content of Sr^{90}, Cs^{137}, calcium, and potassium in samples of 1964-harvested wheat, peas, and potatoes. We see on comparing the data that wheat contains 4.8 times more calcium than potatoes do. The ratio of Sr^{90} present in those products attains the value of 20.3, however. There is no correspondence between the amounts of potassium and Cs^{137} either. Fodder beet foliage accounts for about 96% of the total Sr^{90} and Cs^{137} activity. We can state, in general, that there is no direct relationship between potassium and Sr^{90} content, nor between potassium and Cs^{137} content in plants (e.g., poppy and tobacco, for which see Tables 2 and 3).

The distribution of radioactive materials in the fruits is also nonuniform. Sr^{90} and Cs^{137} distribution in potato tubers was studied, with the edible portion and the skin scrapings analyzed separately. The edible portion of the potato accounts for 45% of the total Sr^{90} activity and 75% of the Cs^{137} activity, whereas the edible portion accounts for 66 to 80% of the total weight of the tubers (Table 7). The amount of this edible portion depends on storage time, brand, and on the size of the potato tubers.

LITERATURE CITED

1. Statisticka rocenka CSSR 1965, [Statistical Almanac of the Czechoslovak Socialist Republic, 1965]. Prague, SNTL-SVTL, (1965).
2. W. Häussermann and W. Morgenstern, Atompraxis, 8, 37 (1962).
3. V. Zboril and T. Trnovec, Chem. zvesti, [Chemical Bulletin], 17, 268 (1963).
4. Report of the UNO Science Committee on Effects of Atomic Radiation (17th session of the UN General Assembly). Appendix 16, New York (1962).
5. E. Mercer and F. Ellis, Report ARCRL, 12, 49 (1964).
6. E. Niemann, Atompraxis, 7, 370 (1961).
7. V. I. Baranov et al., Atomnaya énergiya, 18, 246 (1965).
8. Radioactive Contamination of the Environment. Collection of articles edited by V. P. Shvedov and S. I. Shirokov. Moscow, State Atom press, [in Russian] (1962).
9. H. Squire and L. Middleton, Report ARCRL, 8, 66 (1962).
10. V. M. Klechkovskii and I. V. Gulyakin, Article in the book: Soviet Scientists Speak on the Dangers of Nuclear Weapons Testing. Edited by A. V. Lebedinskii. Moscow, Atom press, [in Russian] p. 58 (1959).

ON THE ANALYSIS OF TRANSITIONAL PROCESSES IN A REACTOR CLOSE TO PROMPT CRITICALITY

Yu. P. Milovanov

UDC 621.039.512

For the case in which there are no neutrons in a reactor up to the onset of the transitional process, the kinetic equation with allowance for delay neutrons can be written as follows:

$$\frac{dn}{dt}=\frac{k(1-\beta)-1}{l}n+\frac{1}{l}\sum_i \beta_i\lambda_i e^{-\lambda_i t}\int_0^t kne^{\lambda_i t}\,dt, \qquad (1)$$

with the usual notation. If we introduce a function

$$\varphi_i(t)=\frac{e^{-\lambda_i t}\int_0^t kne^{\lambda_i t}\,dt}{\int_0^t kn\,dt},$$

then (1) becomes

$$\frac{dn}{dt}=\frac{k(1-\beta)-1}{l}n+\frac{\sum_i \beta_i\lambda_i\varphi_i(t)}{l}\int_0^t kn\,dt.$$

The principal properties of φ_i (t) are as follows:

$$\varphi_i(0)=1;\ \varphi_i(t)<1;\ -\lambda_i\varphi_i<\frac{d\varphi_i}{dt}<0;$$

$$\lim_{t\to 0}\frac{d\varphi_i}{dt}=-\frac{\lambda_i}{2}\varphi_i.$$

The lower limit of the function for increasing neutron flux is found from the formula

$$\varphi_i(t)=\frac{1}{1+\frac{\lambda_i\int_0^t kn\,dt}{kn}}.$$

If the flux decreases sufficiently rapidly, φ_i (t) $\approx e^{-\lambda_i t}$.

As an example of the application of the function φ_i (t), consider the kinetic equation with allowance for delay neutrons, when the reactivity for a prompt-critical reactor has a negative temperature coefficient. The equation has an approximate solution in the form

$$n(t)\approx\frac{e^{\alpha(t-t_0)}}{1+e^{\alpha(t-t_0)}}\cdot\frac{\sum_i \beta_i\lambda_i\varphi_i(t)}{\gamma},$$

where

$$\alpha\approx\sqrt{\frac{\sum_i \beta_i\lambda_i}{l}};$$

Translated from Atomnaya Énergiya, Vol. 21, No. 3, p. 202, September 1966, No. 97/3652
Original article submitted March 17, 1966. Abstract submitted June 1, 1966.

Here t_0 is the time after which the neutron flux increases to half its maximum intensity, and γ is the temperature coefficient of the reactivity.

The kinetic equation in form (1), for a negative temperature coefficient of the reactivity (occurring in the expression for k), is incapable of analytic solution. The introduction of φ (t) simplifies the analysis of the kinetic equation, and in some cases enables us to find a simple approximate solution for the characteristics of the transition process in the reactor (especially in pulsed conditions). To assess the influence of delay neutrons in pulsed conditions, we can conveniently write the kinetic equation in the form

$$n(t) = \frac{\gamma \int ndt}{\gamma \int ndt - \delta k(t) + \frac{l}{n} \cdot \frac{dn}{dt}} \cdot \frac{\sum_i \beta_i \lambda_i \varphi_i(t)}{\gamma}.$$

DOSE BUILD-UP FACTORS FOR LOW-ENERGY γ RAYS IN HOMOGENEOUS AND HETEROGENEOUS BARRIERS

D. B. Pozdneev

UDC 539.122:539.121.72:621.039.58

The author has experimented on the passage of γ rays, from a point isotropic source with primary γ-quantum energy 0.279 or 0.661 MeV, through homogeneous barriers made of graphite, aluminum, iron, cadmium, and lead, and heterogeneous barriers made of combinations of these materials. He used a scintillation dosimeter with energy-dependence compensation, and a scintillation spectrometer; the spectra were processed by the inverse sensitivity-matrix method. The results were plotted as graphs of the dose build-up factor B_D versus the barrier thickness, for the energies studied, and were also tabulated.

Analysis of the data revealed the importance of the end effect at low energies: this means that, especially for light shielding, the factors B_D are appreciably less than for an infinite medium. For two-layer barriers the experimental data agree with the empirical formula of D. L. Broder et al. At the same time, for most of these barriers, within the experimental error (10%), the usual recommendations are satisfied, according to which the dose build-up factor of a heterogeneous shield in which the light element follows the heavy one is approximately equal to the product of the factors for the component homogeneous shields, while if the positions of the components are reversed it is equal to the dose build-up factor of the heavy component with a thickness equal to that of the shield as a whole. The author gives tables comparing their experimental values for B_D with data calculated from the above formulae and recommendations. He also gives data for multi-layer heterogeneous barriers composed of alternating layers of light (graphite) and heavy (cadmium) shielding.

Translated from Atomnaya Énergiya, Vol. 21, No. 3, p. 203, September, 1966, No. 101/3529
Original article submitted December 7, 1965. Abstract submitted May 25, 1966.

ALBEDO OF A HOMOGENEOUS BARRIER OF FINITE THICKNESS FOR LOW-ENERGY γ RAYS

D. B. Pozdneev

UDC 539.122:539.121.72

The author describes an experimental investigation of back scattering of γ rays from an isotropic point source in close contact with scattering barriers, of finite thickness, made of graphite, aluminum, iron or cadmium. The energy of the primary γ rays was $E_0 = 0.279$ or $E_0 = 0.661$ MeV. The values (numerical and energetic) found for the albedo of a barrier of thickness x for the free paths were represented by the empirical formulae $A(x) = A(\infty)(1 - e^{-ax})$ and $A_E(x) = A_E(\infty)(1 - e^{-a_E x})$, where $A(\infty)$, $A_E(\infty)$ are the numerical and energetic albedos, respectively, for a semi-infinite medium, and α and α_E are empirical quantities. The author gives the values of $A(\infty)$, $A_E(\infty)$, α and α_E for the shielding materials under investigation and for the energies of the primary photons used. Data are given on the spectral and angular distributions of the back-scattered γ-quanta. The author compares the experimental energy spectra and angular distributions for graphite, with $E_0 = 0.661$ MeV, with results found for water by the Monte-Carlo method.

The results are displayed as graphs and tables.

Translated from Atomnaya Énergiya, Vol. 21, No. 3, p. 203, September, 1966, No. 98/3577
Original article submitted January 14, 1966. Abstract submitted June 13, 1966.

TWO-CHANNEL SYSTEM FOR SYNCHRONOUS REGISTRATION OF FISSION FRAGMENTS FROM A STANDARD AND A SPECIMEN UNDERGOING ANALYSIS

E. M. Labonov, P. I. Chalov, and U. Mamyrov

UDC 539.16.08:539.173

The capacity of some isotopes to form fission fragments on irradiation with neutrons enables them to be determined by activation analysis. Determinations of the isotope ratio U^{235}/U^{238} [1-3], based on fission fragments, have been made by successive measurement of the rates of fission-fragment formation when a standard and the specimen were irradiated in turn. However, if a nuclear reactor is used as neutron source [3], the accuracy of the measurements can be affected by the following factors: (a) fluctuations in the neutron flux density, slower than the exposure times; (b) similarly slow variations in the neutron energy spectrum. The present authors have therefore tried to carry out synchronized measurements of the rates of fission-fragment formation by a standard and the specimen, in a neutron beam with intensity and energy spectrum which can be varied with time.

The specimen and standard were placed in a pulse-type ionization chamber made of Plexiglas and filled with argon at 1 atm pressure. The chamber had a high-voltage electrode, which simultaneously served as a holder for the specimen and standard, together with two collecting electrodes. Voltage pulses arising at the collecting electrodes were amplified by pre-amplifiers and main amplifiers, and then fed to discriminators. The latter cut out pulses caused by other types of radioactive radiation

Results of Determinations of the Cadmium Ratios of Uranium Standards of Identical Isotopic Composition

No. of measurement	Standard	Measurement of cadmium ratio in first channel			Measurement of cadmium ratio in second channel				Relative value of K_2 when $K_1 = 1$		
		Cadmium ratio K_1	Experimental error, due to statistical fluctuations	Actual deviation of K_1 from mean value	Standard	Cadmium ratio K_2	Experimental error, due to statistical fluctuations	Actual deviation of K_2 from mean value	K_2/K_1	Error in determining K_2/K_1 due to statistical deviations	Actual deviation of K_2/K_1 from mean of the nine measurements
1	2	3	4	5	6	7	8	9	10	11	12
1	A-5	9.340	0.031	0.177	A-4	9.487	0.028	0.146	1.016	0.006	0.004
2	A-5	9.641	0.028	0.124	A-3	9.726	0.024	0.093	1.009	0.005	0.003
3	A-3	9.546	0.036	0.029	A-7	9.584	0.038	0.049	1.004	0.009	0.008
4	A-7	9.619	0.030	0.102	A-8	9.689	0.029	0.056	1.007	0.006	0.005
5	A-6	9.545	0.027	0.028	A-9	9.721	0.028	0.088	1.018	0.006	0.006
6	A-4	9.495	0.031	0.022	A-6	9.649	0.036	0.016	1.016	0.006	0.004
7	A-8	9.587	0.034	0.070	A-1	9.689	0.035	0.056	1.011	0.006	0.001
8	A-11	9.482	0.036	0.035	E-10	9.555	0.054	0.078	1.008	0.010	0.004
9	A-10	9.402	0.035	0.115	E-2	9.594	0.055	0.039	1.020	0.010	0.008
Average		9.402	0.032	0.078		9.633	0.036	0.069	1.012	0.007	0.005

Note. Standards A_i are uranium evaporated from solution on to aluminum with thickness of 1 mm; standards E_i are of uranium electrodeposited on stainless steel with thickness of 1 mm.

Translated from Atomnaya Énergiya, Vol. 21, No. 3, pp. 204-205, September, 1966. Original article submitted February 22, 1966.

(which were appreciably lower in amplitude), and passed only those pulses which were due to fission fragments. These were registered by scaling circuits.

Thus our system for synchronous registration of fission fragments from the standard and specimen consists of two identical recording channels which are used to count the fission fragments [1-3]. Two sensitive volumes, in which fission fragments from the standard and specimen ionize the gas, are combined in one chamber. Simultaneous measurement of fission fragments from the standard and specimen excludes the effects of variations in the intensity and energy spectrum of the neutron beam, and enables us to secure an accuracy limited only by the statistical fluctuations of the number of fission events.

To illustrate these results, the table gives determinations of the cadmium ratios for 18 uranium standards of the same isotopic composition, deposited in thin layers on aluminum and stainless-steel substrates. The neutron source was a horizontal channel of the VVR-S nuclear reactor, with a neutron flux density of $1.75 \cdot 10^8$ neutrons/$cm^2 \cdot$ sec.

The results of nine determinations of the cadmium ratio for the same radioactive preparation in the first recording channel (see column 3 of table) show that, when the error in this quantity due to statistical fluctuations is $\sim 0.3\%$ (column 4), the actual deviation from the mean of the nine measurements was $\ll 1.8\%$ averaging $\sim 0.8\%$. The same pattern is observed in determinations of the cadmium ratio K_2 for the second channel (columns 7-9). This leads us to conclude that uncontrolled factors are operating on the measurements. If one of the channels is used as a reference datum, enabling us to allow for these factors, we can be sure that the accuracy will be limited only by statistical fluctuations. In fact, the ratio of K_2 to K_1 (column 10) (taking the first channel as reference datum) deviates from the mean value (column 12) in all nine cases by less than the errors calculated from the statistical fluctuations of the number of fission events.

Thus we can assume that the introduction of the second channel as standard enables us to eliminate the effects of variations in the neutron flux on the measurements of the relative contents of isotopes in the fission fragments.

It is noteworthy that the ratio K_2/K_1 differs somewhat from unity. If we calculate the weighted mean of this quantity over the nine measurements of varying accuracy, together with its r.m.s. error, we get 1.011 ± 0.002. On interchanging the registration channels, we obtained the values 0.984 ± 0.006, coinciding with K_1/K_2 which is 0.988 ± 0.002. It follows that the channels were not identical for the registration of fission fragments. However, their difference can be allowed for with considerable accuracy, or eliminated by suitable choice of the characteristics of the recording apparatus.

We can thus conclude that, in determining isotopic contents by means of fission fragments from nuclei in neutron beams which have intensities and energy spectra varying with time, a circuit with two-channel registration of the fragments enables us to eliminate the effects of these variations on the results, and to obtain an accuracy limited only by the statistical fluctuations of the fission events. Another advantage of this method is that it halves the time required for a determination.

The authors wish to thank their fellow-workers in the Department of Radioactive Irradiation of the Kazakh State University, E. A. Isabaev and A. Abil'daev, for allowing them to use the pulsed chamber in their experiments, and also the Director of the Institute of Nuclear Physics of the Uzbekhistan Academy of Sciences for permission to work with this institution's reactor.

LITERATURE CITED

1. L. I. Shmonin et al., Bulletin of the Commission for Determination of the Absolute Age of Geological Formations, No. 1, 64 (1955).
2. V. V. Cherdyntsev et al., Geokhimiya, No. 4, 37 (1960).
3. K. A. Petrzhak, I. M. Semenushkin, and M. A. Bak, Geokhimiya, No. 2, 27 (1956).

ABSORPTION OF THE ENERGY OF γ-RADIATION FROM A UNIDIRECTIONAL POINT SOURCE OF γ-QUANTA, IN PLANE GEOMETRY

F.A. Makhlis, L.A. Sugak,
E.A. Plandin, and I.K. Shmyrev

UDC 539.122:539.121.73

It is known [1] that we can use data on the absorption of energy from unidirectional point γ-ray sources to derive detailed information on the dose absorption fields of sources of any shape and size with any angular γ-ray distribution.

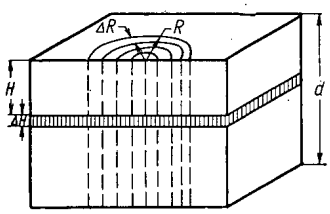

Fig. 1. Geometrical scheme of calculation.

By using the Monte-Carlo method, we have studied the absorption of γ-radiation from a unidirectional point Co^{60} source located on the surface of a plane-parallel water-equivalent plate of infinite extent and finite thickness. From the results we estimated the accuracy of the calculation, using the absorbed-energy build-up factors and the so-called γ method [2]. The calculation was performed with "Minsk-1" computer by a previously-devised method [2]. We calculated the histories of over 5,000 γ-quanta. We summed the energy absorbed in ring-shaped coaxial layers with radial step ΔR equal to 3 or 5 cm. The plate was divided in thickness into plane layers with thickness ΔH, also equal to 3 or 5 cm.

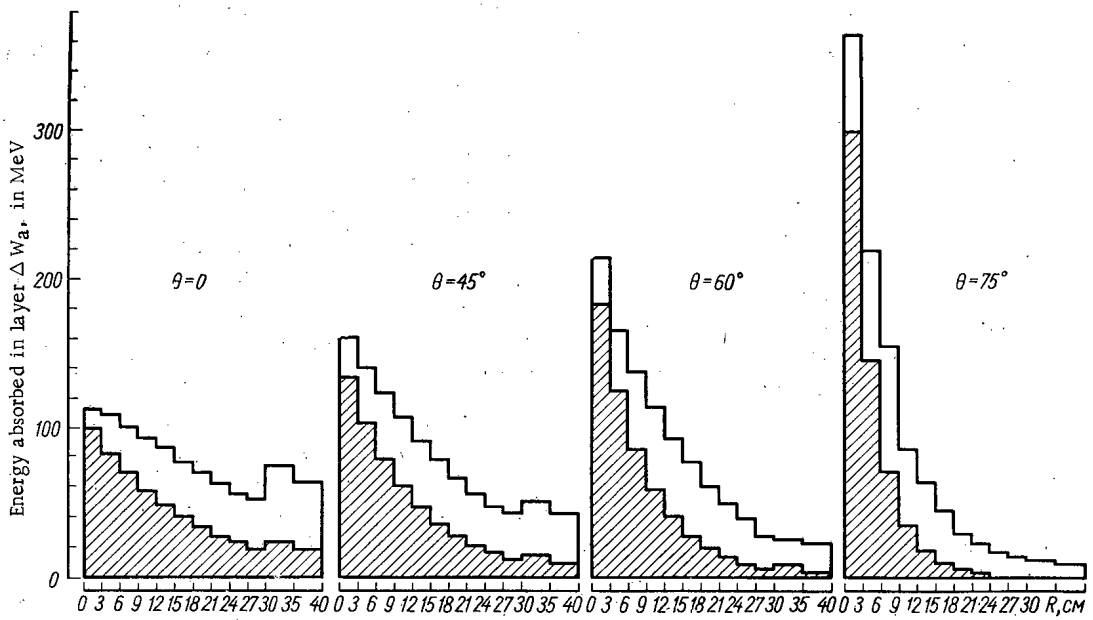

Fig. 2. Distribution of energy, from unidirectional points Co^{60} γ-ray source, absorbed in water-equivalent block of rectangular cross section, found by the Monte-Carlo method. (Crosshatched histograms were calculated without allowing for multiple scattering).

Translated from Atomnaya Énergiya, Vol. 21, No. 3, pp. 205-207, September 1966. Original article submitted December 30, 1965. Revised May 16, 1966.

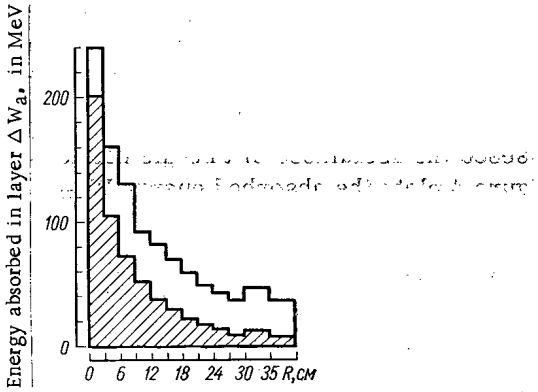

Fig. 3. Distribution of energy, from semi-isotropic point source, absorbed in water-equivalent block of rectangular cross section.

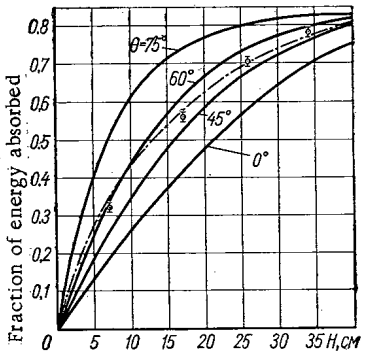

Fig. 4. Absorption in an infinite plane layer of energy of γ-radiation from unidirectional point sources (0, 45, 60, and 75°) and from semi-isotropic Co^{60} sources. (———) unidirectional source (— · —) semi-isotropic source (⊙) semi-isotropic source (γ method).

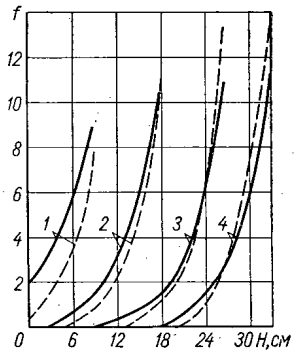

Fig. 5. f (%) versus H, d and θ. In the calculation it was assumed that $\Delta H = 3$ cm, if $H < 30$ cm, and that $\Delta H = 5$ cm, if $H \geq 30$ cm ——— 0°; ----- 75°. (1-4) d = 12, 21, 30 and 40 cm, respectively.

We considered quanta with angles of incidence, θ, varying from 0 to 75° (where θ is the angle between the direction of motion of the γ-quanta and the normal to the object, (Fig. 1)

Figure 2 gives histograms of the distribution of absorbed energy $\Delta W_{a\theta}$ in plane layers ΔH for γ-quanta with angles of incidence of 0, 45, 60, and 75°. It also shows the corresponding values of the absorbed energy calculated without allowing for multiple scattering. We then used the distribution found for the absorbed energy of the unidirectional point radiation sources, $\Delta W_{a\theta}$, to find the distribution for a semi-isotropic point source, ΔW_a. The results, obtained by means of numerical integration with respect to θ, are given in Fig. 3.

It will be observed that the nature of the absorbed-energy distribution depends on the angle of incidence of the γ-radiation. Thus, in the first layer, the absorbed energy ($H = 0$, $\Delta H = 3$ cm) with $\theta = 75°$ is greater than that with $\theta = 0°$ by a factor of 3.3; on the other hand, the energy absorbed in the last layer ($H = 35$ cm, $\Delta H = 5$ cm) with $\theta = 75°$ is less than that with $\theta = 0°$ by a factor of 7. It is interesting to note that, in this case, the total energy absorbed in a thick enough plate (40 cm) hardly varies with changes in the angle of incidence of the γ-rays (to within ~ 10%).

It is rather difficult to allow for multiple scattering when calculating the absorbed energy from an extended source. It is apparently for this reason that some authors consider it permissible to neglect this effect for very thin irradiated objects. However, Figure 2 shows that this assumption is erroneous, because the contribution of multiple scattering exceeds 10%, even for an irradiated object with a thickness of 3 cm (for any θ). If the layer is 12 cm from the source, the contribution of multiple scattering ranges from 45% ($\theta = 0°$) to 75% ($\theta = 75°$); for a semi-isotropic point source, the corresponding value is ~ 54%.

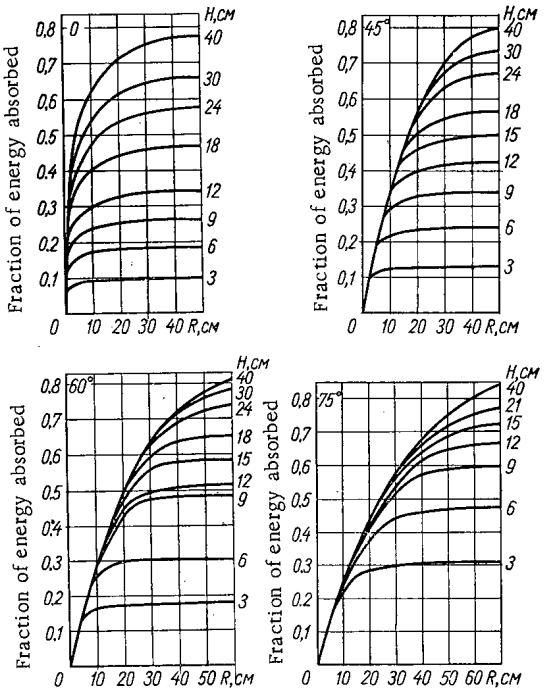

Fig. 6. Radial distributions of absorbed γ-ray energy from undirectional point Co^{60} sources in a semi-infinite water-equivalent medium, with $\theta = 0, 45, 60, 75°$.

We have shown [2], by means of calculations in spherical geometry by the Monte-Carlo method, that the γ method is convenient for calculating the absorption of the energy of γ-radiation from Co^{60}. We have now also assesed the usefulness of this method for plane geometry. Figure 4 plots the absorbed energy W'_{aH}, referred to the power S of a unidirectional point or semi-isotropic radiation source, versus the thickness H of a water-equivalent plane layer of infinite extent. It also plots the corresponding quantities calculated by the γ method. The error in using the γ method is below 5-6%.

Effects of Boundary Conditions. The influence of the finiteness of the object was estimated by means of the quantity

$$f = \frac{W_a(H, \infty) - W_a(H, d)}{W_a(H, \infty)}.$$

Here W_a (H, ∞) is the energy absorbed in layer ΔH located inside a semi-infinite object and at a distance H from the source; W_a (H, d) is the energy absorbed in the same layer ΔH located inside an object of thickness d and also at a distance H from the source. Figure 5 plots f versus H and d for $\theta = 0°$ and $\theta = 75°$, as given by the Monte-Carlo method: it shows that (1) as in the case of spherical geometry, the influence of the finiteness of the medium extends from its boundary by a distance less than the free-path length of the γ-quanta; (2) the influence of the finiteness of the medium is almost independent of the angle of incidence of the γ-rays; in the range considered, the values of f for various values of θ vary only by 3% abs., usually by much less; and (3) the influence of the finiteness of the medium increases with the thickness of the object, because the build-up of scattered radiation increases and the contribution of primary radiation decreases; for an object less than 40 cm thick, $f \leq 14\%$.

We have discussed the distribution of absorbed energy in a layer with finite thickness but infinite extent. However, in calculating the energy absorbed in objects of finite size, we must also know the radial distribution. Figure 6 shows the radial distributions of the absorbed energy for a series of unidirectional point sources (0, 45, 60, 75°). These are displayed as graphs of $W_{a\Theta}/S$, the energy absorbed within a cylinder with the source at the center of its base, versus the radius R and height H of this cylinder. In performing the calculation we added up the energy absorbed in coaxial ring-shaped (ΔR) and plane (ΔH) layers, using the Monte-Carlo method.

LITERATURE CITED

1. L. R. Kimel' and O. I. Leipunskii, Atomnaya Énergiya, 12, 236 (1962).
2. F. A. Makhlis et al., Inzh.-fiz. zh., 8, 675 (1965).

A SOURCE OF LITHIUM IONS FOR AN ELECTROSTATIC GENERATOR

V. M. Korol' and V. S. Siksin

UDC 539.103

Since the first experiments by Allison's group [1] in 1956, nuclear reactions due to accelerated lithium ions have been studied in many laboratories. Many publications on this subject have appeared.

With the aim of further studies of nuclear reactions due to lithium ions accelerated by the ÉG-2.5 E.S. generator, we have built and tested a lithium-ion source. The emitter of lithium ions is an artifically-prepared lithium aluminosilicate, $Li_2O \cdot Al_2O_3 \cdot 2SiO_2$, deposited on a tungsten spiral [3, 2]. When a suitable current is passed through the wire, surface ionization causes the formation of positive singly-charged lithium ions.

In designing the source, special attention was paid to securing maximum operating time without dismantling the source to change the filament, even with a high accelerated-ion current. As seen from diagram a, the source consists of a standard three-electrode focussing lens 1 and a housing (2, lower part; 3, upper part). The middle electrode of the lens is at a positive potential, the end electrodes at negative potentials with respect to the housing. Conical electrode 9 is the extraction electrode. Inside the housing is the filament holder consisting of shaft 6, porcelain insulator 4, molybdenum lobes 7 and copper current leads 5, grounded molybdenum diaphragm 8 and spring contacts 10, 11 (see diagram b). Contact 10 is grounded. Potential is fed to the filament via electro-vacuum lead 13 to contact 11, which is insulated by porcelain sleeve 12. Seven tungsten wires 14 with diameter 0.3-0.4 mm, are spot-welded on to the molybdenum lobes. If the filament burns out or loses lithium-ion emission, it can be replaced by rotating shaft 6. As seen from diagram b, all the filaments can be heated together, reducing the time required for outgassing. An inspection window in the center of the upper part of the housing permits observation of the filament through a system of mirrors. The upper part of the housing carries a motor which rotates shaft 6 slowly (1-2 rev/min) to exchange the filaments. A simple control system with cutout switches enables any filament to be located above the extraction electrode. Fine adjustment of the filaments is monitored by maximum ion current to a Faraday cylinder behind the accelerator tube.

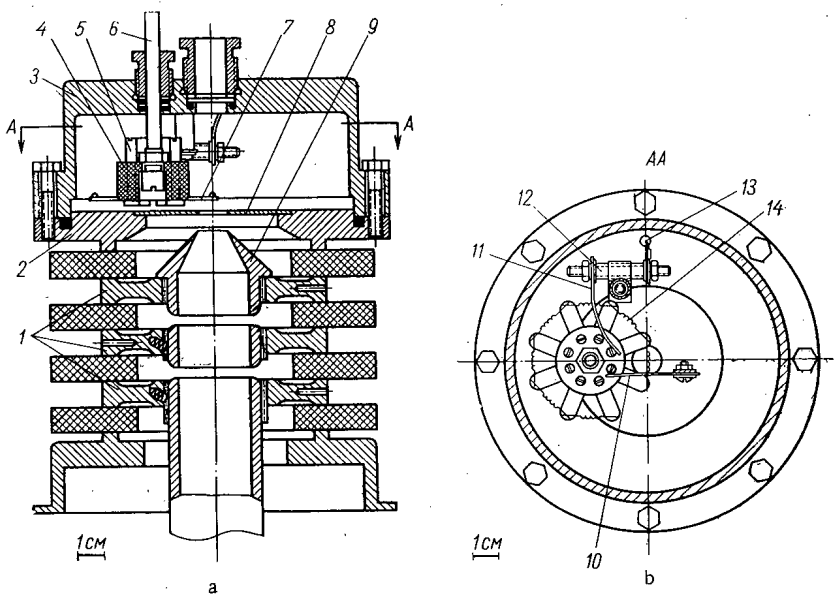

Diagram of lithium-ion source. (a) Vertical section; (b) Section AA.

Translated from Atomnaya Énergiya, Vol. 21, No. 3, pp. 208-209, September 1966. Original article submitted February 18, 1966.

The ion source was subjected to preliminary tests on a test stand. The accelerator tube was part of the ÉG-2.5 accelerator tube, with seven electrodes. The ion optics of the test rig were thus close to those of the source in the electrostatic generator itself. In the tests, the potential of the extraction electrode was up to 10 kV, and the accelerating voltage was 60 kV.

Mass spectrometry showed that, in addition to the main peaks with $m/e = 6$ and $m/e = 7$ ($^6Li^+$ and $^7Li^+$ ions), there are very small peaks with $m/e = 3.5$ (doubly-charged $^7Li^{++}$ ions) and $m/e = 23$ (Na^+ or LiO^+ ions), constituting 0.5% of the $^7Li^+$ peak. By using Li_2CO_3 or Li_2O enriched to 50% ^6Li in preparing the aluminosilicate, it is possible to get approximately equal $^6Li^+$ and $^7Li^+$ beams, thus doubling the number of possible experiments with accelerated lithium ions.

The tests showed that the beam current and focussing depend largely on the diameters of the diaphragm and hole of the extracting electrode, the distance between them, and the shape of the extraction electrode. When all the dimensions are increased, the ion-beam current increases, but the focussing worsens.

Good focussing (1 mm diameter of red spot on quartz screen) can be attained with a diaphragm 6.5 mm in diameter and a 4 mm diameter hole in the extraction electrode, and a distance between them of 4 mm. With these dimensions, the maximum ion current to the Faraday cylinder placed immediately behind the accelerator tube was 370 μA. When all the dimensions were increased to 12 mm, the maximum current became 500 μA.

We tested filaments of two types-cylindrical and conical spirals. No appreciable difference was observed. The current through the filaments was 5.5-10 A, depending on the diameter of the wire, the thickness of the aluminosilicate coating, and the desired ion current. The maximum power expended per filament was below 20 W. The ion current varied from filament to filament by a factor of 1.5-2. This may be due to malpositioning of the filaments relative to the extraction electrode, and to variations in the thickness of the emitter coatings.

LITERATURE CITED

1. S. Allison et al., Phys. Rev., 102, 1182 (1956).
2. S. Allison and M. Kamegai, Rev. Scient. Instrum., 32, 1090 (1961).
3. Ya. M. Fogel' and A. D. Timofeev, Uch. zap. Khar'kovsk. Inst. XCVIII, 177 (1958).

A METHOD FOR SOLVING THE DIFFUSION EQUATION

V. S. Shulepin

UDC 621.039.512.4

It is known [1] that the diffusion equation is reducible to a factorized system of three nonlinear first-order differential equations. We shall show that a homogeneous equation for the neutron flux in a symmetric one-dimensional reactor can be reduced to a system of two nonlinear first-order equations.

Let us write the diffusion equation in the form

$$\frac{1}{r^\nu}\cdot\frac{d}{dr}\left(r^\nu D\frac{d\Phi}{dr}\right)+B^2\Phi=0, \tag{1}$$

where D is the diffusion coefficient; Φ is the scalar neutron flux; $B^2=\frac{\nu_f\Sigma_f}{k_{\text{eff}}}-\Sigma_c$; ν_f is the number of neutrons formed per fission; Σ_c, Σ_f are the absorption and fission cross sections, respectively; ν is 0, 1, 2 for plane, cylindrical, and spherical geometry, respectively.

We introduce the function

$$\beta(r)=\frac{\frac{\Phi}{2}+D\frac{d\Phi}{dr}}{\frac{\Phi}{2}}. \tag{2}$$

From Eq. (2) we obtain

$$\Phi\beta=\Phi+2D\frac{d\Phi}{dr}; \tag{3}$$

$$\frac{d\Phi}{dr}=\frac{\Phi(\beta-1)}{2D}. \tag{4}$$

Applying the operator $\frac{1}{r^\nu}\cdot\frac{d}{dr}r^\nu$, to both sides of Eq. (3), we write

$$\frac{1}{r^\nu}\cdot\frac{d}{dr}(r^\nu\beta\Phi)=\frac{1}{r^\nu}\cdot\frac{d}{dr}(r^\nu\Phi)+\frac{2}{r^\nu}\cdot\frac{d}{dr}\left(r^\nu D\frac{d\Phi}{dr}\right), \tag{5}$$

from which, using Eq. (1) and (4), we arrive at the following equation for β:

$$\frac{d\beta}{dr}=(1-\beta)\left[\frac{\nu}{r}+\frac{(\beta-1)}{2D}\right]-2B^2. \tag{6}$$

From formula (2) we see that when r = 0 (at the center of the reactor), we have $\beta=1$, because at this point $d\Phi/dr = 0$; since the flux is symmetric. The condition at the boundary between the two media is that β must be continuous, which follows from the boundary conditions of the diffusion approximation.

Equation (6) can be solved numerically, e.g., by the Kutta method [2]. To use this method, we must know the value of the right side of the equation at the point r = 0, where it has a singularity. We transform Eq. (6) in order to remove the singularity by multiplying both sides by r and introducing the function $\alpha=\beta r$. We then have

$$\frac{d\alpha}{dr}=\frac{\alpha}{r}+\left(1-\frac{\alpha}{r}\right)\left[\nu+\frac{\left(\frac{\alpha}{r}-1\right)r}{2D}\right]-2rB^2 \tag{7}$$

with the condition $\alpha(0)=0$. The value of α/r on the right side of Eq. (7) is defined for r = 0, since $\lim_{r\to 0}\alpha/r=\beta(0)=1$.

Translated from Atomnaya Énergiya, Vol. 21, No. 3, pp. 209-210, September, 1966. Original article submitted February 22, 1966.

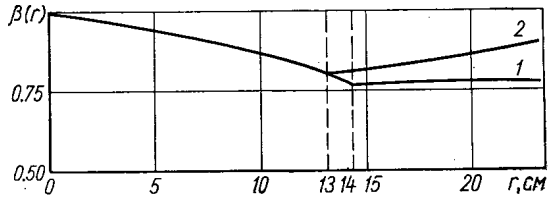

Graph of the function $\beta(r)$.

Calculation Constants

Constants	Active zone	Reflector
D	1.30	1.00
Σ_c	0.028	0.0070
$\nu_f\Sigma_f$	0.040	0.00

If the function $\beta(r)$ is known, the flux Φ can be found by solving Eq. (4), for which $\left.\frac{d\Phi}{dr}\right|_{r=0} = 0$. The analytic solution of Eq. (4) has the form

$$\Phi(r) = C \exp \int_0^r \frac{(\beta-1)}{2D}\, dr,$$

where C is a constant.

It is known that when we solve the problem in the diffusion approximation at the outer boundary of the reactor ($r = R_b$), the condition is

$$\frac{\Phi(R_b)}{2} + D \left.\frac{d\Phi}{dr}\right|_{r=R_b} = 0,$$

which, in accordance with Eq. (2), can be written in the form

$$\beta(R_b) = 0 \qquad (8)$$

The condition (8) enables us to find the value of k_{eff} for a reactor of finite dimensions. To do this, we solve Eq. (7) several times for different values of k_{eff} and then plot the graph of $\beta(R_b)$ as a function of k_{eff}, which will give us the desired value of k_{eff} for $\beta = 0$. This method may be preferable to the iteration method used for solving a factorized system of equations equivalent to Eq. (1), since it enables us to find the value of k_{eff} more quickly when the iteration process converges slowly.

The criterion (8) cannot be used for finding the value of k_{eff} for a reactor with an infinite reflector. In this case, as the numerical calculation shows, β tends to a constant value as the distance from the active zone increases (see figure). By using the analytic solution of Eq. (1), we found that when $k_{eff} = 1$, the critical radius of the active zone is $R_{az} = 14.2$ cm. Equation (7) was solved by the Kutta method with an r interval of 1 cm for the indicated values of k_{eff} and R_{az}. The calculation constants are shown in the table.

As can be seen from the figure, the function $\beta(r)$ decreases with increasing distance from the center of the active zone and tends to a constant value in the reflector (Curve 1). We also carried out the reactor calculations for $k_{eff} = 1$ and $R_{az} = 13$ cm, i.e., for a subcritical reactor. In this case the function $\beta(r)$ increases in the reflector (Curve 2).

The function $\beta(r)$ is not the only function usable for the transition from Eq. (1) to an equation of the type of (4) and (6). In [3] it is shown that using the function $\eta(r) = d\Phi/dr/\Phi$ will also lead to equations similar to (4) and (6).

The method can be extended to the multi-group case if we know the ratios $\frac{\Phi_1}{\Phi_2}, \frac{\Phi_1}{\Phi_3}, \frac{\Phi_2}{\Phi_3} \cdots$ (where the subscripts 1, 2, 3, ... are the numbers of the groups at the center of the reactor; these ratios may be given approximately, e.g., as the ratios of the group fluxes in an infinite medium.

The author thanks G. Ya. Rumyantsev, Yu. I. Orekhov, and L. Ya. Isakova for their valuable critical comments.

LITERATURE CITED

1. G. I. Marchuk, Calculation Methods for Nuclear Reactors [in Russian]. Moscow, Gosatomizdat (1961).
2. E. D. Booth, Numerical Methods [Russian translation]. Moscow, Fizmatgiz (1959).
3. S. Bingulac et al., Report No. 706, presented by Yugoslavia at the Third International Conference on the Peaceful Uses of Atomic Energy (Geneva, 1964), [in Russian].

USE OF GENERAL-PURPOSE ELECTRONIC COMPUTERS FOR COMPLEX EVALUATION OF URANIUM PROSPECTING STUDIES

I. A. Luchin

UDC 550.8

All known uranium deposits have been discovered by radiometric methods. But these methods have a very restricted depth of penetration. They can be used to explore deposits on sites with unconsolidated deposits no thicker than 10 to 12 m. Exploration of deep-lying deposits or of deposits not showing at the surface is pursued at a higher level with liberal use of general geophysical (gravimetric, electrometric, magnetrometric) methods, lithological and petrographic methods, geochemical, and other methods.

TABLE 1. Homogeneous Data File on Deposits. Ore Showings, and Ore Fields

Indices of informational elements	Serial number for indexing characteristic of informational element	Indices of informational elements	Serial number for indexing characteristic of informational element
Principal and subsidiary useful components	1	Differentiation of ore host structures by the resistance method	28
Location in stratigraphic column	2	Differentiation of lithological differences in rock host to, or controlling, mineralization, by the resistance method	29
Position in regional geological structures	3	Differentiation of structural elements by the induced polarization method	30
Relationship to local structures	4	Apparent induced polarizability of ore host lithological differences in rock	31
Host ore-bearing structures	5	Apparent induced polarizability of ore object	32
Relationship to magmatism	6	Regional geological structures in the field of the total magnetic vector	33
Formational control	7	Local geological structures in the field of the total magnetic vector	34
Epigenetic rock changes	8	Ore host structures in the field of the total magnetic vector	35
Presence of precipitant elements	9	Ore host and ore controlling lithological differences in the field of the total mavnetic vector	36
Oxidation and reduction situation	10	Regional structures in the field of the vertical component of the magnetic vector	37
Epigenetic mineralization	11	Local structures in the field of the vertical component of the magnetic vector	38
Satellite elements of the principal component	12	Ore host structure in the field of the vertical component of the magnetic vector	39
Morphology of ore bodies	13	Ore host and ore controlling lithological differences in rock in the field of the vertical component of the magnetic vector	40
Scales of mineralization	14	Regional structures in the gravitational field	41
Orebody outcrops, area	15	Local structures in the gravitational field	42
Size and area of anomaly, with respect to principal component	16	Ore host structure in the gravitational field	43
Size of anomaly, with respect to direct and indirect indicator elements	17	Ore host and ore controlling differences in rock in the gravitational field	44
Area of anomaly with respect to direct and indirect indicators	18	Scales of geological and geophysical surveys	45
Shape, size, and area of emanation anomaly	19		
Size and area of aeroradiometric anomaly	20		
Size and area of auto-anomaly, plow anomaly, γ-anomaly	21		
Size and area of on-foot γ-ray survey anomaly	22		
Magnetic susceptibility of altered rocks and ores	23		
Polarizability of altered and unaltered rocks and ores	24		
Density of altered and unaltered rocks and ores	25		
Differentiation of regional structures by the resistance method	26		
Differentiation of local structure by the resistance method	27		

Translated from Atomnaya Énergiya, Vol. 21, No. 3, pp. 210-215, September, 1966. Original article submitted January 3, 1966.

TABLE 2. Coding of Indexing Characteristics of Elements in Homogeneous Data File on Deposits, Ore Showings, and Ore Fields.

Serial No. and code of indexing characteristic of informational element	Designation of indexing characteristic	What is being coded	Code	
			decimal-coded	binary-coded
1 (1)	Principal and subsidiary useful components	Principal component:		
		molybdenum	01	000 001
		lead	02	000 010
		gold	03	000 011
		uranium	04	000 100
		iron	05	000 101
		copper	.....	.....
		zinc	12	001 100
		Subsidiary component:		
		molybdenum	0001	000 000 000 001
		lead	0002	000 000 000 010
		gold	0003	000 000 000 011
		uranium	0004	000 000 000 100
		iron	0005	000 000 000 101
		thorium	0006	000 000 000 110
		.....	.....	.....
		nickel	0014	000 000 001 110
		No subsidiary component	0	0
2 (10)	Position in stratigraphic column	Pre-Cambrian	01	000 001
		Lower Ordovician	02	000 010
		Middle Ordovician	03	000 011
		Upper Ordovician	04	000 100
		Ordovician (not determined exactly)	10	001 010
		Lower Silurian	11	001 011
		Upper Silurian	12	001 100
		Silurian (not determined exactly)	20	010 100
		Lower Devonian	21	010 101
		Middle Devonian	22	010 110
		Upper Devonian	23	010 111
		Devonian (not determined exactly)	30	011 110
		Carboniferous	31	011 111
		Permian	32	100 000
		Triassic	33	100 001
		Jurassic	34	100 010
		Cretaceous	35	100 011
		Ternary period	36	100 100
		Quaternary period	37	100 101
		Data lacking	0	0

Serial No. and code of indexing characteristic of informational element	Designation of indexing characteristic	What is being coded	Code	
			decimal-coded	binary-coded
3 (11)	Position in regional geological structures	Anticlinoria	01	000 001
		Synclinoria	02	000 010
		Conjugate anticlinal-synclinal zones	03	000 011
		Superimposed troughs	04	000 100
		Regional abyssal fractures	05	000 101
		Intersections or conjugation of fractures	10	001 010
		None, or no data available	0	0
4 (100)	Relationship to local structures	Anticlines	01	000 001
		Synclines	02	000 010
		Brachyanticlines	03	000 011
		Brachysynclines	04	000 100
		Transition zones from anticlines to synclines	05	000 101
		Submeridional fractures	06	000 110
		Sublatitudinal fractures	07	000 111
		North-west fractures	08	001 000
		North-east fractures	09	001 001
		Intersections or conjugation of fractures	10	001 010
		Intersections or conjugation of local and regional geological structures	20	010 100
		.....	.....	.....
		None, or no data available	0	0
5 (101)	Ore host structures	Second-order and higher-order fractures	01	000 001
		Shear fractures belonging to one system	02	000 010

Serial No. and code of indexing characteristic of informational element	Designation of indexing characteristic	What is being coded	Code: decimal-coded	Code: binary-coded
5 (101)	Ore host structures	Shear fractures belonging to two systems	03	000 011
		Shear fractures belonging to three and four systems	04	000 100
		Cleavage fractures	05	000 101
		Schist formation and microjointing zone	06	000 110
		Interformation fissures	07	000 111
		Conjugation and intersections of differently oriented fissures	10	001 010
		No data available	0	0
6 (110)	Relationship to magmatism	Belonging to first igneous complex	01	000 001
		Belonging to second igneous complex	02	000 010
		Belonging to third igneous complex	03	000 011
		Belonging to fourth igneous complex	04	000 100
		Belonging to fifth igneous complex	05	000 101
		Related to central type volcanic apparatus	06	000 110
		Related to fissure type volcanic apparatus	07	000 111
		Related to acidic dike series	08	001 000
		Related to dike series all of one composition	09	001 001
		None, or no data available	0	0
7 (111)	Formational control	Acidic igneous rock	01	000 001
		Acidic basic rock	02	000 010
		Acidic effusive rock, volcanic chimney facies	03	000 011
		Acidic effusive rock, covering	04	000 100
		Acidic effusive rock (not determined exactly)	10	001 010
		Basic effusive rocks	11	000 011
		Amphibolites and amphibolite shales	12	001 100
		Clayey shales	13	001 101
		Coaly-clayey shales	14	001 110
		Clayey-flinty shales	15	001 111
		Sericitic schists	16	010 000
		Mica schists	17	010 001
		Chlorite schists	18	010 010
		Limestones and marbles	19	010 011
		Skarned limestones	20	010 100
		Skarns	21	010 101
		Fine-grained sandstones	22	010 110
		Coarse-grained sandstones	23	010 111
		Conglomerates	24	011 000
		Argillites	25	011 001
		Siltstones	26	011 010
		Breccia	27	011 011
		No data available	0	0
8 (1000)	Epigenetic rock changes	Kaolinization	01	000 001
		Seriticization	02	000 010
		Silicification	03	000 011
		Greisenization	04	000 100
		Albitization	05	000 101
		Potash-feldsparization	06	000 110
		Chloritization	07	000 111
		Hematitization	08	001 000
		Beresitization	09	001 001
		None, or no data available	0	0
9 (1001)	Presence of precipitant elements	Much organic material	01	000 001
		Much ferrous iron	02	000 010
		Much sulfide sulfur	03	000 011
		Many carbonates	04	000 100
		None, or no data available	0	0
10 (1010)	Redox state ΔE_h, mV	0–(+10)	01	000 001
		(+10)–(+20)	02	000 010
		(+20)–(+30)	03	000 011
		(+30)–(+50)	05	000 101
		Above +50	06	000 110
		Negative	07	000 111
		No data	0	0

Serial No. and code of indexing characteristic of informational element	Designation of indexing characteristic	What is being coded	Code	
			decimal-coded	binary-coded
11 (1011)	Epigenetic mineralization	Pitchblende	01	000 001
		Uraninite	02	000 010
		Coffinite	03	000 011
		Sulfides of iron, lead, zinc	04	000 100
		Selenides and tellurides	05	000 101
		Arsenides and diarsenides of nickel and cobalt	06	000 110
		.....	.....	.....
		Carbonates	10	001 010
		Quartz	11	001 011
		.....	.....	.....
		None, or no data available	0	0
12 (1100)	Satellite elements	Molybdenum	01	000 001
		Lead	02	000 010
		Arsenic	03	000 011
		Uranium	04	000 100
		Thorium	05	000 010
		Selenium	06	000 110
		Titanium	07	000 111
		Mercury	08	001 000
		Gold	09	001 001
		Copper	10	001 010
		Tin	11	001 011
		None, or no data available	0	0
13 (1101)	Morphology of ore bodies	Exposed strata of uraniferous sedimentaries	1	001
		Large sheet deposits	2	010
		Sheet-like deposits, columnar deposits, vein deposits	3	011
		Lenticular deposits and pocket deposits	4	100
		Thin veins in ruptures and shear joints	5	101
		No data available	0	0
14 (1110)	Mineralization scales (scale of basic component reserves, tons)	Tens	01	000 001
		Hundreds	02	000 010
		Thousands	03	000 011
		Tens of thousands	04	000 100
		Hundreds of thousands	05	000 101
		No data available	0	0

The volume of information obtained in this research is enormous, and is difficult to process by traditional methods, so that conclusions are subjective to a certain extent. Methods of probability theory, statistical decision theory, and game theory can be utilized for a complex analysis of the results of geological and geophysical studies. The information should be analyzed on electronic computers (preferably digital computers) capable of storing and processing large volumes of information. Regularities and relationships can be discerned from the computer-processed information and statistical criteria can be established.

This approach to processing data on the basis of known geological entities and comparison of data obtained with information on the site studied makes it possible to establish criteria defining the probability of finding deposits and the outlook for exploitation of distinct geological districts, and to evaluate exposed anomalies and ore showings. Results of a computer analysis can provide an objective basis for compiling metallogenetic and prognostic maps.

Localization of a deposit on any one site is known to be the outcome of the combined effect of a large array of factors, some of them firmly established, others presumed. One of the difficulties of a complex analysis is that the investigator not only has to deal with the causes, but also the consequences, and in some cases the same causal factor can be found to lead to different outcomes.

The purpose of the digital computer analysis is to establish statistically verified relationships between certain deposits and geological factors. The following problems call for solution: 1) finding criteria (including numerical criteria) for evaluating exposed anomalies and ore showings, and also establishing the possibility of detecting new deposits within the confines of known ore fields; 2) finding

criteria for singling out promising ore sites on a regional plane, and 3) finding the relationship between the geological factors and the methods used to study them (improvements and selection of efficient prospecting techniques).

The solution of these problems can be attained on the basis of either homogeneous or heterogeneous information files.

In a homogeneous file, the entire available information on the geological entity is taken as the informational element. The form of a homogeneous file of information, concretized for one of the uraniferous ore districts, is indicated in Table 1 (here the informational element, the geological object, has 45 characteristis for indexing). In a heterogeneous file, the informational element is the information available on a discrete factor.

Data on a geological entity are presented in both descriptive and numerical form. They must be presented in digital form for digital computer work, so that a standard digital designation, or digital code, is assigned to each pertinent characteristic (in our case we make use of binary and decimal codes for information processing on the URAL-2 and URAL-4 computers). An example of coding of a homogeneous information file applicable to one of the uraniferous districts is seen in Table 2 (only partially).

In the case of a heterogeneous file, 10 informational elements (nine geological factors plus the name of the geological object) count in the description of the geological object: the structural factor, the lithological-petrographic factor, parameters of the geological object; and the characteristics: geochemical, radiation, physical properties of the rocks and ores, of the magnetic field, electric field, gravitational field. In this field each informational element has from 10 to 16 indexing characteristics.

The total sequence of operations in computer analysis of geological information runs as follows. The files of information compiled as a result of studies of uranium deposits are combined according to distinct metallogenetic provinces, or in terms of entire deposits, or in terms of one of the criterial factors (genetic, structural, lithological-petrographic, etc). Confirmed values of the indexing characteristics, as well as regularities and relationships linking the characteristics and the informational elements, are arrived at on the basis of the combined file. The file of information on a sector investigated (a geological region or part of one, an ore showing, an anomaly) is compared to the combined file (or sequentially with each of the files combined on the basis of some criterial factor), and the problem of the presence or absence of the same regularities in this file and the combined files is resolved. The comparison can be made by converting the file to find the distribution of frequencies with which given indexing characteristics or informational elements with a specified value of the indexing characteristics appear. The results of the file comparison can then be approached as an objective characteristic for the geological object in question.

The solution of problems of this type reduces to sequential data processing on the basis of a system of standard algorithms developed for the files (ordering, convolution and involution, conversion, summing, transformation, selection, combination, checking hypotheses on the pertinent probability distribution law, i.e., normal, Poisson, etc.).

There is great interest not only in the digital computer approach outlined above, but also in complex interpretation of geological and geophysical data based on methods derived from pattern recognition theory [1, 2, 3]. Algorithms developed in pattern recognition theory are useful when applied to complex analysis of geological and geophysical data in the exploration of radioactive ore deposits. All data available on the geological object are recorded as coordinates of some vector $a = (a_1, a_2, \ldots, a_n)$, in which the components $a_1, a_2, \ldots, a_n$ are data obtained through the application of particular geophysical techniques, or the results of a geological study. The same informational elements and their characteristics can be used as components of the vector, as is done in the case of a heterogeneous data file, or values of the characteristics in the case of a homogeneous data file. If the points in n-dimensional space corresponding to geological and geophysical patterns of ore fields and non-ore-bearing fields comprise two distinct regions, then the machine can be "taught" to distinguish between them. After the learning procedure has been completed, and this consists in displaying objects of either category to the machine, the machine is then capable of distinguishing geological objects which it has not enountered previously by reference to the geological and geophysical information store already read into the machine. A similar approach to processing a set of geological and geophysical information can be applied to any other form of minerals.

The author expresses his deep gratitude to D. Ya. Surazhskii, L. I. Vyatkin, and I. M. Konovalov for their kind assistance in the work on the article.

LITERATURE CITED

1. E. M. Braverman, Avtomatika i telemekhanika, 23, 349 (1962).
2. V. S. Fain, Radiotekhnika, 15, 13 (1960).
3. Sh. A. Guberman, Collection of articles "Problems of nuclear geophysics." Moscow, Nedra press, p. 64 [in Russian] (1964).

THE ACTIVATION METHOD FOR DETERMINING FLUORITE

A. P. Bushkov and V. I. Prokopchik

UDC 543.53:539.172.4

The activation method of determining the fluorite (CaF_2) contents of ores, including natural deposits, is attracting much attention in prospecting and mining practice.

The method is based on measurement of the intensity of the γ rays from radioactive isotopes formed by nuclear reactions in fluorine acted on by neutrons (Table 1). However, it is not yet wholly clear which reaction plays the decisive part in the activation determination of fluorite. For example, Bardovskii [3, 4] states that in activation well-logging it is the activity of F^{20} which is measured, i.e., the main contribution is made by reactions of thermal neutrons.

In applied nuclear geophysics, Po-Be sources of fast neutrons are mainly used at present: they have a continuous energy spectrum reaching to about 11 MeV with two maxima at 3 and 5 MeV [5]. Therefore we shall confine ourselves to consideration of fluorine activation by neutrons from a Po-Be source.

The activation of large specimens of fluorite ore irradiated by neutrons is due either to threshold reactions of fast neutrons, or to (n, γ) reactions of thermal neutrons formed by moderation of fast neutrons in the substance.

An approximate calculation of the spatial and energy distributions of neutrons from a Po-Be source in an infinite medium not containing hydrogen shows that, at points 20 cm from the source, the flux of fast neutrons with energies greater than 3 MeV is greater than that of thermal neutrons. The effective cross section of the reaction F^{19} (n, α)N^{16} for fast neutrons is 260 mbarn (for 6 MeV neutrons), which is much greater than either the cross section of the reaction F^{19} (n, p)O^{19} or that of the reaction F^{19}(n,γ)F^{20} for thermal neutrons [6]. If we also remember that in activation well-logging the layer of rock being investigated is less than 15-20 cm thick [7], we can assert that the observed γ-ray intensity is mainly due to the reaction F^{19} (n, α)N^{16}.

To confirm this thesis, we measured the spatial distributions of fast and thermal neutrons in fluorite ore, and also experimented with fluorine activation in a model seam (a box, 1.5 × 1.5 × 1.0 m^3 in size, containing ore, with an iron tube, diameter 100 mm and wall thickness 0.8 mm, passing along its vertical axis). The ore used contained two main chemical constituents - fluorite and quartz, which together made up 80-95% of its weight. In addition it contained approximately equal quantities (up to 4%) of barite, calcite, galenite and aluminosilicates. The experimental results (Fig. 1) showed that the

TABLE 1. Nuclear Reactions of Fluorine Acted on by Neutrons, and Characteristics of the Radioactive Isotopes Formed

Reaction	Reaction threshold MeV [1]	Product nucleus	Half life, sec [2]	Energy, MeV	
				β-particles	γ-quanta
(n, α)	1.57	N^{16}	7.0	10.33 (24%) 4.27 (55%) 3.28 (21%) 1.5 (1%)	6.13 (55%) 7.11 (21%)
(n, p)	4.21	O^{19}	27.0	4.5 (30%) 2.9 (70%)	0.2 (30%) 1.37 (70%)
(n, γ)	Thermal neutrons	F^{20}	10.7	5.42 (100%)	1.63 (100%)

Translated from Atomnaya Énergiya, Vol. 21, No. 3, pp. 215-217, September, 1966. Original article submitted March 21, 1966.

TABLE 2. Results of Activation Well-Logging on Ores of Various Water Contents (Dry Borehole)

Radiation detector	CaF_2 content, %	Water content, vol. %	Mean count rate, pulses/ 30 sec*
VS-9	31.3	2	87
		4	89
		7	83
		9	86
		12	86
Scintillation counter – discrimination level 0.2 MeV	37.0	2	613
		5	619
		7	603
		12	635
Scintillation counter – discrimination level 2.2 MeV	37.0	2	116
		7	121
		12	116
		17	114

* Source power 10^6 neutrons/sec

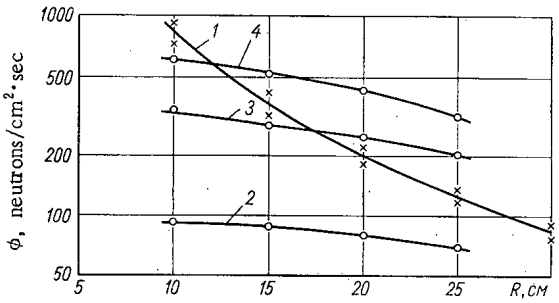

Fig. 1. Experimental data on spatial distribution of neutrons from Po-Be source (10^6 neutrons/sec) in fluorite ore (45% CaF_2). (1) Fast neutrons (average curve for moisture contents of from 6.5 to 18 vol. %); (2, 3, 4) Thermal neutrons, for moisture contents of 3, 6.5, and 18 vol. %, respectively.

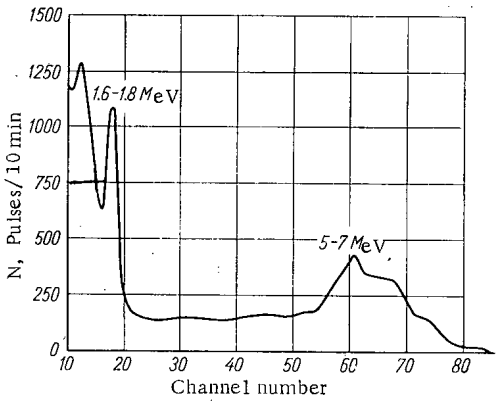

Fig. 2. Instrumental spectrum of γ radiation from activated fluorite ore (45% CaF_2).

thermal neutron flux near the source increases sharply with the moisture content, whereas the fast neutron distribution scarcely changes. This may be explained on the hypothesis that the fast neutron distribution in the medium is mainly determined by the free-path length, which, for neutrons of energies greater than 2 MeV, varies little with the water content [8]. The fast-neutron detector was ZnS in plastic, the thermal-neutron detector was an SNM-13.

The γ radiation from the activated fluorite ores was registered by a scintillation counter (with 40 × 50 mm NaI (Tl) crystal) and a VS-9 gas-discharge counter. The γ-ray spectrum of the activated ore (Figure 2) was measured by irradiating the model seam with a Po-Be source of power $5.4 \cdot 10^6$ neutrons/sec, placed in the "borehole", and detecting the radiation with an NaI(Tl) crystal with dimensions of 40 × 50 mm and an AI-100 analyser. The irradiation time was 30 sec, the delay while the scintillation counter was substitued for the source was 2 sec, and the duration of measurement was

* Al^{28} ($T_{1/2}$ = 2.3 min, E_γ = 1.79 MeV) is formed by the reaction Si^{28} (n, p)Al^{28}.

30 sec. In all we carried out 20 such cycles, the total measurement time being 10 min. The maximum at 1.6-1.8 MeV on the γ spectrum is due to the activities of F^{20} and $Al^{28}*$, and the radiation of higher energies is due to the activity of N^{16}. Without detailed interpretation, this spectrum does not lead to any definite conclusions on the decisive roles of any particular reactions. To solve this problem, we can use material from localized activation well-logging on models. If the reaction involving thermal neutrons played an important role, we should expect a rise in γray intensity when the borehole is filled with water, because in this case the thermal neutron flux would increase near the borehole. However, our experiments showed that when the borehole is filled with water (leaving the ore dry) the γ- radiation intensity falls by 30-35%. This can evidently be explained by supposing that the 3.5 cm water layer somewhat softens the fast-neutron spectrum. When the ore is wetted to 12-17%, despite the fact that this greatly increases the thermal neutron flux near the borehole, the recorded γ-ray intensity does not vary (Table 2).

From what has been said we can conclude that, in measurements in boreholes, it is mainly γ radiation from the radio-isotope N^{16} which is registered, this isotope being formed when the fluorine is activated by fast neutrons; the contribution of reactions involving thermal neutrons is small. This must be remembered when one is interpreting data from activation well-logging in fluorite deposits, in particular when making corrections for water-filled boreholes.

The authors would like to thank V. L. Shashkin for supervising the work and also A. V. Klubkov and V. V. Polzunov for helping with the experiments.

LITERATURE CITED

1. R. Rochlin, Nucleonics, No. 1, 54 (1959).
2. B. S. Dzhelepov and L. K. Peker, Decay Schemes of Radioactive Nuclei. Moscow, Izd. AN SSSR (1958).
3. V. Ya. Bardovskii, In symposium, "Scientific Records of SAIGIMS (Central Asiatic Research Institute for Geology and Minerals)," No. 7, Tashkent, p. 277 (1962).
4. V. Ya. Bardovskii, In: "Geophysical Prospecting", No. 1, Moscow, "Nedra," p. 66 (1964).
5. L. Medvetski, Atomnaya Énergiya, 13, 583 (1962).
6. J. Marion and R. Brugger, Phys. Rev., 100, 69 (1955).
7. F. A. Alekseev et al. In: "Nuclear Geophysics," Moscow, Gostoptekhizdat, p. 65 (1959).
8. K. I. Yakubson, In: "Radioactive Isotopes and Nuclear Radiation in the National Economy of the USSR," Vol. IV, Moscow, Gostoptekhizdat, p. 157 (1961).

A MINIATURE DEVICE FOR MEASURING THE MEAN TOTAL CONCENTRATION OF RADON

V.N. Kirichenko, B.N. Borisov, B.I. Ogorodnikov, V.I. Kachikin, and P.I. Basmanov

UDC 543.52:539.107.37

Although it is now considered that radiation damage to organisms in the mining industry is mainly due to the short-lived daughter products of radon, it is nevertheless necessary to determine the radon concentration, both to estimate the efficiency of anti-radon measures, and also for dosimetric control.

At present, dosimetric control in foreign and Soviet mines is exclusively by way of single samples; however, owing to the continuous variations in the radon content, these cannot reliably characterize the state of the mine air surrounding the operative. This drawback can to some extent be eliminated by means of the device described below. Thanks to its small size, low weight and simplicity of construction, it can be used to estimate the radiation conditions close to the operative throughout his working period.

The device consists of a chamber, shielded from light, into which radon can penetrate by diffusion through a filter which does not pass daughter products or dust. Inside the chamber is a photographic emulsion, which detects the alpha particles emitted by radon and its daughter products. When the device has been in a radon-containing atmosphere for four hours, the density of tracks in the emulsion after development is proportional to the integral of the radon concentration with respect to time,

$$P \sim \int_0^t C(t)\,dt. \qquad (1)$$

The device consists of a housing 1 containing an opaque screen 2 with holes closed by filter 3, a film-holder 4, and a lid 5 which is screwed on to the housing, thus holding together all the components (Fig. 1). The device has the following constructional characteristics:

Area of entry hole in housing		3.1 cm^2
Area of ring-shaped gap between housing and opaque screen		3.0 cm^2
Area of 12 holes in opaque screen		2.4 cm^2
Diameter of opaque screen		35 mm
Volume of opaque screen when assembled (working volume of device)		20 cm^3
Dimensions:	Diameter	50 mm
	Height	35 mm
	Weight	40 g

The filter is of FPP-15-1.7 material, and the alpha particles are detected by an MR (NIKFI) photographic plate with emulsion of thickness 8μ. The density of the tracks in the emulsion is measured with a microscope. For this purpose the film holder has a slot with a length of 18 mm. The lowest mean radon concentration which the device is capable of detecting in 36 h, when the normal inherent background count of the photographic emulsion is 0.3 alpha-particle traces per mm^2, is $5 \cdot 10^{-12}$ curies/liter.

It is obvious that the applicability of (1) presupposes quasistationary exchange of radon between the surrounding atmosphere and the working space of the device. A necessary condition for this is that the time for radon to diffuse into the device should be small in comparison with the time required for appreciable changes in its concentration in the surrounding atmosphere. Calculations and direct

Translated from Atomnaya Énergiya, Vol. 21, No. 3, pp. 217-218, September 1966. Original article submitted March 21, 1966.

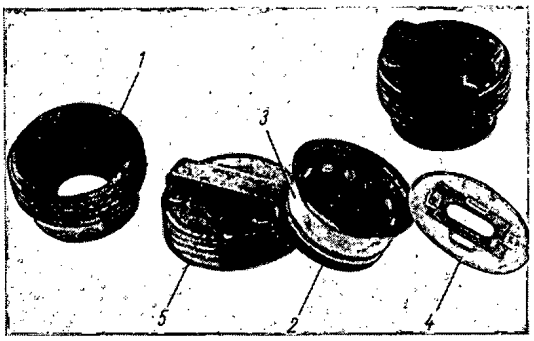

Fig. 1. General view of device.

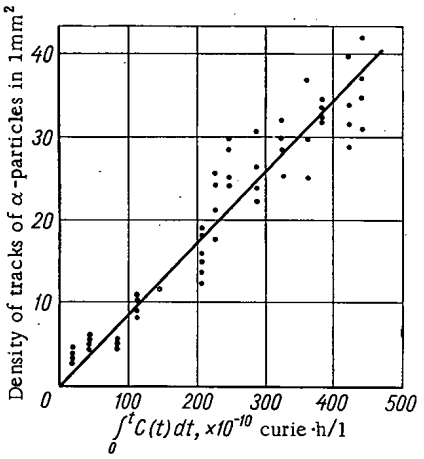

Fig. 2. Dependence of density of tracks of α-particles in the emulsion on concentration of radon and time.

measurements have shown that the ratio of the mean concentration $\bar{C}$ of radon in the working space to the concentration C in the surrounding atmosphere is given as a function of time by the formula

$$\frac{\bar{C}}{C}=1-0{,}76e^{-t/t_2}, \qquad (2)$$

where t_2 is the time of diffusion relaxation of radon in the device (found to be 1.7 min). In industrial tests, 50 devices were simultaneously installed near the mouth of a ventilation drift through which mine air containing radon was being released to the atmosphere. The radon concentration in the region where the devices were placed was monitored at 30-min intervals (on average) by means of single samples. The humidity of the air was 96-100% at +15°C. After certain time intervals the devices were removed in small batches and kept in pure air. Four hours after the removal of the last batch, all the photographic plates were simultaneously developed. From the measurement results in Fig. 2, it will be seen that the readings of the devices correspond to (1) over a wide range of values of $\int_0^t c(t)\,dt$. The standard deviation of the readings from (1) for the 50 devices was 26%.

The above trial of a test batch of radon survey devices, together with individual miners' use of the device, showed that the latter is convenient and reliable in use, and can give extensive and reliable information on the radon content of the air for a relatively small expenditure of time.

USE OF SGD-8 GLASSES FOR DOSIMETRY OF γ-RADIATION FROM THE IGR PULSED REACTOR

S. A. Sharoiko

UDC 621.387.46:621.386.82

The SGD-8 glasses have been used for dosimetry of γ-radiation from the IGR pulsed reactor [2]. In the operating conditions of the reactor, when the glass is irradiated together with the specimen, it is desirable that the dimensions of the detector shall be as small as possible. The size of the glass (15 × 15 mm) is governed by the requirements for measuring its optical density with an SF-4 spectrophotometer. The minimum thickness of the glasses, corresponding to the upper limit of the measurable dose, is 5 mm.

A batch of glasses from the same melt were calibrated in the I. V. Kurchatov Institute of Atomic Energy, by means of a γ unit of activity 2000 Ci. The optical density of the glass was measured one day after irradiation, since regression variation of the optical density is negligible (less than 1%/h) after this period, and errors due to the measurement time are practically eliminated. In addition, this time interval is the most convenient for the operating conditions, because at this time the induced radioactivity of the glass is negligible.

The dose rate at the point of installation of the glasses being calibrated was found by means of a ferrous sulfate dosimeter. The concentration of Fe^{+++} ions formed by the γ-rays was found as follows. Since the range of doses received by the ferrous sulfate dosimeter was already known, it was possible to determine the expected concentrations of Fe^{+++} ions formed. The relation between the optical density of the solution and the concentration of Fe^{+++} ions was found by means of calibration solutions prepared in a given range of Fe^{+++} ion concentrations. The radiation dose was determined, by means of the graph thus drawn, from the measured optical density of the irradiated solution. The calibration curve found for the SGD-8 dosimeter is shown in Fig. 1.

Since the device was calibrated with a Co^{60} source, whereas in use it is irradiated by γ-rays with a wide energy spectrum, it was necessary to eliminate the effect of the energy dependence. For this purpose, following [2], we used lead compensating filters. Furthermore, in using the glasses as dosimeters for pulsed γ-radiation, allowance must be made for the fact that the conditions of calibration differ from those of dosimetry. The IGR reactor, when operating in "flash" conditions, gives γ-ray pulses with a half-width of $\Gamma \leq 0.5$ sec. During calibration with the cobalt source, the irradiation time

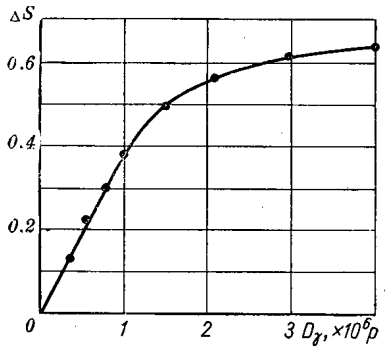

Fig. 1. Calibration curve of SGD-8 dosimeter (λ=740 mμ; ΔS is the increase in optical density).

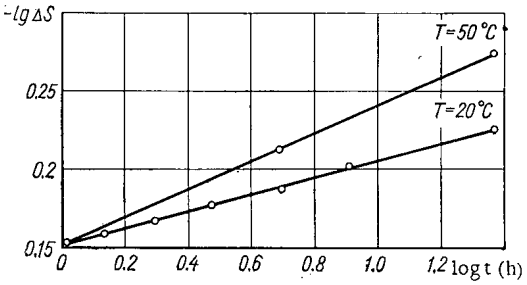

Fig. 2. Regression curves for two storage temperatures.

Translated from Atomnaya Énergiya, Vol. 21, No. 3, pp. 218-219, September, 1966. Original article submitted February 22, 1966. Revised April 30, 1966.

was up to 4 hours. It is obvious that, owing to regression, the optical density, at the same time after irradiation by the same dose, will be greater for glass irradiated by the source than for glass irradiated in the reactor. However, with the chosen time interval (24 h) between the end of irradiation and the measurements, this discrepancy is less than 1%. This value was calculated theoretically from the regression law,

$$\frac{S_{t_2}}{S_{t_1}}=\left(\frac{t_1}{t_2}\right)^K,$$

where S_{t1} and S_{t2} are the optical densities of the glass at times t_1 and t_2 after irradiation, and K, determined experimentally, is equal to 0.056 (for T=20°C and λ =740 mμ).

Since there is a considerable time between irradiation and measurement, the temperature at which the glass is stored during this time will affect the results. For the same dose, there is a 10% difference between the optical densities of glasses stored at T = 50°C and T = 20°C (see Figure 2).

To verify that the glass readings were correct in the case of pulsed reactor radiation, we used nonstationary calorimetry; it was found that SGD-8 glasses give results agreeing to within 10%. For dosimetry of γ radiation from the IGR pulsed reactor, SGD-8 glasses gave consistent readings in repeated tests, and were accurate enough for practical purposes. They are also convenient in use. It appears that the SGD-8 glass γ -ray dosimeter is fairly universal in application, and could be used as a standard method of measuring γ -ray doses in experiments with different sources, including reactors.

LITERATURE CITED

1. I.V. Kurchatov et al. Atomnaya Énergiya, 17, 463 (1964).
2. G.V. Byurganovskaya, E.G. Gvozdev, and A.I. Khovanovich, Atomnaya Énergiya, 21, 38 (1966).

SCIENTIFIC CONFERENCE OF THE MOSCOW ENGINEERING AND PHYSICS INSTITUTE

V. V. Frolov

The annual scientific conference of the Moscow Engineering and Physics Institute, held May 5-20, 1966, attracted an ample audience, as in earlier years. About 300 papers were presented by instructors and students of the institute, and by colleagues from several other scientific bodies, at the 23 sessions of the conference. About 900 of the audience were representatives of different research institutes, plants, factories, and higher educational establishments.

Some interesting reports on high-energy particle physics were heard at the experimental nuclear physics session. V. V. Borog and associates used an ionization calorimeter to investigate electron-photon cascades in iron triggered by cosmic ray muons of $8 \cdot 10^{11}$ eV energy. The findings were compared to the theoretically derived cascade curve at different cascade unit values. The closest fit was obtained at the cascade unit $t = 14$ g/cm^2.

V. S. Demidov et al. reported on pair production of strange particles. This investigation used the Moscow Engineering and Physics Institute (MIFI) 105-cm bubble chamber (propane-freon mixture). The mass spectrum in the $K^0\lambda^0$-system was obtained. A. I. Fesenko and F. M. Sergeev described mass spectral research on secondary particles in the interaction between 80 MeV π^+-mesons and nuclei of the emulsion. The secondary proton yield turned out below 90%. I. L. Rozental' analyzed energy dissipation channels of the electron component of cosmic rays as they pass through the interstellar medium and the atmosphere forming very slow electrons ($E \leq 1$ keV) which play an important role in many processes. It was shown that an appreciable fraction of the energy goes to the ultraviolet portion of the spectrum. Various phenomena due to the appearance of the slow electrons as intermediary factors were examined. V. S. Demidov et al. studied production of K°-mesons and λ-hyperons on hydrogen and light nuclei by π^--mesons of 4 GeV/c momentum. Energy and momentum distributions of the K°-mesons and λ-hyperons were obtained.

Some of the papers presented were devoted to the development of physics research equipment. Yu. M. Grashin and S. V. Somov reported on a nanosecond tunnel diode pulse height discriminator designed for working directly with fast scintillation counters and Cherenkov particle detectors in multiple coincidence systems. L. P. Kotenko et al. reported calculations of the expected relativistic growth of bubble density in bubble chambers. The possible use of relativistic bubble growth in the identification of particle energies was discussed.

A report by V. M. Galitskii and S. R. Kel'ner on computations of bremsstrahlung cross section in scattering of a fast muon on electrons at rest highlighted the theoretical nuclear physics session. The calculations were based on covariant tensor integration. An interesting discussion followed the report by A. S. Kompaneits, who spoke on possible regularization of the equations of quantum electrodynamics at the cost of a partial rejection of the Lagrangean formalism, taking account of the existence of two fermions of different mass.

A. V. Berkov and Yu. P. Nikitin gave an account of the spin structure of the photoproduction amplitude at high energies based on the concept of moving singularities in the complex j-plane. Low-energy resonance nuclear reactions involving particles of spins 0 and $\frac{1}{2}$ were discussed in a paper by V. V. Grushin and Yu. P. Nikitin, on the basis of the Regge moving poles concept and the Khuri method. Yu. B. Ivanov and E. E. Lovetskii presented a theory to account for stability of a current-carrying plasma pinch contained by a conducting shell. They derived the dispersion equation of the current plasma oscillations. The stability conditions of the system were investigated.

Papers submitted by V. V. Khromov, I. S. Slesarev, A. M. Kuz'min, and others dealt with reactor numerical calculations, precision techniques in neutron field mapping, and effective methods for finding

Translated from Atomnaya Énergiya, Vol. 21, No. 3, pp. 220-222, September, 1966.

criticality conditions and neutron distributions in multidimensional geometries. The algorithms proposed shorten computer time encouragingly and are particularly useful in variational computations. The results have materialized in concrete computer programs. Reports by S.B. Shikhov, M.N. Nikolaev, A.A. Ignatov, V.I. Davydov dealt with new methods for solving the transport equation. The method of subgroups employed by these authors greatly improved the exactness of neutron flux calculations near interfaces in the resonance energy range. They also described an efficient analytical method for criticality calculations which eliminates the iteration process in transport equation solutions. An existence and uniqueness proof of the solution of the neutron transport equation discussion of nonlinear reactor dynamics (self-sustained oscillations) are found in papers by S.B. Shikhov, L.K. Shishkov et al. on reactor theory. A paper by S.B. Stepanov et al. on an experimental study of diffusion parameters of hydrogenous media stimulated much interest. These authors found a mutual relationship between the neutron diffusion coefficient and the self-diffusion coefficient of the medium.

L.K. Shiskov and S.B. Shikhov proposed a higher-order perturbation theory for solving some reactor calculation problems. A change in the eigenvalue of the neutron transport operator and in its eigenfunction (neutron flux) can be obtained even without a knowledge of the set of all eigenfunctions. This method has made it possible to calculate k_{eff} more accurately, even in the first approximation, than by using conventional perturbation theory.

V.I. Deev and G.P. Dubrovskii presented results of an experimental investigation of heat transfer and burnout heat flux in bulk water boiling under vacuum conditions. An analogy between boiling of water and boiling of liquid metals at low pressures was demonstrated. L.S. Kokorev et al. reported an ingenious technique for determining the contact wetting angle of liquid metals by measuring the maximum pressure in a gas bubble. New data on contact wetting angles for sodium and potassium were reported. A new approach to calculating velocity distrubution and hydraulic drag in jacketed tube bundles with arbitrary rod spacing in the bundle was discussed in a paper by V.I. Petrovichev et al. This led to a theory aiding in hydrodynamical calculations checking the state of the fuel rod assembly on the LENIN nuclear-powered icebreaker.

B.I. Nikolaev et al. reported experimental results on isotope separation on a mercury mass diffusion column standing one meter high. Constructional features of the diffusion column were given. A peak separation factor of 17 was attained by using a two-ply diaphragm (an expanded stainless steel grid) on neon isotopes with no outgoing materials.

N.G. Volkov et al. described a calorimetric method for indentifying isotopes by their γ emission, using three Geiger counters with different energy-recording efficiency relations. V.K. Lyapidevskii et al. discussed results of research on the emission spectra of alkali halide crystals exposed to α-particles and electrons. The difference between these spectra was established. An attempt was made at a separate analysis of the spectra of the fast and slow components of a burst.

P.L. Gruzin, L.A. Alekseev, G.N. Shlokov et al. presented results on the properties of solids based on the nuclear γ-ray resonance method (Mössbauer effect). Papers dealing with studies of the properties of tin-containing ferrites in the magnesium-manganese system, for which Zeeman splitting spectra have yielded information on internal effective magnetic fields on Sn^{110} nuclei in these ferrites, and for which the temperature variations have been determined, were of particular interest. An account was given of practical application of the Mössbauer method to the solution of ferrite fabrication problems in order to produce ferrites having predetermined magnetic properties.

Yu.F. Babikova, V.I. Kazakevich et al. reported on a study of diffusion, thermodiffusion, and impurity distribution in semiconducting materials (silicon, germanium) by radioisotope methods. Autoradiographic studies of breakdown sites in alloy junction indium-germanium diodes were reported.

A group of reports was devoted to applied neutron physics. E.Z. Vintaikin, V.V. Gorbachev et al. presented results of an investigation of Cu—Ni alloys by inelastic neutron scattering methods. An attachment to a conventional neutron diffractometer which adapts the diffractometer to the needs of crystal dynamics research was designed. A.Z. Kichev, V.T. Samosadnyi et al. reported the development of neutron isotope sensors. The sensor head in a neutron isotope level gage was tested on stream in propylene and acetic acid production plants.

I.E. Konstantinov and B.Ya. Narkevich reported the development of a novel procedure for scintillation spectrometer measurements of the space distribution of electron dose and electron flux in

the passage of a thin beam of β - particles through lightweight material, in a paper presented at the shielding physics session. This measurements procedure (using thin scintillation films) and a detector designed to go with it make it possible to carry out measurements without introducing disturbances in the object or plant investigated. The absorbed dose is accurately determined not only within the beam but outside it as well. Measurements of absorbed dose of beta radiation of unknown spectral composition were discussed by V. F. Baranov et al. A method for determining the specific activity of thick-layer β - ray sources by the measured electron yield from the surface of the source was put forth. Results of studies of a tissue-equivalent ionization chamber made of current-conducting plastics and a conductively coated polyethylene chamber were presented in a paper by I. M. Dmitrievskii and Yu. N. Martynov. A simple method for extruding plastic ionization chambers has been developed.

Several papers submitted by A. A. Viktorov, V. A. Klimanov, V. P. Mashkovich, and others discussed passage of radiations through inhomogeneities or discontinuities in shielding (channels, slits, voids). This is the least studied topic in radiation shielding. Results of calculations of the differential albedo characteristics of γ radiation by electronic computer Monte Carlo techniques were presented. G. M. Budyanskii employed stochastic computational techniques in a study of the passage of neutron emission through labyrinth mazes. L. R. Kimel' and associates gave an account of the attenuation pattern of scattered neutron emission belonging to various energy groups.

Papers devoted to theoretical and experimental research and development projects on linear accelerators and automatic accelerator control systems were read at the session on electrophysical equipment, along with reports on the development of high energy particle separators and on investigation of 1000 GeV cybernetic accelerator accelerating systems.

A. V. Shal'nov discussed wavelength assignments in supplies for constant-geometry linear accelerator sections. He showed how the wavelength of the driving oscillator affects the energy, the length of the accelerator, and the efficiency of the machine. Yu. N. Serebryakov et al. derived analytical formulas for calculating the transverse beam instability (pulse shortening effect) in constant and variable waveguide structures.

A new method for measuring the frequency of oscillation modes in vacuumtight waveguides has been proposed and worked out (N. P. Sobenin, V. S. Anis'kin). The precision of this technique has been estimated at $\pm$ 0.2 mHz, which is not inferior to the precision of currently available techniques for tuning collapsible waveguides. E. V. Armenskii et al. discussed the possible application of the MN-7 analog computer to obtain operational data on the output variables of a linear electron accelerator. A consultative computer for facilitating control and adjustments of accelerators has been proposed. An interesting paper was submitted by E. R. Aleshkin and colleagues on the possibility, in principle, of using traveling-wave iris-loaded waveguides over the required frequency band as an accelerating section for the 1000 GeV cybernetic accelerator.

Papers on controlled thermonuclear fusion were read at the plasma physics session. V. V. Kosachev and B. A. Trubnikov discussed the stability of closed plasma systems with magnetic surfaces of circular cross section in which stabilization is achieved by establishing a variable field on the system axis. They showed that the stability criterion can be met by a judicious choice of axis geometry and periodic modulation of the field. V. M. Smirnov dicussed a criterion he found for the stability of stationary potential distributions in a plasma gap with respect to slow particle current feedback. N. A. Gorokhov described equipment and techniques for measuring the electromagnetic radiation of a quasistationary plasma in the millimeter and submillimeter wavelength ranges. He found that a plasma of this type acts as an intense radiation source, and is one of the manifestations of the two-stream instability developing in such cases. V. A. Kurnaev et al. described a double-focusing mass-monochromator in a sector magnetic field. They employed an arc discharge source in a longitudinal field. Papers on plasma injectors were received with interest. V. F. Demichev presented results of studies on the operating modes of plasma injectors designed to produce tight and relatively pure accelerated bunches. E. A. Azizov and V. S. Komel'kov presented data on the performance of a pulsed cascade type plasma accererator consisting of a coaxial conical injector and one or two subsequent slaved acceleration cascades. They showed that the velocity of the plasma leader bunch in the downstream cascades can be increased three- to sixfold with a total number of particles present in the 10^{17}-10^{18} range.

G. A. Mochalov et al. submitted a paper discussing the properties of high-pressure fluid-extruded molybdenum, at the session on metallurgy and metals science. Hydroextrusion techniques make it

possible not only to plastically deform molybdenum of different initial state and processing history, but also to obtain material exhibiting improved plasticity and strength.

Several reports described methods for growing molybdenum single crystals by the zone melting method, and the resulting zone-refined products (E. M. Savitskii, G. I. Burkhanov), a study of the fine structure of molybdenum single crystals grown by deposition from the vapor phase (A. A. Rusakov et al.), plastic flow features of molybdenum single crystals in rolling and tension (A. I. Evstyukhin et al.), and methods for determination of gases in pure molybdenum (N. F. Litvinova).

Yu. F. Bychkov et al. described the properties of metastable β- and ω-modifications of pure zirconium. These phases exist in many zirconium alloys, but could be obtained in pure zirconium as modifications stable at room temperature only by applying elevated pressures. G. B. Fedorov and V. S. Kolesnikov studied diffusion in zirconium and zirconium-tin alloy by internal friction techniques and I. I. Korobkov et al. discussed the corrosion strength of zirconium intermetallic compounds and the effect of these added constituents on the properties of the zirconium. Some of the papers (N. A. Sokolov, Yu. F. Bychkov et al.) were devoted to a study of the relationship between fine structure and superconducting behavior in zirconium-niobium alloys.

The most interesting paper presented at the solid-state physics section was one by V. F. Elesin and É. A. Manykin on the possible realization of absolute negative conductivity in semiconductors under highly off-equilibrium conditions, and the spectral characteristics of photoeffects closely related to this phenomenon.

A good number of the papers will be selected for publication in the topical scientific symposia of the Moscow Engineering and Physics Institute.

THE FIRST SOVIET-MADE INDUSTRIAL SEMICONDUCTOR ELECTRON-HOLE DETECTOR DEVICES

V. V. Matveev, Yu. P. Sel'dyakov, and A. D. Sokolov

Development work on the first detector units incorporating semiconductor detectors and the requisite electronic equipment, which includes a 9063-02 set (the Amur-1) designed for large-batch production, was completed in 1965 at the Union Instrumentation Research and Development Institute. This equipment has given positive results in State standards tests in the branch institute of the State Committee on standards, measures, and measuring instruments.

The system is made up of four types of detection units incorporating semiconductor detectors, and two table stands for mounting electronic equipment.

The detection units are intended primarily for recording heavy charged particles (three of the units serve this function), but also recording thermal neutrons (the remaining unit). The operating features of the semiconductor detectors were taken into account in the design of the detection units: the need for light shielding, reduced pressure in performing spectrometric measurements, the effect of geometric factors on resolution, among others. Materials selected in the design of the detection units must be amenable to surface deactivation.

The 6965-02 detection unit is designed for precision spectrometric measurements of α-particle flux with 1% resolution for energies in the neighborhood of 5 MeV, and is designed to work with emitters 35 mm in diameter. Seven emitters can be loaded in the detection unit, and measurements can be taken successively without disturbing the vacuum. The spacing between detector and emitter surfaces is set within the 6 to 40 mm range. A built-in vacuum gage monitors the state of the vacuum. The detection unit measures 194 × 220 × 168 mm.

α - particle fluxes can be measured spectrometrically with 1-3% resolution at 5 MeV energy at both reduced and atmospheric internal pressure by using the 6965-01 general-purpose detection unit. The unit is provided with a collimator for enhanced accuracy in measurements at atmospheric pressure. This detection unit is designed to work with emitters 35 mm in diameter. This type of detection unit differs from the spectrometric type in its simpler design, with easily replaceable emitters and detectors. The unit measures 90 × 76 × 100 mm.

The 6465-01 detection unit is designed to record α particles emitted from open surfaces and to determine the degree of surface contamination of materials by α - emitting isotopes. The resolution is 13% for 5 MeV α particles. The unit is 42 mm in diameter and stands 80 mm high.

The 6845-01 detection unit is capable of recording thermal neutron flux with 0.1% efficiency against a γ-ray background of 28 mR/sec. The unit measures 47 mm in diameter and 83 mm in height.

The electronic equipment consists of two independent instruments: a preamplifier positioned in the immediate vicinity of the sensor, and the main amplifier placed in the immediate vicinity of the analyzing or recording instruments. The following circuit employing these units is utilized in most cases: detection unit-preamplifier-amplifier; less frequently, a detection unit-preamplifier arrangement is utilized.

The amplifier is employed in those cases where pulses from the preamplifier have to be further amplified, or where the partial height distributions of the pulses must be investigated to a high order of precision (to within 1-5% error or better). The amplifier can also be operated independently with other equipment (such as scintillation counters, ionization chambers). It is for this reason that the equipment is designed in the form of separate and independently operated units.

Translated from Atomnaya Énergiya, Vol. 21, No. 3, pp. 223-224, September, 1966.

A 514-05 preamplifier amplifies pulses received from the semiconductor detectors and applies bias voltages to them. The preamplifier consists of the following: a 514-02 amplifier, a bias voltage source (591-55) for the semiconductor detectors, 591-56 and BN-65M power supplies for the preamplifier. The preamplifier has three amplification ranges corresponding to the 0-10, 0-30, 0-100 MeV energy ranges of recorded particles (using silicon detectors). The equivalent noise level does not exceed 10 keV in the first amplifying range, and the sensitivity is $2 \cdot 10^{12}$ V/C.

The 514-04 amplifier is designed to amplify and expand voltage pulses. The expander makes it possible to use AI-50, AI-100, AI-128, and AI-256 analyzers to study moderate spreads in input pulse heights. The amplifier contains the four components: 514-03 amplifier, 503-68 supply voltage indicator, and amplifier power supplies BN-40 and BN-34.

The instrument contributes to the solution of many problems in the spectrometry of ionizing radiations. Preliminary testing also indicates some possibility of using the electronic equipment developed to go along with it in spectrometric research on light charged particles and γ emission, using the proper semiconductor detectors. Designs of the individual components are now being worked out to completion.

Further research and development work on new semiconductor detectors should lead to improved electron physics equipment along these lines.

TEN YEARS OF THE "ATOMS FOR PEACE" EXPOSITION

V. Mikhailin

An exhibit of the achievements of the Soviet Union in the peaceful uses of atomic energy has been underway both here and in foreign countries since 1956. The exhibit was initiated in the wake of the first international conference on the peaceful uses of atomic energy in 1955 [at Geneva].

In the ensuing decade, 107 "Atoms for Peace" exhibits displaying achievements of science and industry have been organized, 69 of these in 43 foreign countries, plus 38 exhibits on special topics in the leading cities and industrial centers of our country.

A total of 42 million visitors to these exhibits have been recorded, 28 million abroad and about 14 million in the USSR alone. The "Atomic Energy" pavilion at the Exposition of Achievements of the National Economy of the USSR [Moscow] is visited annually by one million people. The pavilion makes a systematic display of topical exhibits and conducts seminars on subjects related to the exploitation of atomic energy in industry, biology, agriculture, and medicine. Designers, manufacturers, and users of isotope hardware and nuclear-physics equipment usually participate in the seminars.

Seminars and exhibits of this type are often arranged in other sections of the country where there is some experience in utilizing the advances of atomic science in specific fields. For example, an exhibit based on the theme "Applications of isotopes and nuclear radiations in mining" was organized in Lugansk in 1965, and about a thousand specialists took part in the seminar held during the time the exhibit was open to the public. The best exhibits and displays are selected and recommended for inclusion in the national exposition. Over the 10-yr period about 150 plants and organizations participating in the "Atomic Energy" pavilion of the national exposition were awarded prizes and medals struck for the Exposition of the Achievements of the National Economy of the USSR, for the best displays

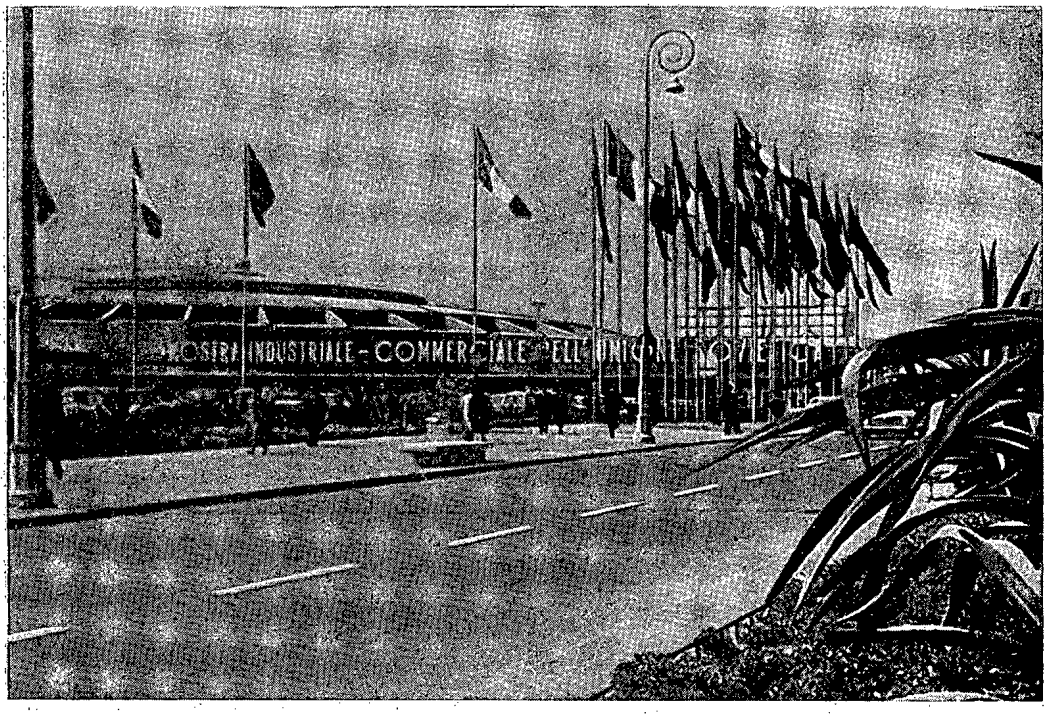

Soviet commercial and industrial exhibit in Genoa (Italy).

Translated from Atomnaya Énergiya, Vol. 21, No. 3, p. 229-230, September, 1966.

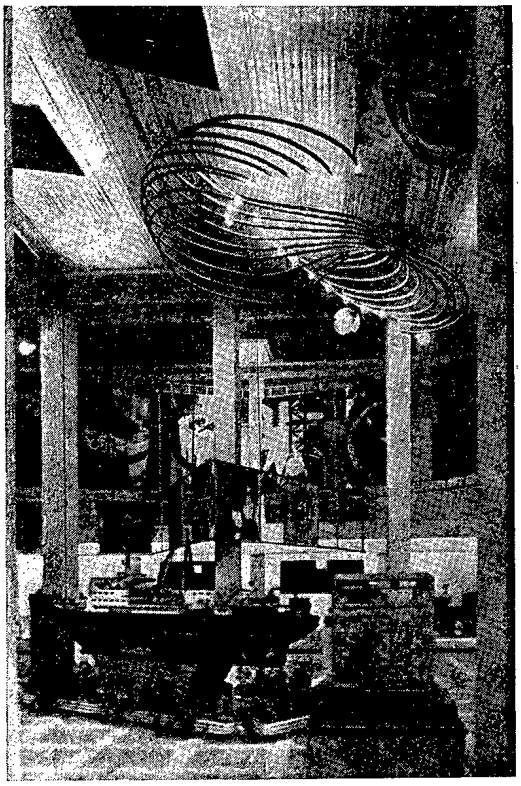

"Atoms for Peace" bay at the Izmir International Fair (Turkey).

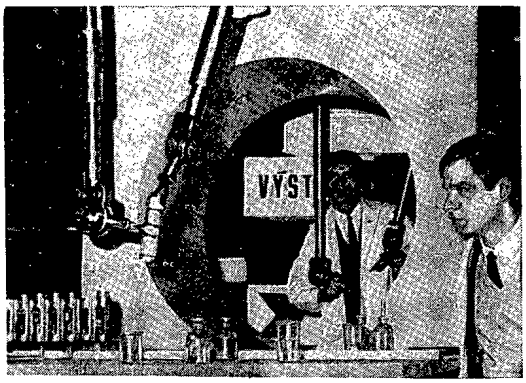

Mobile "Atoms for Work" exhibit at the Prague Technical Museum.

showing new techniques and their use in the national economy, 1230 individuals were awarded gold, silver, and bronze medals for their contributions in this area.

A dozen or so movable exhibits giving a general picture of the mainstream of scientific work in atomic energy and applications (as part of "Atoms for Peace" and "Atoms for Work") are on display in different cities throughout the USSR. The All-Union "Znanie" [Knowledge] Society organizes lectures and reports on the peaceful uses of atomic energy wherever these displays are open to the public. A photographic "USSR-Atom-Peace" exhibit consisting of fifty panels is now being prepared, and will be reproduced for widespread display.

Material on international collaboration between Soviet scientists and scientists in other countries, on the participation of the Soviet Union in IAEA activities, international conferences, and various international bodies, is being presented at the "Atoms for Peace" exhibits. The activities of the Joint Institute for Nuclear Research is generously reflected in these exhibits.

Special scientific and industrial exhibits have been set up on several occasions in Geneva, at international conferences on the peaceful uses of atomic energy, at Rome at international congresses on electronics, atomic energy, and telekinematography, where the Soviet exhibits won prizes.

The section "Nuclear power development in the USSR" shows mockups and activated models of nuclear electric power generating stations, nuclear power facilities, and materials on the development of nuclear power in the USSR from the world's first nuclear-fuel electric power generating station producing power at industrial levels to date. The exhibit which stimulates greatest interest in all countries is the mockup of the Romashka direct-conversion reactor designed for direct conversion of nuclear energy to electrical energy.

Beta type isotope sources were exhibited in the 1965 shows along with the automatic hydrometeorological station ARMS-N. This exhibit won a "Gold Medal" at the spring 1965 Leipzig international fair.

The "Atoms for Peace" exhibits include mockups and models of thermonuclear fusion apparatus for controlled fusion and plasma research, isotope instruments and facilities, nuclear physics equipment, dosimetric and radiometric equipment.

The "Isotope production and applications" sections familiarize visitors with isotope production and with equipment fabricated for this purpose in the USSR, and provide information on the achievements of Soviet scientists in application of isotopes and isotope-based devices to various sectors of the national economy.

As a rule, visitors are particularly interested in the exhibit sections illustrating the application of nuclear radiations and isotopes in medicine and radiation safety.

Experience has shown that the "Atoms for Peace" exhibit is of enormous significance in publicizing the use of the latest achievements of nuclear physics and nuclear industry in the various sectors of the national economy.

CANADIAN SCIENTISTS VISIT THE USSR

In response to an invitation to collaborate in the field of the peaceful uses of atomic energy, and by agreement between the USSR State Committee on the uses of atomic energy and the Canadian governmental body "Atomic Energy of Canada Ltd.," a delegation of Canadian scientists headed up by R. F. Harrington, director of the Canadian Nuclear Society, visited in the Soviet Union in April, 1966. The delegation also included A. B. Billey, head of the scientific division of the society, D. V. Anstey, head of the isotope production division, and J. F. S. McDonald, senior physicist of the London clinic of the cancer research center.

These scientists expressed interest in the design of equipment for experimental and industrial irradiation of foodstuffs, sterilization of medicinals, radiation chemistry and radiobiology, and the production and use of radioisotopes in a variety of research and industrial processes. Members of the delegation were familiarized with the work of several research institutes, were given an opportunity to meet with Soviet scientists, exchanged views on ways of utilizing isotopes, and discussed the development of means and techniques for radiation processing of different materials and radiation modification of processes.

The Canadian scientists were brought up to date on the status of research in radiation and spectrometry laboratories, in their visit to the L. Ya. Karpov Physical Chemistry Research Institute. They were very interested in the K-120000 general-purpose radiation-chemical facility, which is designed for a wide variety of radiation-chemical research experiments under any physico-chemical conditions. One of the principal advantages of this facility is the way the irradiator geometry can be altered as desired, and the way the effective volume of the internal irradiator cavity can be altered, and with it the dose rate in that cavity. The facility can be used with dry storage of radiation sources or with electromechanical source lifting techniques.

Canadian scientists showed keen interest in an experimental γ-ray facility designed for agricultural research, which used irradiators of different configuration (cylindrical, planar, linear, etc.), which they saw at the All-Union Institute of Electrification of Agriculture. The facility has a viewing window and a manipulator, making it possible to observe the irradiated object visually and to vary the dose rate as required.

The delegation of Canadian scientists flew to Tashkent on April 19, to visit the Nuclear Physics Institute of the Academy of Sciences of the Uzbek SSR. The scientists inspected the housing of a γ-ray facility accommodating three wells with Co^{60} γ-ray sources of total activity 500,000 gram-equivalents of radium. They also inspected the J-150 cyclotron, a reactor, and the departments of scientific chemical dosimetry, radiation effects, and activation analysis. Particular attention was given to the γ-ray facilities and dosimetry of high-level γ radiation flux.

The Canadian scientists were quite enthusiastic about their visit to the Boguchar branch of the All-Union Food and Vegetable Canning and Dehydration Research Institute , one of the leading organizations of the USSR in radiation processing of foodstuffs. V. N. Rogachev, vice-director of the Institute, informed the visitors of the lavish attention bestowed in the USSR on utilization of atomic energy for peaceful uses and on the development of food irradiation research on a broad scale. This research — in the areas of microbiology and physiology, biochemistry and biophysics, physical chemistry and engineering physics, radiation technology and radiation design — smoothes the way for comprehensive solutions of many problems involved in the practical utilization of ionizing radiations in processing agricultural raw materials and finished products.

The Canadian scientists were familiarized with an experimental production facility whose irradiator consists of two parallel planes sandwiching a cage holding irradiated materials and riding on a suspended chain conveyor. The spacing between the parallel planes can be varied over a wide range in

Translated from Atomnaya Énergiya, Vol. 21, No. 3, p. 231, September, 1966.

order to vary the dose rate from 60,000 to 15,000 rad/min. This facility is used to make thorough checks on methods and conditions for irradiating foodstuffs, as an aid to eventual industrial production.

In their visit to the central institute for advanced training of physicians under the USSR Ministry of Public Health, the guests were shown the quantity-produced rotational convergence γ-ray therapeutic cobalt irradiator "Rokus," with its 4000 C total source activity.

On the last day of their stay in the USSR, the Canadian scientists visited the V/O "Izotop" organization to acquaint themselves with its activities, and with the scale of application of radioisotope devices, facilities, shielding techniques, and isotopes in the USSR and deliveries of those items to other countries. The scientists also inspected samples of radiation work in the exhibit hall of the "Izotop" building.

In his concluding talk, R. F. Harrington expressed the gratitude of the Canadian delegation for the warm reception they encountered, and acknowledged the usefulness of mutual exchanges of delegations of specialists between different countries.

BIBLIOGRAPHY

PLASMA PHYSICS AND CONTROLLED NUCLEAR FUSION RESEARCH VOLS. 1 AND 2. CONFERENCE PROCEEDINGS, CULHAM, SEPTEMBER 6-10, 1965*.

Publication is now complete of the proceedings of the Second International Conference on Plasma Physics and Controlled Nuclear Fusion, held at Culham (Great Britain) in September, 1965. The papers presented run to two volumes totalling 1600 pages: detailed summary is to be found in "Atomnaya Énergiya", 20, 174 (1966). Each paper is in the original language, with summaries in English, French, Russian and Spanish. The Proceedings also include discussions of the papers in English, and a survey of the conference results by L. Spitzer and B. B. Kadomtsev in English and Russian. The papers give a clear idea of the state of plasma physics and are of interest to all workers in this field. The book is well produced, but unfortunately we must remark on the very low quality of the Russian translations in this publication.

A. E. Green and J. Wyatt. ATOMIC AND SPACE PHYSICS†.

This book is written by Professors of the Universities of Florida and California, U.S.A.; it is intended for readers who are familiar with higher mathematics. Even in Chapter 1, "Newtonian Dynamics and the Solar System" use is made of vector analysis and differential equations. This chapter concludes with a section on the dynamics of rocket flight. In Chapter 2 the reader will find a detailed exposition of topics in atomic physics and quantum theory, as far as the energy levels of diatomic molecules. Chapter 3 analyses the influence of solar radiation on the earth's atmosphere. The next chapter discusses various aspects of the behavior of the plasma in interplanetary space. There are also paragraphs on the solar wind, the radiation belts of the earth and how they are affected by high nuclear explosions. Chapter 5 gives details of the principles of quantum mechanics. It is followed by chapters on atomic spectroscopy and molecular energy levels. Chapter 8 deals with the transmission of radiation in planetary atmospheres and stars. It is followed by two chapters on spectroscopy in the infra-red (Chapter 9) and ultra-violet (Chapter 10) regions of the spectrum. Chapter 11 discusses details of radio astronomy. The last chapter, Chapter 12, deals with such applications of atomic and molecular physics as masers, lasers, etc.

The appendices contain detailed lists of names and subjects.

* Published by IAEA, Vienna, Vol. 1, 778 pp.; Vol. 2, 1000 pp., 1966.
† Published by Addison-Wesley, Reading, Mass. XVI+620 pp., 1965

Translated from Atomnaya Énergiya, Vol. 21, No. 3, pp. 232-238, September, 1966.

K. W. Gatland. SPACECRAFT AND BOOSTERS*. (The First Comprehensive Analysis of More Than Seventy U.S. and Soviet Space Launchings, 1961).

This is a beautifully produced and richly illustrated book containing brief characteristics of more than seventy objects launched from American and Sovient sites in 1961. The format is that of a handbook; the material is grouped in two parts: "satellites, probes and test rockets," (in chronological order), and "carrier rockets" (in alphabetical order).

In the section on satellites of the "TRANSIT-4" series, detailed descriptions are given of the SNAP-ZV radio isotope generator (with plutonium 238) used in this equipment as a source of electrical energy.

SATELLITE ENVIRONMENT HANDBOOK†. Second Edition, Edited by F. S. Johnson

This handbook contains eight sections written by scientists from Texas University, together with three short appendices and a subject index.

Section 1 deals with the structures of the upper layers of the earth's atmosphere; Section 2 deals with the structure of the ionosphere. Chapters 3 and 4 contain concentrated information on penetrating cosmic rays and solar radiation. Section 5 deals with the micrometeorite hazard; Section 6 gives data on radio noise. In the next two sections the reader will find material on the thermal radiation of the earth and on geomagnetism. Each section has a detailed bibliography.

The appendices give information on the solar system, the commonest physical constants and coefficients for converting one system of units to another.

There is a short subject index.

FIRST INTERNATIONAL CONFERENCE ON ELECTRON AND ION BEAM SCIENCE AND TECHNOLOGY ‡. Edited by R. Bakish

This book contains the proceedings of the First International Conference on Electron and Ion Beams, which took place in Toronto (Canada) in May 1964. All 47 papers are published in English, regardless

* Published by Iliffe Books Ltd., London 296 pp., 1964.
† Published by Stanford University Press, Stanford Cal. 196 pp., 1965.
‡ Published by John Wiley, N. Y. 986 pp., 1965 .

of the language of the original, and are divided into seven sections:- (1) Physics of electron and ion beams (6 papers); (2) Use of electron and ion beams in microelectronics (8 papers); (3) Use of electron and ion beams for recording and storing information (2 papers); (4) Electron beams in the processing of materials (12 papers); (5) Electron beam welding (8 papers); (6) Electron beams in microanalysis (5 papers); and (7) Ion motors (6 papers).

The book concludes with a short subject index.

MEASURING THE CHARACTERISTICS OF NUCLEAR REACTIONS AND PARTICLE BEAMS*. Compilers: K. L. Lyuk, Yuan and Vu Tszen'-Syun. Translated from the English, Edited by L. A. Artsimovich.

This book is a translation of the second part of Volume 5 of the Encyclopedic Series "Methods of Experimental Physics", published in the U. S. A. Chapter 1 analyses methods of determining the characteristics of nuclear reactions; Chapter 2 analyses the intensities of ion beams and γ-quanta. Chapter 3 describes various radioactive sources. Chapter 4 gives systems of ion beam transport. Chapter 5 contains information on statistical fluctuations in nuclear processes; a short appendix to this chapter discusses methods of presenting experimental results. Each survey has a full bibliography, mainly of articles from learned journals.

G. R. Keepin. PHYSICS OF NUCLEAR KINETICS†.

This book, written by the Director of the Physical Section of the Research and Laboratories Division of the IAAE, is a fundamental monograph on topics in nuclear reactor kinetics. It contains ten chapters. A short introduction is followed by Chapter 2 on the energy, mass, and charge distributions in the fission of heavy nuclei. Chapter 3 collects and analyses the data on instantaneous neutrons and γ-quanta from nuclear fission. The role of delay neutrons and their precursors is discussed in Chapter 4, while Chapter 5 gives data on delayed γ radiation from nuclear fission and photoneutrons. The basic ideas of reactor kinetics are formulated in Chapter 6. Chapter 7 deals with period-reactivity ratios. Chapter 8 gives a detailed analysis of methods of determining the kinetic parameters and reactivity, while Chapter 9 deals with transient functions. The last chapter, Chapter 10, deals with reactor stability.

Lengthy appendices give the period-reactivity ratios for U^{235}, Pu^{239} and U^{233}, the characteristic parameters of the fundamental equations of a linear reactor, the transient functions for zero power reactors based on U^{235}, Pu^{239} and U^{233}, and detailed subject and name indices. Each section has an extensive bibliography.

* Published by "Mir" Moscow, 416 pp., 1965.

† Published by Addison-Wesley, Reading, Mass., 436 pp., 1965.

L. E. Weaver. SYSTEMS ANALYSIS OF NUCLEAR REACTOR DYNAMICS* (An AEC Monograph).

This book was developed from a course of lectures on the use of linear systems analysis to analyse the dynamics of a nuclear reactor. The book contains 8 chapters and an appendix, containing, in particular, a large number of diagrams for the simulation of transient functions of a nuclear reactor. The bibliography contains 50 items, mostly from journal articles. There is a detailed subject index.

UTILIZATION OF THORIUM IN POWER REACTORS†. (Technical Reports Series, No. 52).

In Vienna in 1965 was convened a Symposium on the Use of Thorium in Power Reactors, organized by the IAAE. The participants included 45 specialists from 12 countries and two international organizations. The proceeding of the symposium were published by the IAAE in April 1966.

It is known that world thorium resources are greater than those of uranium. In addition, thanks to the nuclear properties of thorium, its use can to some extent reduce the fuel component costs of nuclear electric power. The problem of using thorium in a nuclear reactor is therefore very important in nuclear power production. Thorium is already in use in 12 reactors, and studies of this problem are being made in 9 countries.

This symposium consists of two interlinked sections: the first section summarizes the proceedings of the symposium and gives recommendations, while the second consists of the papers which were read.

Both sections comprise practically all aspects of the use of this type of nuclear reactor. One might somewhat arbitrarily pick out the following problems which are discussed: the physics of thorium in a reactor, the technology of thorium fuel, the design of reactors with thorium fuel, the role of thorium in plans for the development of nuclear power production, thorium fuel cycles, the economics of thorium as a fuel, the behavior of thorium fuel under irradiation, and the regeneration of the fuel.

The papers include one by a Russian author: "Fuel Breeding in an Intermediate-Energy Uranium-Thorium Reactor with Water Moderator" (by I. K. Levin).

The symposium presented the IAAE with a number of recommendations, most of which deal with the selection and systematization of nuclear-physical constants for thorium, and also the behavior of power reactors using thorium.

This symposium will undoubtedly be found useful by specialists in the field.

* Published by Rowman and Littlefield Inc., N. Y., 286 p., 1964.

† Published by IAEA, Vienna, 376 pp., 1966.

NUCLEAR ENERGY FOR WATER DESALINATION*. (Technical Reports Series, No. 51).

The IAAE Press has published a collection of papers read at the Fifth Symposium on the Use of Heat from Nuclear Reactors for the Distillation of Salt and Brackish Water, convened in April 1966. The symposium was attended by 37 specialists from 17 countries and international organisations.

This symposium reflects the interest of many countries in the problem of water supply and is one item in the IAAE program in this region of atomic energy utilization.

This collection contains 18 papers from the symposium, including one from the USSR on the economics of distillation. Little attention was paid to the actual technology of distillation. Attention was mainly focussed on nuclear power reactors as heat sources for distillation, their characteristics, the use of reactors in two-purpose nuclear stations, and plans for developing such stations. In the papers, a considereable place was occupied by questions of the economics of distillation. The scale and tempo of adoption of the nuclear method of distilling salt and brackish waters depend on the economic prospects of the use of reactors for this purpose. Studies in this direction have shown that in certain technical conditions quite obtainable in the present state of reactor construction, nuclear fuel can successfully compete with ordinary fuels. Several countries are therefore constructing two-purpose nuclear distillation stations. A number of the reports deal with this work.

A separate section of the collection gives brief summaries of the reports, conclusions and recommendations of the symposium. A brief description is also given of work to be undertaken in the near future by IAAE.

The book ends with a list of participants in the symposium and the organisations which they represent, together with the resolutions of IAAE symposiums on the same theme held in September 1963 and April 1966.

This book will undoubtedly be useful to specialists in the field of "nuclear distillation", since publications in this promising field of nuclear energy are very few.

G. Mau, V. Gassner, and H. Völcker. KOSTENUNTERSUCHUNG VON SCHIFFEN KONVENTIONELLEM UND KERNENERGIEANTRIEB†. (Costs of Nuclear-Powered and Conventional Ships).

This book is based on work by the West German Society for the Use of Atomic Energy in Navigation (G. K. S. S.). The results were presented at the Third Conference on Navigational Reactors in May 1964 at Kiel, and have now been augmented and edited.

The nine chapters of this book compare the economics of conventional and atomic vessels such as tankers and cargo ships.

The first three chapters give the basic assumptions and general considerations used in the investigation, together with a detailed discussion of running costs as a function of load, distance, speed, and type of ship.

* Published by IAEA, Vienna, 133 pp., 1966.
† Published by Thiemig, Münich, 90 pp., 1965.

The next two chapters determine the economic characteristics of a tanker and a cargo ship with conventional (diesel or steam) engines, with various displacements and speeds, as a function of the running costs, fuel costs, and voyage lengths. The reliability of the initial data is established and the method and results of the calculations given, these being compared with results obtained in the U. S. A.

Chapters 4 and 7 study the economics of six projected atomic ships. The initial data here were obtained from the shipbuilding firms. The costs of nuclear fuel were taken from data from the U. S. A.

Chapter 8 considers some of the economic prospects of atomic ships and gives the principal characteristics of the reactor of the nuclear ship "Savannah", together with the projected nuclear ship reactors CNSG, 630A, and SCLMR.

The short concluding chapter discusses defects in the initial data for the determination of the economic characteristics of atomic ships; these are mainly explained by the lack of adequate experience in their use.

An appendix to the book gives tables and graphs of the initial data and calculated results.

M. Taube. BREEDING OF FISSIONABLE FUEL*.

This book, by a well known Polish specialist, is a survey of current journal literature (304 references) on fissionable fuel breeding. The monograph is in Polish, and consists of six main sections:- (1) fissionable materials; (2) fuel breeding; (3) breeding in fast reactors; (4) breeding in a fast reactor with salt-type fuel; (5) breeding in thermal reactors; (6) the economics of breeding reactors.

R. P. Gottlib. UNTERSUCHUNG VON UNVERDICHTETEM UND VERDICHTETEM REAKTOR-GRAPHIT MIT HILFE VON GAS-DIFFUSIONS UND SORPTIONSMESSUNGEN†. (Study of Compressed and Noncompressed Reactor Graphite based on Gas Diffusion and Sorption).

This book is a detailed exposition of experimental investigations of the permeabilities of various types of the permeabilities of various types of graphite for fragment gases. A short introduction (Section 1) gives the aim and main courses of the work; Section 2 gives the theory and calculates the dynamic adsorption of inert gases and nitrogen on the surface of granules and in the capillaries of

* Published by Nuclear Energy Information Center, Warsaw, 404 pp., 1965.

† Published by Brown Boveri und Krupp Reactorbau GmbH, Dusseldorf, 148 p., 1964.

graphite. Section 3 describes the experiments and gives details of tests of the substance and the gases and apparatus. The radioactive tracer was Kr^{85}. Sorption-desorption isotherms are obtained and are compared with earlier published results in Section 4, and are discussed in detail in the concluding Section 5. The references include 53 items.

J. Spinks and R. Woods. AN INTRODUCTION TO RADIATION CHEMISTRY*

Reviewed by Senyavin

As the authors correctly point out, processes of radiation chemistry have accompanied the study of nuclear science from its very first steps, for x-rays and radioactivity were discovered via radiation-chemical phenomena—the interactions of electromagnetic radiation and charged particles with photographic emulsions. With the advance of atomic power, during the last 70 years much progress has been made in radiation chemistry. This is demonstrated, not only by the many publications on the subject, but also by the growing tangible and practical applications, including industrial uses, of these processes, which are considered to be an important factor in the economic viability of power production by nuclear means (dual-purpose power-chemical reactors).

We can cite a number of monographs on radiation chemistry covering various aspects of its application (water and aqueous solutions, polymers, etc.), but so far there has been no attempt to give a brief summary of the results obtained in this interesting and important branch of knowledge. This book, described by the authors as a textbook, in the reviewer's opinion successfully fills this gap.

In about thirty printer's sheets, the authors, who are professors at the University of Saskatchewan (Canada) fulfil their aims by expounding the topics briefly, comprehensively, and at a high scientific level. After a brief discussion of the meaning of "radiation chemistry" and of how it differs from "nuclear chemistry" and "radiochemistry", they describe radioactive-isotope radiation sources (including mixed sources in nuclear reactors), γ-ray generators, and accelerators. The principles of radiation chemistry are discussed in comparatively great detail: they include the interaction of radiation with matter, and the mechanisms of processes associated with the formation of ions, excited molecules, and free radicals.

A large part of the book deals with the results of the action of radiation on various systems—gases, water and aqueous solutions, organic compounds, and solids. A separate chapter is devoted to the industrial applications of radiation for sterilization, chemical synthesis, and the irradiation of monomers and polymers; the same chapter briefly describes industrial radiation sources. Finally, the book discusses the solution of some problems associated with calculations of radiation doses, source powers, energy absorption, etc. The book contains more than 800 references to original papers; unfortunately, however, Soviet authors are far from completely represented.

This book will be read with interest by many specialists, such as chemists, physicists and engineers in various fields, and also by advanced students of chemistry. It would be very useful to have a Russian translation of it.

*Published by J. Wiley & Sons, N. Y., London-Sydney, 477 pp., 1964.

A. J. Duivenstijn and L. A. Venverloo. PRAKTISCHE GAMMASPEKTROMETRIE *. (Practical γ-spectrometry).

Reviewed by Yu. V. Sivintsev

This is a textbook on γ-ray spectrometry, intended for persons without specialist training in nuclear techniques but who have to make practical use of the corresponding apparatus. Chapter 1 is a brief introduction, defining the place of γ-quanta in the frequency-energy scale of electromagnetic radiation. Chapter 2 gives information on stable and radioactive atoms and ionizing radiations. Chapter 3 is a brief description of the main processes of the interaction of γ-rays with matter.

Scintillation detectors are described in comparative detail in Chapter 4 (scintillators and photomultipliers are dealt with separately). Chapter 5 summarizes information on γ-ray spectrometers (mainly single-channel models), and also describes the principal electronic equipment associated with them. Methods of identifying γ-rays from the shape of the energy spectrum are given in Chapter 6, which gives many numerical and graphical examples. Chapter 7 deals with the use of γ-spectrometers for the quantitative measurement of radioactive substances. It ends with data on the statistical nature of the phenomena involved in the recording of γ-ray quanta and the resultant accuracy of the analysis results obtained. A short final chapter briefly enumerates other methods of γ-spectrometry.

Appendices give tables of frequently-required physical constants, K_α-lines, characteristic radiations, and half-life versus quantum energy for γ-emitters, and information on the energies of β and γ- radiation from radioactive isotopes from H^3 to No^{254}. The bibliography is short and consists mainly of Anglo-American journal articles published in special editions.

G. Dearnaley and D. Northrop. SEMICONDUCTOR COUNTERS FOR NUCLEAR RADIATIONS†.

This is the first fundamental monograph on the use of semiconductor detectors to record ionizing radiation. In ten chapters the authors discuss various aspects of these new aids to experimental nuclear physics and compare them with previously known detectors. After a brief authors' introduction and a list of symbols, Chapter 1 discusses the properties of ionizing radiation and the energy losses in a medium for ions, electrons, γ-quanta, and neutrons. Chapter 2 is a survey of methods of detecting ionizing particles. The references to each of these chapters include 30 items. In Chapter 3 the reader will find a detailed discussion of the physical properties of semiconductor detectors. It includes sections on ionization, charge collection, secondary radiation, and electronic pulse shaping. Chapter 4 deals with noise and energy resolution limits of semiconductor detectors: some higher mathematics is used here. Chapter 5 describes homogeneous counters based on silicon, germanium, cadmium sulfide, and other materials. Other types of semiconductor detector—surface-barrier, germanium-lithium, etc.—are described in Chapter 6. Chapter 7 gives details of methods of preparing semiconductor detectors and their properties. (This chapter has a list of 25 references, while the preceding chapters have only 10-15 each). Chapter 8 describes the apparatus required in the use of semiconductor detectors. Various applications of the new detectors are described in great detail in Chapter 9, which

* Published by Centrex Verlag Philips Technische Bibliotek), Eindhoven, 150 pp., 1964.

† Published by E. and F. N. Spon Ltd., London, 332 pp., 1964.

gives actual examples of investigations in various branches of contemporary nuclear physics and engineering. The references here include over 70 times. The final tenth chapter gives information on radiation damage to semiconductor detectors.

The book ends with appendices containing tables of the physical properties of silicon and germanium, a full bibliography (30 pp.), and detailed author and subject indexes.

L. V. Loeb. ELECTRICAL CORONAS: THEIR BASIC PHYSICAL MECHANISMS*.

Chapter 6 of this book gives a detailed description and analysis of processes occurring in gas-discharge counters for charged particles (proportional, with self-stable discharge, or halogen-quenched). Throughout this chapter, the authors proceed by comparing the measured effects with the predictions of the theory of electrical coronas.

E. I. Hamilton. APPLIED GEOCHRONOLOGY†.

This book opens with an introduction which deals with the comparative geochronology of potassium, rubidium, calcium, argon, strontium, uranium, thorium, and lead. A short historical survey (Chapter 1) is followed by Chapter 2 which deals with the principal methods of measurement used in this field.

The author briefly but clearly describes the methods of radiometry, dilution of stable isotopes, and mass-spectrometry. The radiocarbon method is discussed in detail in Chapter 3. Here the reader will find information on the sources of C^{14} in the atmosphere. methods of measuring it by means of various types of counters, and applications to dating. The potassium-argon method is dealt with in Chapter 4. It also deals with the flame photometry and neutron-activation methods, in addition to mass spectrometry, and also gives data on the losses of argon in geological materials. Chapter 5 describes the rubidium-strontium method for measuring the ages of rocks. Special attention is paid to the use of this method in petrography, including the analysis of meteorites. The short sixth chapter briefly describes the principle of the rhenium-osmium method and its applications to geochronology. Chapter 7 is an extended description of the uranium-thorium-lead method. Special details are given of the complex case of the analysis of samples not containing individual members or final products of radioactive families, and of the method of Pb^{210} (RaD) dosing.

* Published by California University Press, Berkeley and Los Angeles, 694 pp., 1965.
† Published by Academic Press, London, XVI + 268 pp., 1965.

The compact eithth chapter describes the relatively new method of estimating the ages of rocks by radiation damage. The conventional lead method is discussed in detail in Chapter 9. Together with a description of methods of separating lead from the sample, much attention is paid to the interpretation of the data on the dissemination of the lead isotopes. The book ends with three short sections on dating geologically recent sediments (Chapter 10), on the ages of meteorites (Chapter 11), and the scale of geological epochs (Chapter 12). The appendices contain a detailed list of references (18 pp.) and full author and subject indexes.

RADIATION, PART OF LIFE*.

This is a short popular-science book on the action of ionizing radiation on the human body. A short historical survey (Chapter 1) is followed by a discussion of the nature of radiation (Chapter 2). Chapter 3 introduces the reader to the idea of sources of radiation, including ionizing radiation; various effects of radiation are described in Chapter 4. The last, fifth chapter tells of the applications of atomic energy. The book ends with a vocabulary of unfamiliar terms and a short subject index.

M. M. Link. SPACE MEDICINE OF PROJECT MERCURY†.

This monograph describes the development of work in space medicine and gives data obtained as a result of the launching of the first American man-carrying satellites (Project "Mercury"). An introduction written by several specialists is followed by eleven chapters and an appendix with a list of members of various NASA committees dealing with space medicine. The book contains many photographs, and each chapter has a list of references (mainly NASA reports) with a few dozen items. The appendices include detailed author and subject indexes.

* Published by Consumer Publications, London, 124 pp., 1961.

† Published by National Aeronautics and Space Administration, Washington (NASA SP-4003). 198 pp., 1965.

PROBLEMS OF ATMOSPHERIC DIFFUSION AND AIR CONTAMINATION*.

(Work of A. I. Voikov Principal Geophysical Observatory, No. 158). Edited by M. E. Berlyand.

This symposium contains 18 original papers, mainly on the calculation and measurement of contamination of the lower atmosphere based on ejection and smoke tubes. Some of the papers discuss the influence of relief and urbanization on the distribution of smoke plumes (dust, ashes, sulfur dioxide). Some of the articles deal with radiometry of contaminated air (aerosols and gases) and soil surfaces. This book will interest specialists working in the field of discharge of gaseous radioactive waste through ejection tubes and of external dosimetry.

INDUSTRIAL WASTEWATER CONTROL. A TEXTBOOK AND REFERENCE WORK†. Edited by G. Fred Gurnham.

A new handbook on the control of industrial effluents, prepared by a group of specialists from the Illinois Technological Institute (Chicago). Chapter 24 deals with liquid radioactive wastes formed during the use of atomic power. The chief topic discussed is nuclear reactors of various types.

BIOLOGY OF RADIO-IODINE ‡. (Proceedings of the Hanford Symposium). Edited by L. K. Bustad.

This book contains the papers from a symposium organized by the AEC of the USA at Hanford in July 1964, dealing with various aspects of the biology of radioactive iodine isotopes. Except for eight of the papers, the texts of the reports are printed in full and are grouped under seven headings: (1) physical methods of obtaining and dispersing radioactive iodine (4 papers, 1 summary); (2) incorporation of I^{131} into biological systems and human food (8 papers); (3) relative accession of iodine isotopes into animals and men via various food chains (19 papers, 4 summaries); (4) immediate and remote effects of acute and chronic action of I^{131} on young and old organisms (3 papers, 1 summary); (5) comparative radiobiology of I^{131} and x-rays used with iron shields (2 papers, 1 summary);

* Published by Gidrometeorologicheskoe izd., Leningrad, 136 pp., 1965.

† Published by Academic Press (Chemical Technology: A Series of Monographs, Vol. 2), N. Y. – London. 476 pp., 1965.

‡ Published by Pergamon Press (Symposium Publication Division), Oxford – London 346 pp., 1964.

(6) the carcinogenic effect of I^{131} in comparison with x-rays (2 papers); (7) prophylactic and therapeutic methods (4 papers, 1 summary). The book also includes the texts of lectures by E. E. Pochin on "What is a Permissible Dose"? and by K. Morgan on "Biomedicinal Consequences of Accidental Discharge of Radioactive Iodine", read by participants in the symposium.

CURRENT RESEARCH IN LEUKAEMIA*. Edited by F. G. J. Hayhoe.

This book contains material from a course of lectures given at Cambridge University in August 1964 by eminent specialists in the leucoses. Brief prefaces by the publishers and compilers are followed by seven sections. Section 1 contains four reports on cytology and electron microscopy of blood cells in animals and man. Three lectures deal with cytogenetic investigations (Section 2). The study of the growth and fission of cells occupies a specially large place (Section 3, eight lectures). A very specialized section (Section 4) deals with lymphoma in children in a region of Africa. Section 5 deals with biochemical aspects of the leucoses, and contains the texts of two lectures. Section 6 deals with work on the treatment of acute leucoses by bone-marrow grafting. Section 7 deals with epidemiological aspects of the leucoses (3 lectures).

Each section has an extensive bibliography, and there is a detailed subject index.

S. K. Krasnov. RADIATION SICKNESS, POISONING, AND SHIELDING AGAINST THEM†.

This book is intended for readers without special training in radiation and chemical protection. It is divided into two sections as indicated in the title. The first section (8 chapters) deals with radiation sickness. After an exposition of the biological action of ionizing radiation in man (Chapters 1 and 2) there follow chapters on radiation sickness, caused by external (Chapter 3) and internal (chapter 4) irradiation. This section is followed immediately by Chapter 5 on the medical treatment of radiation poisoning and radiation sickness. Chapter 6 deals with methods of dosimetry and radiometric investigations, and Chapter 7 with deactivation and shielding of food products and water; Chapter 8 deals with collective means of shielding against high-fallout weapons.

* Published by Cambridge University Press, XII+306 pp., 1965.
† Published by Saratovskogo Universiteta, Izd., 136 pp., 1965.

E. W. Webster and K. C. Tsien. ATLAS OF RADIATION DOSE DISTRIBUTIONS*. VOL. 1. SINGLE-FIELD ISODOSE CHARTS.

The main content of this atlas is 155 isodose x-ray and γ-ray distributions, measured by means of ionization chambers at various depths in a water phantom man. This section contains four subsections. The first two of these contain diagrams for Co^{60} (25 items) and Cs^{137} (62 items) teletherapy units, starting with short-focus power 10 curie and going to units with long focal length (up to 1 m) with powers of several kilocuries. The third subsection gives isodose diagrams for x-ray units with high anode voltages of 2 to 70 megavolts, five different betatrons, and five linear accelerators (43 diagrams in all). In the fourth section the reader will find twenty-five isodose diagrams for electron beams, with particle energies of 7 to 35 MeV, produced by betatrons or linear accelerators.

For convenience in use, the atlas has a detailed foreword containing information on methods of isodose measurement, the parameters of the measurement equipment, and the characteristics of the shaping of the radiation beam. It also gives clear indexes which facilitate the location of the required diagram for the apparatus in use.

P. S. Russell and A. P. Aronaco. THE BIOLOGY OF TISSUE TRANSPLANTATION†.

This book, written by two well-known American radiobiologists, discusses the present state of the problem of tissue transplantation, in particular that of bone marrow after over-irradiation of the human body. The monograph contains a short foreword, a brief introduction, an explanation of the terminology (Chapter 1), four main chapters, and an enclosure. The bibliography is very extensive (612 items). There is a detailed subject index.

INDEXED BIBLIOGRAPHY OF CURRENT NUCLEAR SAFETY LITERATURE-4‡.

This symposium is the fourth issue of a quarterly bibliographic handbook published by the Nuclear Safety Information Center. This new issue contains references to articles, books, and AEC reports

* Published by IAEA, Vienna, 52+155 pp.

† Published by Little, Brown & Co., Boston, 208 pp., 1965.

‡ Published by ORNL-NSIC-14, Oak Ridge National Laboratory, Nuclear Safety Information Center, 214 pp., March 1966.

published later than September 1964. The data was processed by means of a computer. The material is divided into nineteen sections: (1) general safety criteria; (2) choice of sites for nuclear installations (3) transport and handling of radioactive substances; (4) safety in space flights; (5) analysis of accidents; (6) reactor kinetics and stability; (7) extraction, transition functions, transfer and disposal of fission products; (8) sources of the energy emitted in accidents; (9) nuclear-physical instruments, control and safety systems; (10) energy-producing systems; (11) shielding envelopes; (12) aspects of safety in large installations; (13) safety in radiochemical plants; (14) transport of radioactive substances in an enveloping medium; (15) external dosimetry service and irradiation of the population; (16) meteorological aspects; (17) experience in use and safety; (18) reports on the analysis of plans for safety systems; (19) bibliography. The book has detailed subject and author indexes.

ISOTOPES AND RADIATION IN SOIL-PLANT NUTRITION STUDIES*.

The IAAE has published the papers from a symposium on the uses of isotopes and radiation in soil studies, held from May 28 to July 2, 1965.

This collection comprises 45 reports on various topics in soil chemistry and physics, accumulation of elements, and their exchange between the soil and vegetation, divided under four sections.

Most of the reports give interesting results obtained by studying various processes of element exchange in the soil and vegetation (foods and toxic compounds, soil water, etc.) by means of tagged compounds.

For regions with sufficiently homogeneous soils and level surfaces, H. Sharpansel' et al. (German Federal Republic, Bonn University) proposed a system of continuous automatic control of irrigation by means of a neutron detector. P. Kirchman et al. (Belgium) reported on the accumulation of Fa^{226} in plants and gave a comparison with the corresponding balances of calcium and strontium in identical experiments.

E. Weldt et al. (Federal German Republic) gave the results of an investigation of the feasibility of tracing potassium compounds by means of Rb^{86}.

The symposium as a whole will be of interest to workers in agricultural research institutions, and also to those who use isotopes in plant growing and agrochemistry.

* IAEA, Vienna, 609 pp., 1965.

PLANT NUTRIENT SUPPLY AND MOVEMENT*. REPORT OF A PANEL HELD IN VIENNA, 9-13 NOVEMBER 1964.

This book contains an introductory address by the president of a panel of experts, and the texts of 17 reports on topics in plant nutrition (in English). Most of the reports deal with ion-exchange properties of soils; the work was performed with such radioactive isotopes as Na^{24}, Mg^{27}, and Mg^{28}, P^{32}, S^{35}, Cl^{38}, K^{42}, Rb^{86}, Sr^{89}, etc. Four of the reports consider the possibility of using activation analysis to study the dynamic relations of soil and vegetation. The brochure also contains the panel's conclusions and recommendations(in English, French, Russian, and Spanish). The authors emphasize the importance of their investigations for the most effective use of phosphate and nitrogen fertilizers.

MANIPULATION OF RADIOACTIVE WASTES IN WORK WITH RADIO-ISOTOPES†. (Series of Publications on Safety, No.12).

This is a handbook of practical rules based on reports by a panel of experts (a list of the reports is given at the end of the brochure). A short introduction on the aims and terms of reference of the collected recommendations (Chapter 1) is followed by Chapter 2 which deals with control in the use of radioactive isotopes and disposal of radioactive wastes. Special interest attaches to a report on the permissible limits of discharge of radioactive substances into the earth, water, and town dumps. Chapter 3 deals with the handling of radioactive wastes by individual consumers; Chapter 4 deals with methods of treating radioactive wastes which are not separated from the isotopes by the consumers. Chapter 5 gives information on methods of temporary and long-term storage of radioactive wastes in the surrounding medium. A short appendix (Appendix I) characterizes the types of wastes which have to be manipulated in work with a number of radioactive isotopes; Appendix II gives examples of the national regulations of the USSR, USA, and Great Britain, governing disposal of radioactive wastes by isotope users.

* Published by IAEA, Vienna, (Technical Reports, Series No.48), 158 pp., 1965.

† Published by IAAE, Vienna, 70 pp., 1966.

RADIOACTIVITY (RECOMMENDATIONS OF INTERNATIONAL COMMISSION ON RADIATION UNITS AND MEASUREMENTS REPORT 10 C, 1962), SERIES OF TECHNICAL REPORTS (No.47)*.

This book has an introduction, containing information on the aims, activities, program and composition of the International Commission on Radiation Units and Measurement (ICRUM). Chapter 1 contains a survey of present methods of absolute and relative measurements of radioactivity (4π-counters, coincidence circuits) and information on the results of international comparisons of radioactive standards. In Chapter 2 the reader will find a description of methods of measuring low levels of radioactivity and information on natural and artificial radioactive contamination of constructional materials, chemical reagents, and photographic emulsions. Chapter 3 summarizes data on radioactive standards. Methods of measuring radioactivity in biological samples and living organisms are described in Chapter 4. Attention is paid mainly to scanning apparatus and spectrometers for human irradiation. There is also an extensive bibliography on topics in radiometry. The appendices give recommendations (ICRUM, 1959) on radioactivity standards and radiation units.

E. Fenyves and O. Haiman. DIE PHYSIKALISCHEN GRUNDLAGEN DER KERNSTRAHLUNGSMESSUNGEN†. (Physical Principles of Measurements of Nuclear Radiations).

This monograph consists of nine chapters, three appendices and a subject index. The first chapter contains an introduction and historical survey of methods of recording ionizing radiation. Chapter 2 describes the main processes of the interaction of radiation with matter. In the next chapter the reader will find information on the transmission of ionizing radiation through a layer of absorbent. Chapter 4 analyses physical processes occuring in various detectors (from ionization chambers to photographic emulsions and Cerenkov detectors). Chapter 5 (150 pages) describes in special detail the action and construction of charged-particle detectors, and contains an extensive bibliography. The physical bases of methods of determining the main properties of particles and quanta are discussed in Chapter 6, which also contains an extensive bibliography. Chapter 7 gives information on methods of determining the characteristics of fields of ionizing radiations and their doses. Chapter 8 describes detectors of particle trajectories and tracks (Wilson cloud chamber and photographic emulsion). Chapter 9 deals with methods of identifying particles by analysis of their trajectories.

Appendix I gives brief information on experiments which have led to the discoveries of the various elementary particles (from the neutron to the antihyperons); Appendix II gives the elements of statistics as far as they apply to methods of recording ionizing radiations; Appendix III gives information on electronic methods of registration and discriminations applicable to experimental nuclear physics. The book concludes with a detailed subject index (12 pages).

---

* Published by IAAE, Vienna, XVI+128 pp., 1965.

† Published by Akademiai Kiado, Budapest, Verlag der Ungarischen Akademie der Wissenschaften, 728 pp., 1965.

R. L. Egan. MAMMOGRAPHY*.

This book is a well-produced handbook on the use of x-rays to diagnose malignant growths in the mammary glands. It is richly illustrated with numerous x-ray photographs made with various contrast techniques.

T. Venkei and J. Sugar. EARLY DIAGNOSIS, PATHOHISTOLOGY AND TREATMENT OF MALIGNANT TUMORS OF THE SKIN† .

This book, written by specialists from the Oncological Institute at Budapest, consists of an introduction, eight sections, a detailed bibliography, and author and subject indexes. In the sections which deal with the conditions favoring the appearance of a neoplasm (Chapter 2) and malignant tumors of the skin (Chapter 3), much attention is paid to overirradiation by ionizing radiations, i.e., x-rays and rays from radioactive substances. In Chapter 4 in the main subsection there is information on acute and chronic radio-dermatitis. Some chapters contain data on the therapeutic use of x-rays, and penetrating γ-rays from Ra^{226}, Co^{60}, and Cs^{137}, and also β-particles from P^{32}.

* Published by Ch. Thomas, Springfield, Illinois, 448 pp., 1964.

† Published by Akademiai Kiado, Publishing House of the Hungarian Academy of Sciences, Budapest, 368 pp., 1965.

Solid State Transformations

Edited by N. N. Sirota, F. K. Gorskii, and V. M. Varikash

Institute of Solid State Physics and Semiconductors Academy of Sciences of the Belorussian SSR, Minsk

Translated from Russian by Geoffrey D. Archard
Corrected by the editors for the American edition.

A well-balanced summary of the mechanism of phase transformations, beginning with the theoretical concepts of thermodynamics and leading on to the practical significance of these in the structure of crystals, their formation and growth, defects and dissolution, reaction to magnetic and electric fields, and physical and chemical properties. The papers included consider some general questions on the thermodynamics of critical phenomena based on Gibbs' research on the thermodynamic instability of phases with discussions of phase transformations and associated ultrasonic, x-ray, and other forms of scattering. Articles on transformations and recrystallization in the solid state concern polymorphism of elements in connection with their position on the periodic table, experimental crystal growth in the solid state during polymorphic transformations, the effect of vacancy diffusion on crystal growth during recrystallization, and peculiarities of martensite transformations.

This volume is a translation of two sections of the Russian work entitled *Mechanism and Kinetics of Crystallization* containing articles presented at the All-Union Conference on the Theory of Crystallization, Thermodynamics, and Kinetics of Phase Transformations. The remaining two parts are being published simultaneously in a translation entitled *Crystallization Processes*. Both volumes have been thoroughly corrected by the editors.

OF INTEREST TO: solid state physicists, crystallographers, physical chemists, metallurgists, and scientists and engineers concerned with semiconductor devices and research.

169 pages $22.50

Solid State Transformations: $22.50
Crystallization Processes: $22.50

Set price: $40.00

CONSULTANTS BUREAU 227 West 17th Street, New York, New York 10011
A DIVISION OF PLENUM PUBLISHING CORPORATION

Declassified and Approved For Release 2013/03/12 : CIA-RDP10-02196R000700040003-1